

Editor-in-Chief B.E.Paton

Editorial board:

Yu.S.Borisov	V.F.Khorunov
A.Ya.Ishchenko	I.V.Krivtsun
B.V.Khitrovskaya	L.M.Lobanov
V.I.Kirian	A.A.Mazur
S.I.Kuchuk-Yatsenko	
Yu.N.Lankin	I.K.Pokhodnya
V.N.Lipodaev	V.D.Poznyakov
V.I.Makhnenko	K.A.Yushchenko
O.K.Nazarenko	A.T.Zelnichenko
I.A.Ryabtsev	

International editorial council:

N.P.Alyoshin	(Russia)
U.Diltay	(Germany)
Guan Qiao	(China)
D. von Hofe	(Germany)
V.I.Lysak	(Russia)
N.I.Nikiforov	(Russia)
B.E.Paton	(Ukraine)
Ya.Pilarczyk	(Poland)
P.Seyffarth	(Germany)
G.A.Turichin	(Russia)
Zhang Yanmin	(China)
A.S.Zubchenko	(Russia)

Promotion group:

V.N.Lipodaev, V.I.Lokteva
A.T.Zelnichenko (exec. director)

Translators:

A.A.Fomin, O.S.Kurochko,
I.N.Kutianova, T.K.Vasilenko
PE «Melnik A.M.»

Editor

N.A.Dmitrieva
Electron galley:
D.I.Sereda, T.Yu.Snegiryova

Address:

E.O. Paton Electric Welding Institute,
International Association «Welding»,
11, Bozhenko str., 03680, Kyiv, Ukraine

Tel.: (38044) 287 67 57

Fax: (38044) 528 04 86

E-mail: journal@paton.kiev.ua

http://www.nas.gov.ua/pwj

State Registration Certificate
KV 4790 of 09.01.2001

Subscriptions:

\$324, 12 issues per year,
postage and packaging included.
Back issues available.

All rights reserved.

This publication and each of the articles
contained herein are protected by copyright.
Permission to reproduce material contained in
this journal must be obtained in writing from
the Publisher.

Copies of individual articles may be obtained
from the Publisher.

CONTENTS

SCIENTIFIC AND TECHNICAL

<i>Gook S., Gumenyuk A., Lammers M. and Rethmeier M.</i> Peculiarities of the process of orbital laser-arc welding of thick-walled large-diameter pipes	2
<i>Khorunov V.F., Maksymova S.V. and Zelinskaya G.M.</i> Investigation of structure and phase composition of alloys based on the Ti-Zr-Fe system	9
<i>Gvozdetsky V.S.</i> Analytical study of current controller of power source for microplasma welding	15
<i>Derlomenko V.V., Yushchenko K.A., Savchenko V.S. and Chervyakov N.O.</i> Technological strength and analysis of causes of weldability deterioration and cracking	20
<i>Kobernik N.V., Chernyshov G.G., Mikheev R.S. and Chernyshova T.A.</i> Treatment of the surface of aluminium-matrix composite materials by concentrated energy sources	24

INDUSTRIAL

<i>Lobanov L.M., Pashchin N.A., Loginov V.P., Poklyatsky A.G.</i> and <i>Babutsky A.I.</i> Repair of ship hull structures of aluminium alloy AMg6 using electrodynamic treatment	31
<i>Martinovich V.N., Martinovich N.P., Lebedev V.A., Maksimov S.Yu., Pichak V.G. and Lendel I.V.</i> High-quality hose packs for underwater welding and cutting	33
<i>Troitsky V.A., Dyadin V.P. and Davydov E.A.</i> Ultrasonic diagnostics of service defects in structures of oil and gas industry	36

NEWS

10th Jubilee European Conference-Exhibition on Non-Destructive Testing	41
International Conference on Welding Consumables	42
10th International Conference-Exhibition «Problems of Corrosion and Anticorrosion Protection of Structural Materials. Corrosion-2010»	45
L.M. Lobanov is 70	46

INFORMATION

News	48
Developed in PWI	49



PECULIARITIES OF THE PROCESS OF ORBITAL LASER-ARC WELDING OF THICK-WALLED LARGE-DIAMETER PIPES

S. GOOK, A. GUMENYUK, M. LAMMERS and M. RETHMEIER

Federal Institute for Materials Research and Testing (BAM), Berlin, Germany

The results of development and testing of hybrid laser-arc welding of large-diameter pipes are given. The main results of the research, in particular, on the peculiarities of weld formation in different regions of circumferential joints, mechanical properties of the welded joints, and potentialities of the available equipment for construction of main pipelines are generalized.

Keywords: *hybrid laser-arc welding, orbital welding, high-pressure pipelines, fibre-optic lasers*

One of the key components of the world energy system is a network of main pipelines. Construction of these pipelines demonstrated advantages of manual and mechanised methods of arc welding, such as manual covered-electrode arc welding, mechanised gas-shielded welding using solid or flux-cored wire, and mechanised twin-arc tandem welding. Worthy of note among the non-arc processes is flash butt welding, which has not yet found wide application for construction of modern oil and gas pipelines despite the simplicity of its principle of operation [1]. Position butt welding of pipelines is a labour-consuming process, which determines to a considerable degree the rate of laying a line as a whole. The arc welding methods employed are characterised by a relatively low speed. This limitation may be quite appreciable, for example, in construction of pipeline with a diameter of 1229 mm and wall thickness of 35 mm or more. Furthermore, the oil and gas industry is in a state of search for solutions concerning application of modern high-strength structural materials, as this would allow reducing wall thickness of pipelines in order to cut their metal intensity or increase a working pressure in the pipeline to provide a more efficient transportation of product. Instead of standard pipeline steel grades of strength classes X60 and X70 with a yield point of up to 500 MPa, according to classification of the American Petroleum Institute, steels of a higher strength class, such as X80 or X100, are introduced into practice, as a result of which the working pressure in new pipelines that are designed now can be raised from 7–10 to 15–20 MPa. Despite the fact that increase of strength characteristics of steel in terms of welding metallurgy leads to deterioration of its weldability, traditional arc welding is capable of providing the required quality of welded joints, and the use of fully automated welding processes solves the problem of its reproducibility. It is likely that the choice of

these welding processes or the other for construction of advanced pipelines from high-strength steel will be based primarily on the technical-economical factors, allowing for the volumes of construction and assurance of the quality of building and assembly operations. This strategy is inseparably connected with application of the latest achievements in the field of welding technologies, among which the most attractive ones today are highly efficient combined (hybrid) welding processes based on the synergic, complex effect of the laser beam and electric arc on the weld.

The idea of using beam welding to make circumferential welds on pipelines is not new. For instance, the possibilities of using electron beam [2], gas CO₂-laser [3] and solid-state Nd:YAG-laser [4] to implement the orbital welding process have been considered in a number of publications approximately since 2000. The feasibility of applying electron beam welding for making single-pass circumferential welds was demonstrated on the 762 mm diameter pipes with a wall thickness of 19 mm. However, the use of the said welding method under field conditions is hampered by technical difficulties associated mainly with the need of creating vacuum within the welding zone and ensuring protection from X-radiation generated when electrons hit a workpiece. In the case of the laser beam, the maximal wall thickness of a pipe is limited to 10 mm, which is caused by the maximal output power of laser units employed at that time (12 kW for the CO₂-laser, and 4.4 kW for the Nd:YAG-laser).

With emergence of the high-power solid-state lasers, such as fibre-optic and disk ones, the welding industry began using up to 20 kW continuous-wave laser units featuring an excellent quality of emission and compact design. Utilisation of the said advantages of modern lasers combined with the hybrid laser-arc welding process made it possible, for the first time ever, to perform single-pass butt welding of materials with a wall thickness of up to 20 mm [5].

Potentialities of the up-to-date fibre-optic lasers for welding pipelines have been intensively studied at a number of research centres of Germany and other



countries. Studies of the highest current importance in this field, the results of which have been published in special literature in the last two years, include those performed by the German Welding Research and Education Centre (Schweisstechnische Lehr- und Versuchsanstalt Halle GmbH – SLV Halle) [6]. The 10 kW fibre-optic laser was used as part of the hybrid process for joining segments of pipes with a wall thickness of 10 mm. Hybrid welding with V-groove and 8 mm high root face was performed by using the 6.5 kW laser at a maximal welding speed of 0.61 m/min. The covering layer of the weld was made by automatic gas-shielded welding. At the Structural Materials Research Centre (CSM, Rome, Italy) the circumferential welds on 36 mm diameter pipes with a wall thickness of 16 mm were made by using the process of laser and hybrid laser-arc welding in two passes [7]. In this case, the point is a roll butt welded joint, which was made in flat position by rotating a pipe. The Yb:SiO₂-laser with an output power of 10 kW (IPG Company) was used as a laser radiation source. The arc power supply was the ESAB welding inverter Aristo MIG 500 operating at a maximal current of 500 A. The first pass with the V-groove and 5 mm root face was made only by laser welding using the 10 kW laser unit. This provided filling of the groove only to half of the pipe wall thickness. Remaining 8 mm were filled with the second pass made by hybrid laser-arc welding. The welding speed in making both passes was 1 m/min. Study [8] reports the field test results on hybrid welding of 610 mm diameter pipes. The 4.4 kW solid-state Nd:YAG-laser combined with the process of automatic metal-arc welding was used to make the root pass of a multilayer orbital U-groove weld. At a root face 4 mm high, the semi-orbital welding process can be implemented, starting from the flat position to the overhead one at a speed of 1.8 m/min.

Within the frames of this study, the authors planned to try out the fibre-optic Yb-laser with an output power of 10 kW, which is used to make the root passes of circumferential joints. However, by the time of the publication only a number of experiments on flat samples with the U-groove and 4–7 mm root face had been performed to investigate the penetration shape and select the welding parameters. Study [9] discusses a variant of using the 10 kW disk laser for hybrid welding of pipes with a diameter of 30 mm or more. The results presented concern flat position welding of the 10.4 mm thick flat samples of pipe steel X80. The V-groove with a 6 mm root face and 60° opening angle was filled up in two passes: the first pass was made by hybrid laser-arc welding using the 9 kW laser at a speed of 2 m/min, and the second one – by automatic metal-arc welding at a speed of 1 m/min. The authors of the said study also mention optimisation of the hybrid process on the circumferential welds.

The above literature data give a general idea of the state-of-the-art in development of hybrid laser-arc welding for large-diameter thick-walled pipelines. It can be concluded on their basis that no scientifically grounded results required for practical application of the hybrid laser-arc welding processes, which could provide high reliability and quality of the circumferential joints on pipes, are available so far. The results discussed apply to the pipes about 10 mm thick, which are usually joined by the multilayer welding technology. Potential of the modern lasers, which can provide deeper penetration of a material, is underutilised so far. Partly, this can be explained by the fact that power of the lasers employed is limited to 10 kW, and single-pass welding of the pipes with a wall thickness of 16 mm or more, which could be interesting in terms of cost effectiveness, is unfeasible. Moreover, no quantitative results of investigation into reliability of the welded joints on pipes made by hybrid laser-arc welding are available, the causes of hot cracking have not been studied to a sufficient degree, and no recommendations for prevention of hot cracking have been worked out.

In collaboration with a number of companies representing the industry, and with a support provided by the German Federal Ministry of Education and Research, BAM is active in studies of the orbital hybrid welding process by using the 20 kW fibre-optic laser. Utilisation of laser systems with a power of 15 kW or more is attractive for construction of large-diameter thick-walled pipelines, as lasers of the said power can provide such a penetration depth that allows achievement of a substantial economic benefit due to application of this equipment. This is associated, first of all, with modification of the groove for welding, so that the quantity of passes and, hence, consumption of filler material can be substantially reduced. As shown by comparison, consumption of welding wire for joining the 1020 mm diameter pipes with a wall thickness of 20 mm can be cut down by a factor of 4 owing to the use of the hybrid laser-arc welding process, compared to twin-arc tandem gas-shielded welding, which by now has been regarded as one of the most efficient methods for welding pipelines, and more than by a factor of 10, compared to manual arc welding. The higher speed of the hybrid laser-arc welding process, compared to the traditional methods, allows reducing the time needed to make one pass, thus leading to a higher rate of laying a line. Despite a comparatively low efficiency of the fibre-optic lasers (approximately 30 %), the power consumed with the hybrid welding method is commensurable with that consumed for the tandem arc welding process, and is an order of magnitude lower than for manual arc welding. Some parameters of the welding methods under consideration are given in Table 1.

As follows from the data presented, hybrid laser-arc welding is a promising resource-saving technology.

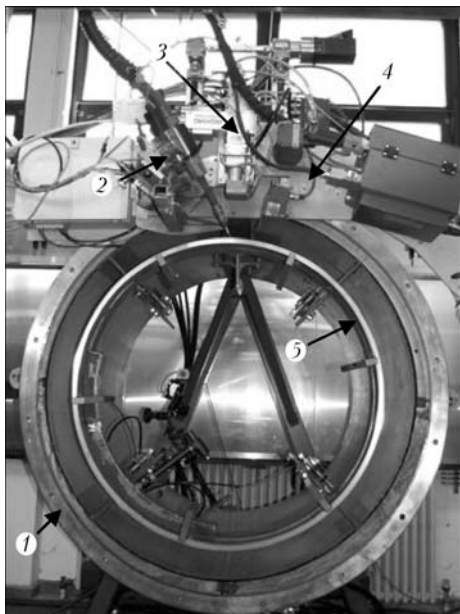


Figure 1. Device for orbital laser-arc welding

However, the necessary condition for successful commercial application of this technology is its correspondence to requirements of the quality standards with regard to permissible defects in the welds, as well as ensuring the required mechanical-technological properties of the welded joints specified in corresponding regulatory documents. One of the goals of the research conducted at BAM is to answer the question whether the welded joints on pipelines made by hybrid laser-arc welding meet the appropriate requirements.

The focus of this study is on two aspects of orbital welding of large-diameter thick-walled pipes. Considered is the feasibility of utilisation of the 20 kW fibre-optic laser to address the above problems, as well as peculiarities of the above methods for welding in different spatial positions. The mechanical-technological properties of the produced welded joints have been analysed, and methods for affecting their values have been suggested in this study.

Equipment and materials. The IPG 20 kW fibre laser YLR-20000 was used as a laser radiation source, and the Cloos automatic pulsed arc welding device of the GLC 603 Quinto type, providing the maximal welding current of 600 A, was used as the arc power supply. The device for orbital laser-arc welding of pipelines (Figure 1), which makes it possible to weld circumferential joints with a diameter of 914 to 1070 mm, was designed and supplied for welding tests by Vietz GmbH, a partner of BAM in the given project.

Table 1. Comparison of pipeline welding methods by an example of making one joint on 40 mm diameter pipes with 20 mm wall thickness

Welding method	Wire consumption, kg/h	Welding time, min	Power consumption, kW
Manual metal-arc welding	6.40	190	30.0
Gas-shielded twin-arc tandem welding	1.90	12	2.7
Hybrid laser-arc welding	0.33–0.44	1.5	2.2

Main components of the device are guide ring 1 and orbital carriage 4, which is moved on the circumference of the ring by using a gearwheel. Position of the laser beam with regard to the joint during welding is adjusted by means of three extra electrically driven axles. The device as a whole is controlled by the Siemens SINUMERIK programmed numerical control system, which provides the ±0.1 mm positioning accuracy. The hybrid welding head consisting of the HighYag optical head 3 with a focal distance of 300 mm and gas-shielded welding head 2 was fixed on the orbital carriage. To conduct welding experiments under laboratory conditions, design of the device was adapted to welding of pipe rings 5 fixed at the guide ring centre. Laser radiation was transported from the laser to optics via an optical fibre with a core diameter of 200 µm. Diameter of the laser beam in the focal plane was 0.5 mm. Some experiments were carried out by using scanning optics. In this case, diameter of the focal spot was 0.42 mm. 120 mm wide rings cut from the 914 mm diameter pipes with a wall thickness of 15 and 16 mm were used as samples for welding.

The pipes were made from steels X56 and X65, according to the API 5L classification. Approximate analogues of these steels are Russian steels K52 and K56, which correspond to steels L360MB and L450MB (EN 10208-2). The materials investigated are characterised by a low content of carbon (about 0.09 % C). The contents of sulphur and phosphorus also were within the permissible ranges for the laser welding process [10]. Chemical compositions of the materials investigated are given in Table 2.

High values of yield stress of steels X56 and X65, combined with good impact toughness, are achieved due to controlled rolling of plates (strips). Mechanical properties of the steels under investigation are given in Table 3.

Table 2. Chemical compositions (wt.%) of investigated materials

Strength class of steel	C	Si	Mn	P	S	Cr	Ni	Nb	Cu	Al	Mo	V	Ti	Fe
X56	0.07	0.03	1.33	0.008	0.001	0.03	0.04	0.05	0.02	0.04	0.02	<0.01	0.02	Base
X65	0.09	0.36	1.57	0.011	0.001	0.03	0.05	0.04	0.02	0.04	0.01	<0.01	0.02	Same



The filler was 1.2 mm diameter welding wire G3Si1, according to DIN EN 440. Gas mixture ARCAL 21, consisting of 92 % Ar and 8 % carbon dioxide (M21 according to DIN EN 439) was used as a shielding gas. Argon (Ar 4.6) was utilised to shield the weld root. The hybrid welding process was implemented with the leading arc, deepening of beam focus Δz to 4 mm, and angle of inclination of the torch to the laser beam axis equal to 25°. Distance between the points of incidence of the welding wire and laser beam on the workpiece surface was 3 to 4 mm. Prior to welding, two rings were tack welded from inside by using six clips uniformly spaced on the perimeter. Welding was performed by the butt method without groove preparation. The maximal welding gap in some regions of the butt joint was 0.2 mm, and the maximal edge displacement ranged from 0.5 to 1.0 mm.

Semi-orbital welding of circumferential joints.

The rings were downhill welded (from the flat position to the overhead one) to make the circumferential weld in two stages with two fading out regions. In our opinion, at this point it is reasonable to introduce a notion of the semi-orbital process and, to designate separate spatial welding positions, use a change in the tangent inclination angle to the circumference relative to the initial flat position. Therefore, position with the 0° angle (flat position) corresponded to the beginning of welding, and position with the 180° angle (overhead position) corresponded to the end of the process. When welding the second semi-ring, coordinates of the process start and stop points were shifted along the weld to provide its closing. Five sets of welding parameters P were used to make one semi-orbital weld. All operations associated with smooth variation and monitoring of these parameters were carried out by using the Siemens SINUMERIK digital control system. Figure 2 explains the procedure used to weld a semi-ring. Also, it shows strength symbols of process parameters P for different welding positions.

Welding was performed at laser power $P_L = 19$ kW, which was constant for all welding positions, and at average welding speed $v_s = 2$ m/min. The speed was slightly adjusted within ± 0.2 m/min relative to its average value depending on the welding position. The volume of the weld pool formed by fusion of the welding wire had a higher effect on formation of the external surface of the weld. The required penetration shape was provided by corresponding adaptation of welding wire feed speed v_d in transition from one welding position to the other. For example, the flat position is characterised by a high value of welding wire feed speed v_d (about 14 m/min). And it gradually decreases to 9 m/min with distance to the vertical position of 90°. Quality weld formation in the overhead position can be provided at such a volume of the molten metal that does not cause its flowing out from the weld pool. The maximal welding wire feed speed for the overhead position was limited (6 m/min).

Table 3. Mechanical properties of steels X56 and X65 (according to API 5L classification)*

Strength class of steel	Yield stress, MPa	Tensile strength, MPa	Elongation, %	Impact energy at 68 J/cm ² (T = 20 °C)
X56	386	489	25.5	68
X65	450	530	23.5	68

*Minimal values of parameters are given.

When changing the welding position, arc length L_{LB} was adjusted from +5 to -12 % with respect to its nominal value at the preset welding parameters, in addition to adaptation of the wire feed speed. For example, welding in the overhead position was performed with the short arc at a correction factor of -12 %. In this case, forces of the gas- and electrodynamic impact of the arc on the weld pool metal had a positive effect, thus resulting in formation of the quality weld bead. Figure 3 shows macrosections and appearances of some characteristic regions of the semi-orbital welds.

It can be concluded from the character of occurrence of the process that at the correct settings of the main welding parameters (see Figure 2) the weld formation in the positions starting from the flat one (0°) to vertical (90°) is sufficiently stable. Welding was performed at an increased speed of 2.2 m/min, at which no sag of the weld root takes place, and its complete penetration is provided. The welds have a favourable shape of their cross sections with a smooth transition to the base metal, and feature a stable formation of the root with low spattering. However, visual assessment of the weld formation quality showed that the joint region from 50 to 80° is characterised by some sag of the weld front face. Despite

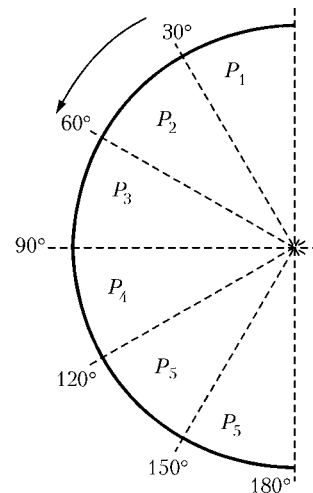


Figure 2. Schematic of semi-orbital laser-arc welding of circumferential weld with 914 mm diameter and 16 mm wall thickness: constant parameters $P_L = 19$ kW and $\Delta z = -4$ mm; variable parameters: P_1 ($v_d = 14$ m/min, $L_{LB} = +5\%$, $v_s = 2.2$ m/min); P_2 ($v_d = 12$ m/min, $L_{LB} = 0\%$, $v_s = 2.2$ m/min); P_3 ($v_d = 9$ m/min, $L_{LB} = -5\%$, $v_s = 2.2$ m/min); P_4 ($v_d = 7$ m/min, $L_{LB} = -10\%$, $v_s = 1.9$ m/min); P_5 ($v_d = 6$ m/min, $L_{LB} = -12\%$, $v_s = 1.7$ m/min)

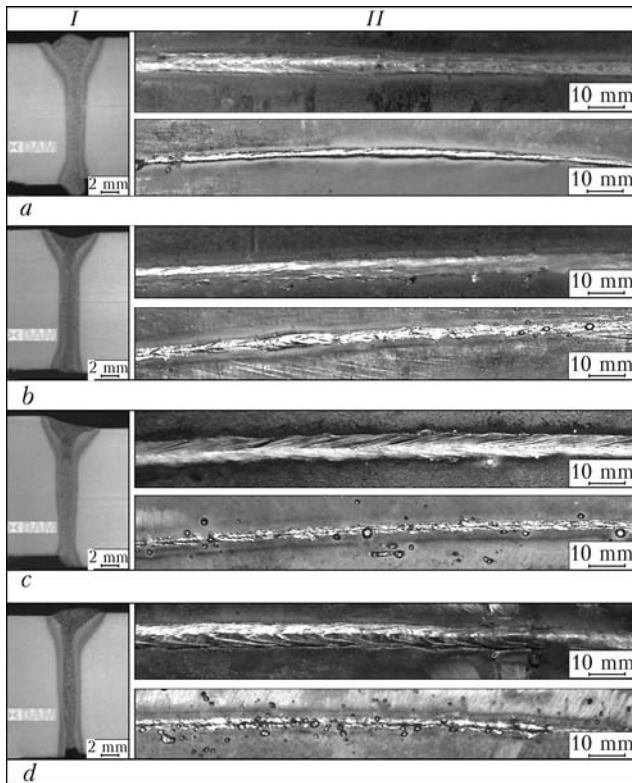


Figure 3. Macrosections (I) and appearance of the hybrid laser-arc weld (II) made on X65 steel pipe with 914 mm external diameter and 16 mm wall thickness: *a* – 0° angle ($v_d = 14$ m/min, $v_s = 2.2$ m/min, $L_{LB} = +5\%$, $I_a = 364$ A, $U_a = 35.5$ V); *b* – 60° ($v_d = 10$ m/min, $v_s = 2.2$ m/min, $L_{LB} = -5\%$, $I_a = 245$ A, $U_a = 28.9$ V); *c* – 120° ($v_d = 7$ m/min, $v_s = 1.9$ m/min, $L_{LB} = -10\%$, $I_a = 180$ A, $U_a = 22$ V); *d* – 180° ($v_d = 6$ m/min, $v_s = 1.8$ m/min, $L_{LB} = -12\%$, $I_a = 174$ A, $U_a = 21.5$ V)

the fact that the sag is insignificant, deposition of a covering layer will probably be required to form the weld reinforcement in the given region.

High sensitivity of the process to the weld pool volume was noted in transition to the 90° position. Even an insignificant excess of some critical value of the wire feed speed (9 m/min at an angle of 90°) led to spreading of metal over both sides of the weld. The process in this case occurred with increased spattering, and the reverse side of the weld might have metal rolls and partial penetration.

While approaching the 120° position, the heat input of the hybrid process decreased together with decrease in the welding wire feed speed to 7 m/min, thus leading to growth of the probability of lack of penetration of the weld root. Complete penetration with satisfactory formation of the weld root was achieved in this position at a simultaneous decrease of the welding speed to 1.9 m/min.

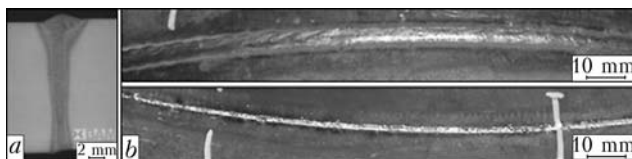


Figure 4. Macrosection (a) and appearance (b) of the overhead hybrid laser-arc weld made by using scanning optics and forming gas: $P_L = 19$ kW, $v_d = 6$ m/min, $v_s = 1.8$ m/min, $L_{LB} = -12\%$, $I_a = 174$ A, $U_a = 21.5$ V

In welding in the overhead position, the sound bead with a small reinforcement was formed at a process speed of 1.7 m/min starting approximately from 120° and to 180°. In this region of the weld, it was very difficult to provide acceptable formation of the weld root. In this position, the critical problem was the absence of fusion on the reverse, upward-looking side of the weld. On the one hand, this defect was caused by shortage of molten metal in the root zone of the weld because of its sagging under the effect of gravity and spattering. On the other hand, high sensitivity of the process to the accuracy of positioning of the welding head relative to the joint also involved a problem. For example, shifting the laser beam even to 0.3 mm led to one-sided melting of the edges and, as a result, to the absence of fusion in the root zone of the hybrid weld. Variation of the main welding parameters had almost no effect on this defect (constant parameters $P_L = 19$ kW and $\Delta z = -4$ mm).

Encouraging results were obtained with the scanning optics of Company «HighYag», which provides the possibility of linearly oscillating the laser beam in a direction normal to the welding direction at maximal amplitude of 13 mm and frequency of up to 1 kHz. The scanning optics was applied to stabilise the process in oscillation of the laser beam and increase cross section of the weld in order to ensure better coverage of the edges and their fusion. Reproducible results on satisfactory formation of the weld root in the overhead position were obtained at scanning with the 0.7 mm amplitude and 200 Hz frequency. These settings of the scanner provided complete penetration with no need to adapt other welding parameters. The pure argon gas was used to improve the quality of formation of the weld root. The gas was fed from the reverse side of the weld by using a specially made pool deposited on the joint and copying the internal contour of the parts welded. Macrosection and appearance of the overhead weld made by using the scanning optics and forming gas are shown in Figure 4.

We investigated the capabilities of the scanning optics, including for determination of the maximal

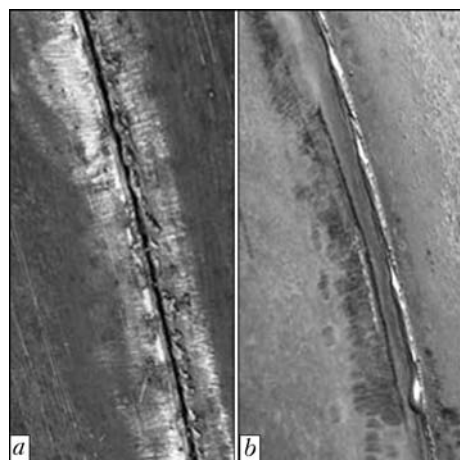


Figure 5. Defects in the weld root (a), and repair weld (b)



Figure 6. Sample made by semi-orbital hybrid welding

gap in the joint, which could provide reliable fusion of the edges [11]. As proved by a series of experiments conducted on 16 mm thick flat samples of steel X65, the stable process without fusion defects can be achieved at a maximal gap of 0.7 mm, with the conventional optics this gap being approximately 0.3 mm. The maximum permissible edge displacement is about 2 mm. The above tolerances apply only to the flat welding position, and it will be necessary to conduct a number of experiments to determine values of tolerances for other welding positions.

Some repair welds were tested to estimate the possibility of repairing defects in the hybrid weld. The tests were carried out both in flat position and in vertical position in a region from 60 to 70°. Regions of the circumferential welded joint with defects of the type of lack of fusion in the weld root were welded by the hybrid method over the existing defective weld by using the forming gas. All the repair welds thus made were characterised by formation of the satisfactory quality of the weld root. One of the examples of such a weld made in the vertical position is shown in Figure 5. The tests proved the feasibility of repairing defective regions of the welds by making the second pass. No systematic studies in this area, including in

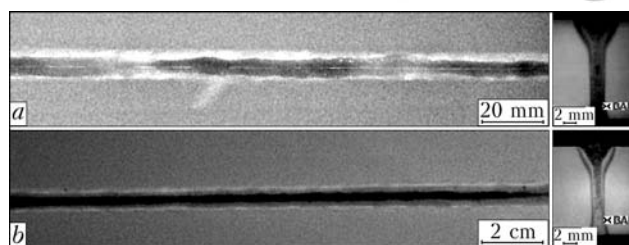


Figure 7. X-ray photos and macrosections of the hybrid welds on steels X65 (a) and X56 (b)

the overhead position, had been conducted by the time of preparation of this article.

The knowledge and experience accumulated as a result of research allowed us to make a series of samples (Figure 6), which were demonstrated at the «Schweißen & Schneiden 2010» Fair in Essen, Germany.

Internal defects and mechanical properties of welded joints. Non-destructive and destructive testing methods were used to assess the quality and mechanical properties of the welds made. Metallographic and X-ray examinations of the welded joints on steel X65 revealed the presence of extended solidification cracks along the central line of the weld in parallel to the weld edges, the cracks locating deep, approximately in the middle of the pipe wall thickness (Figure 7, a). No such defects were detected in the welded joints on steel X56 (Figure 7, b).

The steels under investigation are characterised by complex chemical compositions (see Table 2). Hybrid welding of rings of both steel grades was carried out under identical conditions. One of the probable reasons of increased sensitivity of steel X65 to solidification (hot) cracking is the effect of zonal segregation, as well as the properties of structure of the pipe metal caused by thermomechanical rolling parameters. The structure of steel X65, in contrast to steel X56, is characterised by the presence of pearlitic streakiness (Figure 8), causing high anisotropy of mechanical properties of the rolled stock. At present, we are investigating the issue of the effect of its structure on hot cracking in laser and laser-arc welding.

Microhardness of the weld and HAZ zones was measured according to DIN EN 1043-2 on circumferential test samples of steel X65 with carbon content

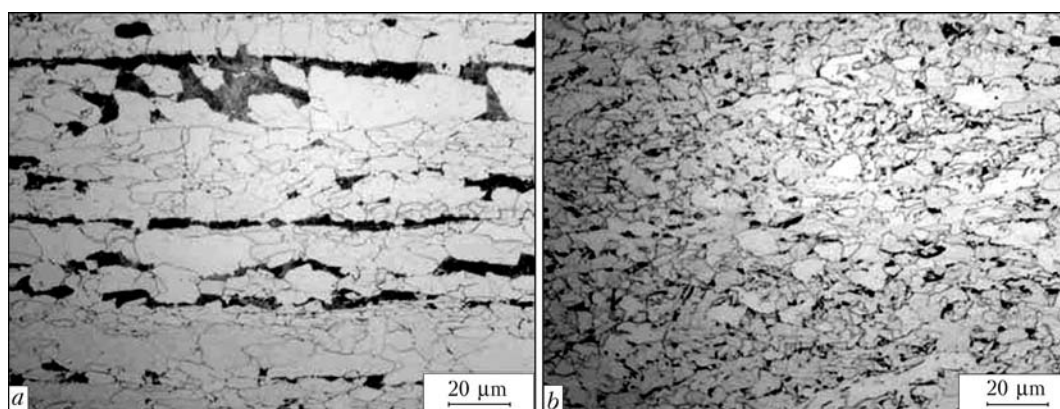


Figure 8. Microstructures of base metal: a – steel X65; b – X56



HV0.5

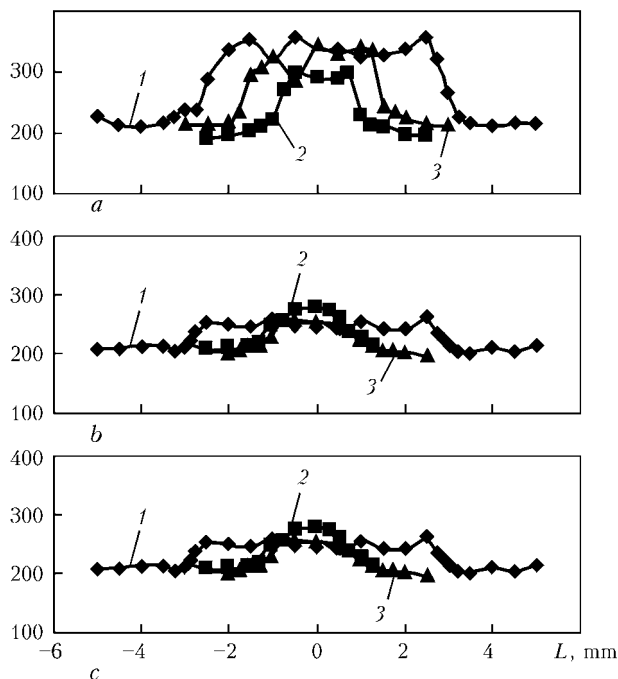


Figure 9. Distribution of microhardness across the welded joints made without preheating (a) and with preheating to 200 (b) and 300 (c) °C: 1–3 – upper, central and lower (root) weld zones; L – distance from the weld centre

of 0.09 wt.%. It was found that the maximal values of microhardness did not meet requirements of the above standard. Therefore, it was decided to use preheating to provide the required values of microhardness. The welding tests with preheating were carried out on segments of rings in the flat position. The parts were heated before welding by using resistance heaters to a temperature of 150 to 350 °C with a step of 50 °C. Thermocouples of the K type (nickel-chromium-nickel), mounted on the reverse side of a sample at a distance of 0.7 mm from the joint, were used to monitor the preheating temperature, as well as to measure the welding thermal cycle. The results of measuring microhardness of the weld metal and HAZ in welding with and without preheating are shown in Figure 9.

It was found that increase in the preheating temperature allows implementing the welding process with a lower laser beam power than that required for welding the «cold» samples. The laser power at a preheating temperature of 350 °C can be reduced to 17 kW. Cooling time $t_{8/5}$ measured in the HAZ (in a temperature range of 800 to 500 °C) is about 1 s in welding without preheating, while in welding with preheating it increases to 16 s. Maximal microhardness of the weld metal in this case is at a level of that of the base metal (HV 220). The values of microhardness achieved with preheating correspond to requirements of the active standards on production of pipes from materials that are not designed for operation in acid environment, e.g. DNV-OS-F101.

When using resistance heaters to preheat the entire circumference of a joint, it is necessary to take into account that this is a time-consuming operation, which

may have a negative effect on the pipeline laying rate. As an alternative, we consider local preheating of the joint edges, e.g. by using an inductor moved together with the welding head. Depending on the configuration and location of the inductor, it is possible to provide extra heat input into the material both immediately prior to welding and after welding. In this case, power of the inductor should provide heating of the workpiece material through its entire thickness at a preset welding speed.

The possibility of welding the circumferential joint with two semi-orbital downhill passes at an average speed of 2 m/min and laser power of 19 kW was successfully demonstrated by an example of the 914 mm diameter pipes with a wall thickness of 16 mm. The overhead welding position (region from 150 to 180°) is most difficult in terms of ensuring the quality formation of the weld root.

Adaptation of the wire feed and welding speeds, and utilisation of the forming gas provide a marked improvement of the root quality in the overhead welding position. The scanning optics proved to be an efficient means for widening tolerances on the gaps in joints, allowing compensation for insignificant errors in positioning of the welding head relative to the joint. The gap established for the 16 mm thick metal, at which the stable welding process without fusion defects is still possible, is 0.7 mm, whereas in conventional welding it is 0.3 mm. Increase in cooling time $t_{8/5}$ from 1 to 16 s was achieved by using preheating, which led to a substantial decrease of microhardness in the heat-affected zone.

These studies are conducted under project MNPQ FK19/07 with the financial support provided by the Federal Ministry of Education and Research of Germany. The authors express gratitude to industrial partners, companies «Vietz GmbH» and «HighYag», for their fruitful cooperation and providing equipment to conduct experiments.

1. Widgery, D.J. (2005) Mechanised welding of pipelines. *Svet-saren – the ESAB welding and cutting journal*, 1, 23–26.
2. Koga, S. et al. (2001) Study on all position electron beam welding of large diameter pipeline joints. Rep. 1, 2. *Welding Int.*, 5, 28–33, 92–99.
3. Gainand, Y. et al. (2000) Laser orbital welding applied to offshore pipe line construction. *Pipeline Techn. Elsevier Sci.*, 2, 327–343.
4. Fujinaga, S. et al. (2005) Development of an all-position YAG laser butt welding process with addition of filler wire. *Welding J.*, 19, 441–446.
5. Rethmeier, M. et al. (2009) Laser-hybrid welding of thick plates up to 32 mm using a 20 kW fibre laser. *Transact. of JWRI*, 27(2), 74–79.
6. Neubert, J. et al. (2009) Influence of tolerances to weld formation and quality of laser-GMA-hybrid girth welded pipe joints: IV-1003–09.
7. Fersini, M. et al. (2009) Circumferential welding of gas pipeline pipes using hybrid technology with fibre-delivered laser beam. *Welding Int.*, 23(6), 450–459.
8. Harris Ian, D. et al. (2008) Hybrid laser/gas metal arc welding of high strength steel gas transmission pipelines. In: *Proc. of 7th Int. Pipeline Conf.* (Sept. 29–Oct. 3, 2008, Calgary, Alberta, Canada).
9. Begg, D. et al. (2008) Development of a hybrid laser arc welding system for pipeline construction. *Ibid.*
10. (1996) *Guidelines for approval of CO₂-laser welding in ship hull construction classification societies unified.*
11. Gumenyuk, A. et al. (2009) High power fibre laser welding for pipeline applications. In: *Proc. of 5th Congress on Laser Advanced Materials Processing* (July 2009, Kobe, Japan).



INVESTIGATION OF STRUCTURE AND PHASE COMPOSITION OF ALLOYS BASED ON THE Ti–Zr–Fe SYSTEM

V.F. KHORUNOV¹, S.V. MAKSYMOVA¹ and G.M. ZELINSKAYA²

¹E.O. Paton Electric Welding Institute, NASU, Kiev, Ukraine

²G.V. Kurdjumov Institute for Metal Physics, NASU, Kiev, Ukraine

Melting temperature ranges for alloys of the Ti–Zr–Fe system were investigated, and liquidus surface of the ternary system in 2D and 3D graphic presentations was plotted. The eutectic pit comprising alloys that show promise for development of brazing filler metals was determined. Microstructure and morphological peculiarities of the alloys at different cooling rates were investigated. Filler metals for brazing titanium aluminides were developed on the basis of the investigation results.

Keywords: *brazing, filler metal, eutectic, structure, liquidus temperature, adhesion-active alloys, cooling rate, phase composition*

The basic system that shows promise for development of adhesion-active filler metals for brazing titanium alloys, including titanium aluminides, is the Ti–Zr system, which features formation of a continuous series of solid solutions. Alloying this system with other elements, such as manganese, iron and chromium, allows the melting temperature to be decreased to some extent owing to formation of low-temperature eutectics.

Alloying titanium with iron leads to formation of eutectic on the titanium side at a temperature of 1085 °C [1], while according to other references the temperature of the eutectic is 1100 °C. Solubility of iron in β -titanium is 22 at.%. The Zr–Fe system containing approximately 23 at.% Fe also has the low-temperature eutectic at a temperature of 928 °C between β -Zr and Zr₂Fe. Owing to their acceptable melting temperature range and good wettability, alloys of the Ti–Zr–Fe system are of interest for use as a base to develop filler metals for brazing titanium alloys, including intermetallic alloys. Unfortunately, the states of phase equilibrium in the Ti–Zr–Me ternary systems, which are good candidates for use as a base to develop filler metals, are little investigated so far.

The purpose of this study is to investigate adhesion-active alloys based on the Ti–Zr–Fe system, their melting temperature ranges and peculiarities of their structure formation at different cooling rates.

An experiment was designed to plot the liquidus surface of alloys of the Ti–Zr–Fe system. 36 experimental alloys of the Ti–Zr–Fe system marked by points in the diagram (Figure 1) were melted according to the experimental design. The contents of elements in the alloys were varied within the following ranges, at.%: 8.25–71.75 Zr, 6.0–79.75 Fe, and 4.0–76.75 Ti. Figure 1 also shows the binary diagrams according to [2].

Melting temperatures were determined by using differential thermal analyser VDTA-8M3 in BeO crucibles at a heating rate equal to 40 °C/min. The liquidus surface of the Ti–Zr–Fe ternary system* (Figure 2) was plotted by the experimental design simplex-lattice method [3–5], which is used to plot the liquidus surfaces of ternary systems bounded by two binary systems of the eutectic type and one system with a continuous series of solid solutions, as well as by using literature and experimental data (melting temperature range).

The eutectic pit can be seen on the 3D liquidus surface. The pit comprises eutectics with a minimal melting temperature, which is acceptable for their use as filler metals. A typical representative of such eutectic alloys is Ti–19Zr–20Fe with a melting temperature range of 940–960 °C, whose structure consists of solid-solution primary dendrites and eutectic (Figure 3, *a*).

Alloying the Ti–19Zr–20Fe alloy with aluminium (up to 11 %) and increasing the amount of zirconium by 8.5 % affect morphological peculiarities of the structure (Figures 3, *b* and 4). The primary phase enriched with zirconium and containing 21.5 % Fe and 15.26 % Al (Figure 4, Table 1, spectrum 1) was found to solidify in the form of dendrites. It is the main phase having a small amount of the Ti–22.5Zr–7.65Al–5.1Fe phase between the dendrites. The finely dispersed phase (Figure 4, Table 1, spectrum 3) with an increased content of zirconium (35.32 %) precipitates in the form of isolated white spot-like inclusions. This alloy differs from the previous compositions in brittleness.

It is a known fact that cooling rate has a high effect on structure formation of alloys, including the eutectic ones [6].

*The calculation procedure was developed by M.O. Karateev and V.V. Voronov.

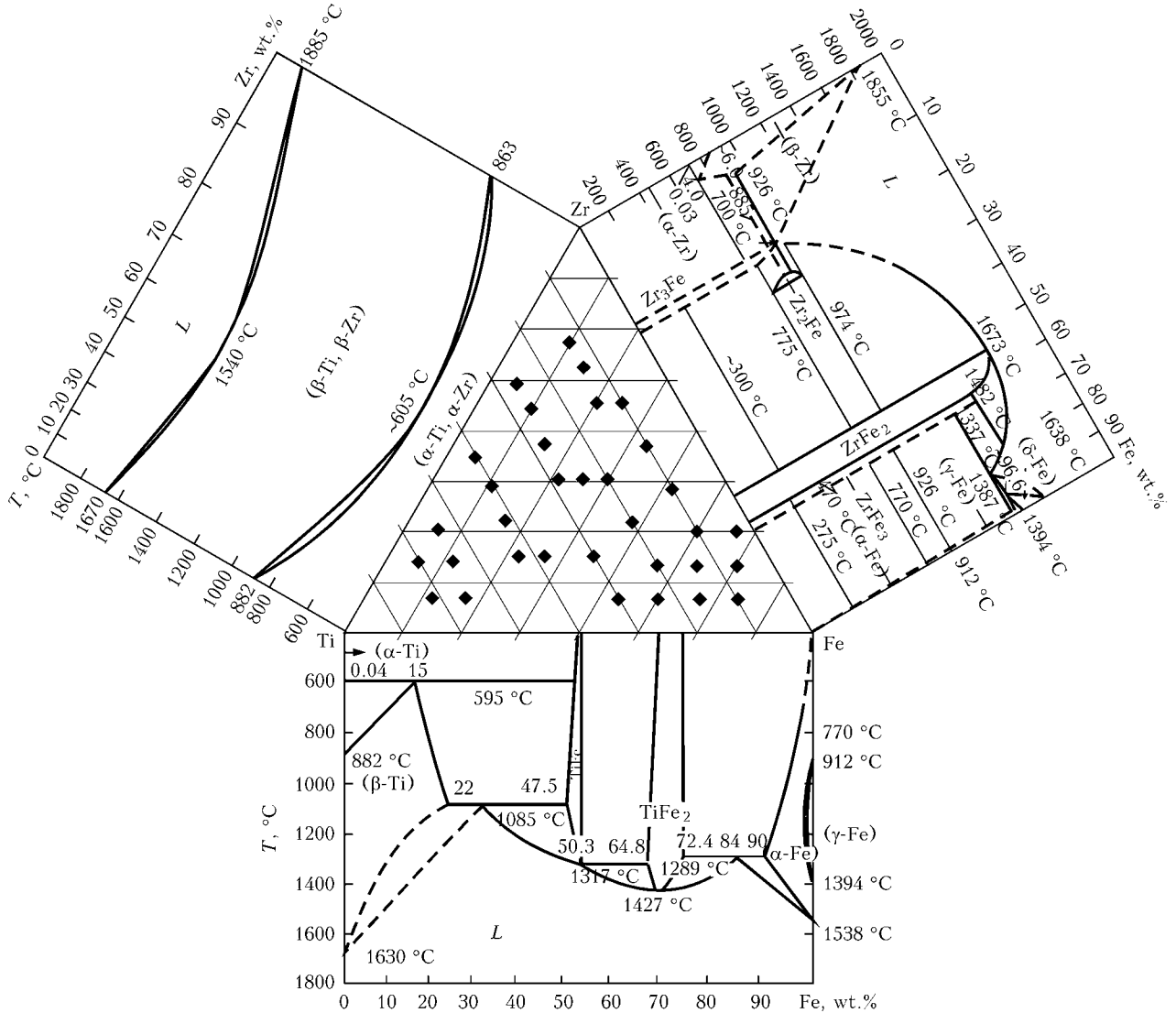


Figure 1. Positions of experimental alloys of the Ti–Zr–Fe system with adjoining binary diagrams

The said alloys were melted in a laboratory electric arc furnace on a copper water-cooled bottom plate.

The method of dispersion from liquid state (using electron beam heating) was used to provide a more homogeneous and finer structure of the alloys under investigation. The main point of the method is as follows. The metal melt is poured from the cold hearth onto a rotating drum mould, where it is built on to provide the required thickness of the skull [7, 8]. Then the drum mould with the skull is imparted a high rotation speed (about 2000 rpm), and the skull surface is melted with a concentrated electron beam. Under the effect of centrifugal forces, the molten metal is

torn away in the form of a flow of liquid fine drops from the skull surface at a tangent to the focal spot of the concentrated electron beam. The flow of liquid drops of the melt, having a small diameter (about 1 mm) and high velocity (about 10 m/s), is directed to the shape-forming surface (mould). There the drops spread into a thin (about 0.1 mm) layer under the effect of the forward pressure and solidify with no formation of the molten pool. Some of them solidify in the form of spherical particles with a diameter of 1–3 mm, and others – in the form of particles of irregular shape.

The structure of the Ti–19Zr–20Fe alloy produced by electron beam remelting consists of rounded, coarse primary crystals of 73.8Ti–15.3Zr–10.9Fe (Figure 5, a) and eutectic, the main phase of which is the (TiZr)₂Fe compound with a high atomic content of iron (31.23 %) (Figure 6, Table 2, spectrum 1). The second component of the eutectic is a phase with a chemical composition that is close to composition of the primary crystals (Figure 6, Table 2, spectrum 2). The degree of dispersion of structural components

Table 1. Chemical composition of calculated alloy Ti–27.5Zr–17.7Fe–11.4Al, at. %

Spectrum number	Al	Ti	Fe	Zr
1	15.26	33.51	21.50	29.73
2	7.65	64.76	5.10	22.50
3	9.39	43.57	11.72	35.32

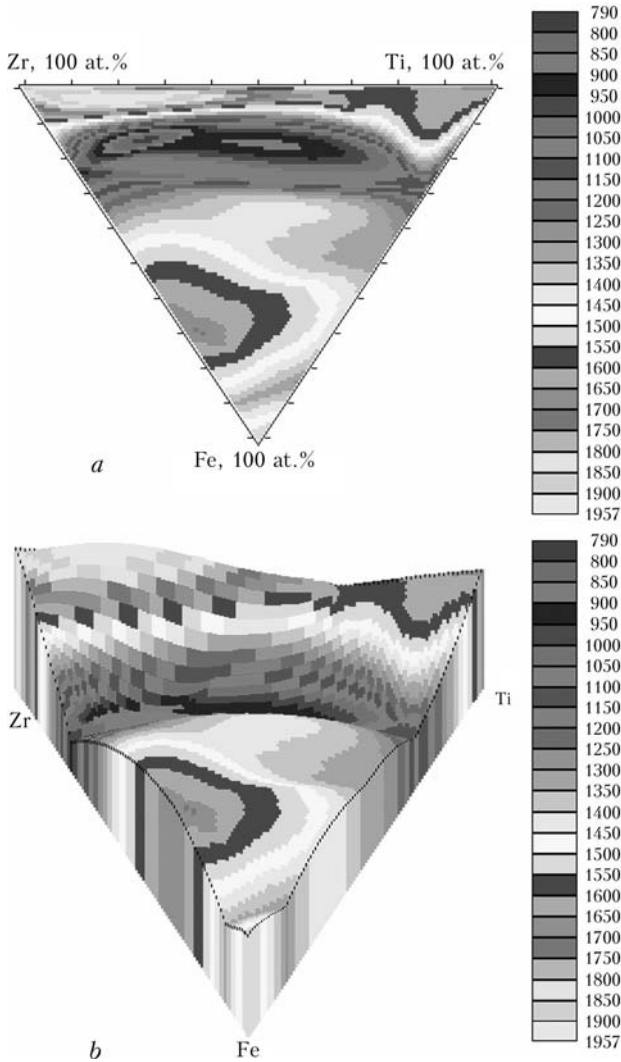


Figure 2. 2D (a) and 3D (b) picture of liquidus surface of alloys of the Ti-Zr-Fe system

grows with increase of the cooling rate (Figure 5, b-f). The cooling rate was determined by calculations in modelling of thermal processes occurring in rapid solidification of the dispersed melts [8, 9].

The structure of the alloy at a cooling rate of 10^2 °C/s differs from the previous one not only in size of the primary dendrites, but also in morphological peculiarities of the eutectic caused by a temperature gradient [6]. The smaller the diameter of spherical particles, the higher is the cooling rate, the smaller

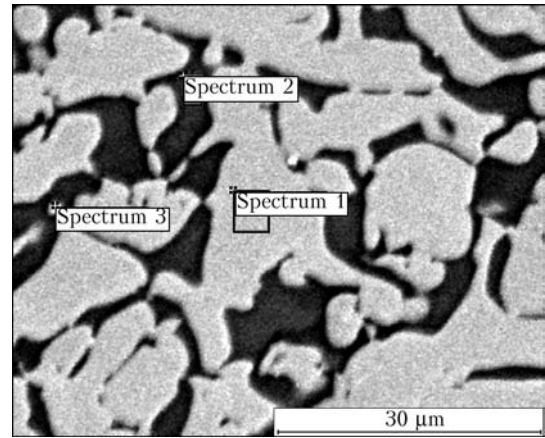


Figure 4. Microstructure and regions of chemical analysis of structural components of calculated alloy Ti-27.5Zr-17.7Fe-11.4Al

is the size of structural components of the eutectic, and the higher is the degree of its dispersion (Figure 5, d, e).

With further increase of the cooling rate to $6 \cdot 10^4$ °C/s, even in solidification of drops in the form of a thin strip, structural components of the alloy continue decreasing in size (Figure 5, f).

The use of super rapid quenching in the high-purity helium atmosphere allowed producing a homogeneous structure and uniform distribution of chemical components of the Ti-19Zr-20Fe filler metal in width of the strip (Figure 7, a-d). The cooling rate of the melt (i.e. the rate at the time point of solidification – formation of the strip) was estimated at $(2-5) \cdot 10^5$ °C/s. The strip can be used as an embedded element for brazing, which is very important, but it has an insufficient ductility. Even if it is in the amorphous state at the time point of solidification, a dramatic decrease of the cooling rate to $(2-5) \cdot 10^3$ °C/s after removing it from the disk may lead to partial crystallisation, and at the outlet it will be in the amorphous-crystalline state.

Results of X-ray diffraction analysis are in good agreement with metallographic examinations (Figures 8 and 9, a). The phases in solutions β -TiZr and $Fe(TiZr)_3$ were detected in X-ray pattern of the rapidly quenched Ti-19Zr-20Fe strip (diffractometer DRON-3, K_α radiation) against a background of the diffuse halo (Figure 8). It is a known fact that the

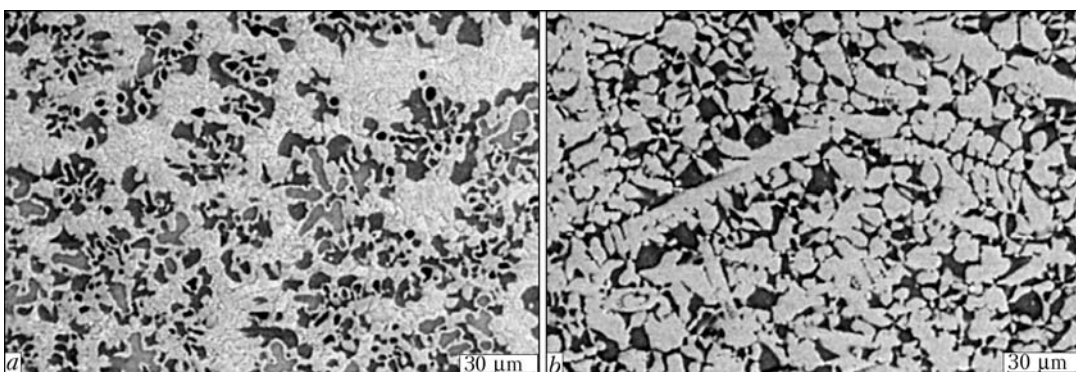


Figure 3. Microstructures of alloys Ti-19Zr-20Fe (a) and Ti-27.5Zr-17.7Fe-11.4Al (b) in as-cast condition

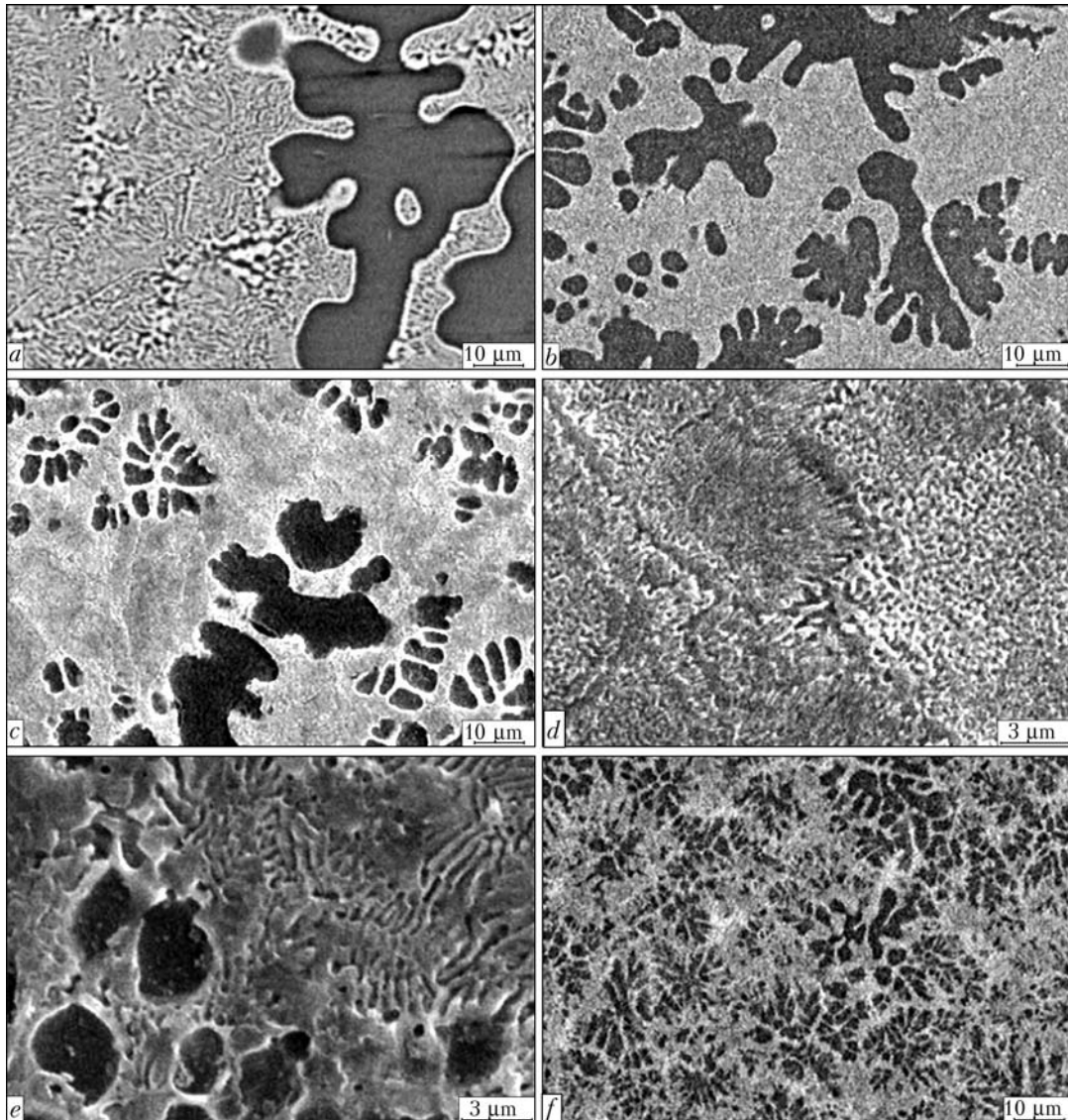


Figure 5. Microstructures of the Ti-19Zr-20Fe alloy produced at different cooling rates: $a - v_{cool} = 2-5$; $b-e - 2 \cdot 10^2$; $f - 6 \cdot 10^4 \text{ } ^\circ\text{C/s}$

structure of the alloys is affected, in addition to the cooling rate, also by the melting parameters, such as time of holding of the molten pool, and its temperature at the time point of solidification (formation of strip). Other structural components may form in production of rapidly quenched strips under other conditions.

It should be noted that the parameter of height of structural factor $i(s)$ related to packing density of

atoms is a very sensitive characteristic, which makes it possible to estimate the presence and content of the crystalline phase in the amorphous strip, this being associated with a number of technological factors taking place in production of amorphous strips from the melt [10]. Height of the structural factor (Figure 10) is a confirmation of the amorphous-crystalline state of the Ti-19Zr-20Fe alloy.

As seen, a typical diffraction pattern in the form of diffuse maxima and a clearly defined effect with a split second maximum, which is always characteristic of amorphous materials [11], is observed for the Ti-27.5Zr-17.7Fe-11.4Al alloy strip (Figure 11). The

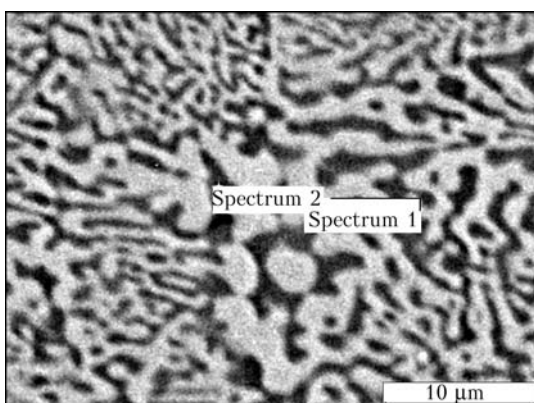


Figure 6. Microstructure and investigated regions of eutectic

Table 2. Chemical composition of eutectic, at.%

Spectrum number	Ti	Fe	Zr
1	43.97	31.23	24.81
2	67.93	15.62	16.45

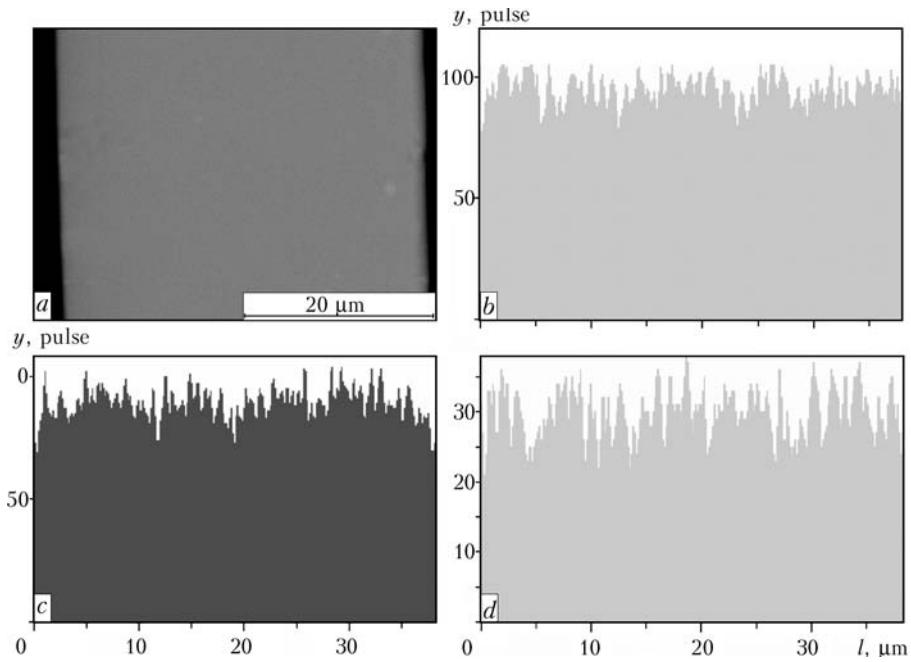


Figure 7. Microstructure of the Ti-19Zr-20Fe rapidly quenched strip (in reflected electrons) (a) and qualitative distribution of titanium (b), zirconium (c) and iron (d) in width of the strip along the scanning line

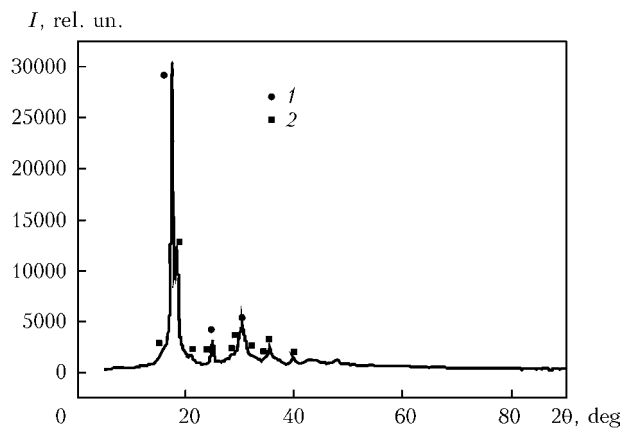


Figure 8. X-ray pattern of the Ti-19Zr-20Fe amorphous-crystalline strip: 1 – solution β -TiZr; 2 – solution $Fe(TiZr)_3$

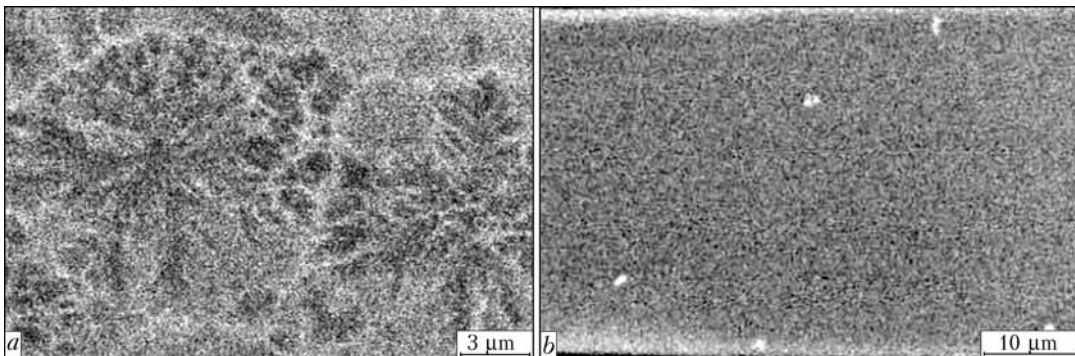


Figure 9. Microstructures of the Ti-19Zr-20Fe (a) and Ti-27.5Zr-17.7Fe-11.4Al (b) rapidly quenched strips

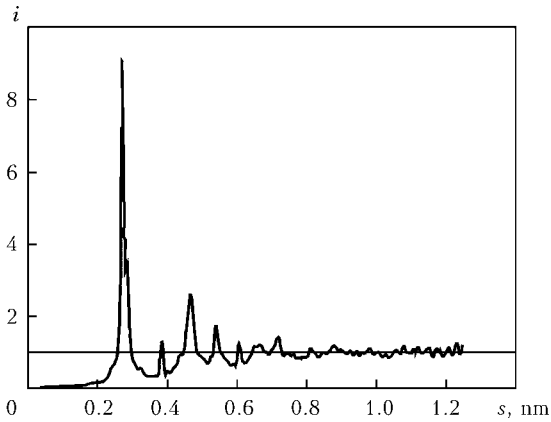


Figure 10. Structural factor of the Ti-19Zr-20Fe amorphous-crystalline strip

rapidly quenched Ti-27.5Zr-17.7Fe-11.4Al alloy strip turned out to be amorphous (Figures 9, *b* and 11).

CONCLUSIONS

1. Alloys based on the Ti-Zr-Fe system were investigated within a wide concentration range. The plotted liquidus surface made it possible to find position of the eutectic pit, on which the alloys with a low melting temperature are located.

2. The Ti-19Zr-20Fe filler metal with a minimal solidus temperature was developed on the basis of the results obtained. It was determined that at a cooling rate increased to 10^2 °C/s the alloy structure consists of primary crystals of the 73.8Ti-15.3Zr-10.9Fe solid solution and eutectic.

3. Increasing the cooling rate (to 10^2 °C/s) of the Ti-19Zr-20Fe alloy in dispersion by electron beam melting leads to approximately 3-4 times decrease in size of its structural components.

4. The use of the super rapid quenching method ($v_{cool} = (2-5) \cdot 10^5$ °C/s) provided a homogeneous strip of the Ti-19Zr-20Fe alloy in the amorphous-crystal-

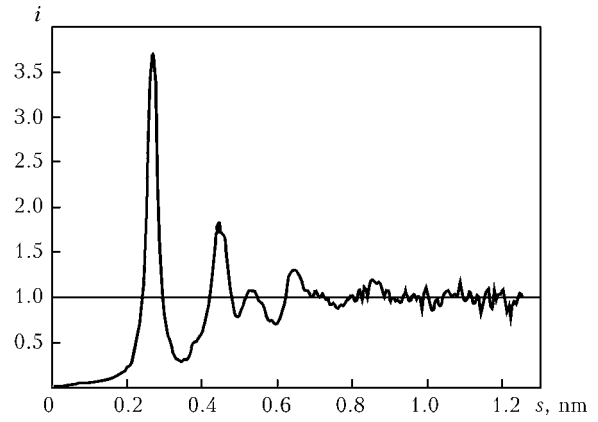


Figure 11. Structural factor of the Ti-27.5Zr-17.7Fe-11.4Al amorphous strip

line state. X-ray phase analysis showed the presence of the β -TiZr solid solution and $Fe(TiZr)_3$ phase.

1. (1997) *Constitutional diagrams of binary metallic systems*: Refer. Book. Vol. 2. Ed. by N.P. Lyakishev. Moscow: Mashinostroenie.
2. Massalski, T.B. (1990) *Binary alloy phase diagrams*. 2nd ed. Ohio: ASM Int., Materials Park.
3. Ganiev, I.N., Zheleznyak, L.V. (1983) Plotting of liquidus surface of the Al-Si-Ge system by the experimental design simplex method. *Metally*, **4**, 184-187.
4. Zedgenidze, I.G. (1976) *Experimental design to study multi-component systems*. Moscow: Nauka.
5. Scheffe, H. (1958) Experiments with mixtures. *J. Roy. Stat. Soc.*, **20(2)**, 334.
6. Eliot, P. (1987) *Control of eutectic solidification*. Moscow: Metallurgiya.
7. Zhuk, G.V., Trigub, N.P. (2002) New method for dispersing the melt in electron beam units and equipment for its realization. *Advances in Electrometallurgy*, **4**, 15-16.
8. Paton, B.E., Trigub, N.P., Kozlitsin, D.A. et al. (1997) *Electron beam melting*. Kiev: Naukova Dumka.
9. Zhuk, G.V., Kozlitsin, D.A., Pap, P.A. (1993) Modelling of thermal processes of quick solidification in casting of dispersed melts. *Problemy Spets. Elektrometallurgii*, **3**, 44-49.
10. Nemoshkalenko, V.V., Romanova, A.V., Iliinsky, F.G. (1987) *Amorphous metallic alloys*. Kiev: Naukova Dumka.
11. Golder, Yu.G. (1978) Metallic glasses. *Tekhnologiya Lyog. Splavov*, **6**, 74-93.



ANALYTICAL STUDY OF CURRENT CONTROLLER OF POWER SOURCE FOR MICROPLASMA WELDING

V.S. GVOZDETSKY

E.O. Paton Electric Welding Institute, NASU, Kiev, Ukraine

An area of stable converter operation as regards arc voltage was determined. Dependence of the converter coefficient current amplification on its efficiency, voltage of power supply unit and arc voltage drop was established. An analytical dependence of arc current on arc voltage drop, voltage of power supply unit and switching frequency was found. The necessity of application of ferrite core in a choke, inductance of which decreases with current increase, was shown. The need for buffer capacitor was substantiated.

Keywords: *microplasma welding, plasmatron, plasma, plasma plume, arc voltage drop, transistor module, snubber, inductance, choke, buffer capacitor, switching frequency*

Investigations of microplasma welding at the E.O. Paton Electric Welding Institute started in the second half of 1960s. The work was conducted in parallel both on fundamental studies of low-amperage arc, and on applied issues of development of technologies and equipment. Features of each welding process required development of not only advanced technologies and arc powering circuits, but also new specialized power sources, taking these features into account.

Large-scale introduction of microplasma welding in all the industrial sectors took place in 1970–1985s. More than 15,000 units of equipment and automatic machines for welding thin metals, including aluminium and its alloys, were manufactured and provided to industry. Equipment and technology were sold to foreign companies of Sweden, Japan, France and other countries.

At present the demand for microplasma welding is much lower. One of the main causes is old-fashioned equipment. It is large-sized, power- and material-consuming, and difficult-to-repair because of outdated components. It cannot be applied for high-speed processes of welding sheet structures from aluminium and its alloys.

Therefore, development of small-sized highly dynamic equipment based on batch-produced inverter power supply units and converters is an urgent and promising task.

Modern industry produces a great variety and number of small-sized inverter power supply units with a high energy intensity (about 536 W/kg), as well as powerful field and bipolar transistors at affordable prices. All this creates the necessary prerequisites for development of a new generation of equipment for microplasma welding with high dynamic properties with analog or numerical control of welding modes.

The purpose of this work is comprehensive analysis of downconverter operation for the case of development of microplasma welding power source, as well

as revealing new capabilities for development of advanced technologies, meeting modern requirements, thus allowing increase of the demand for a simple, reliable and efficient method of welding thin metals.

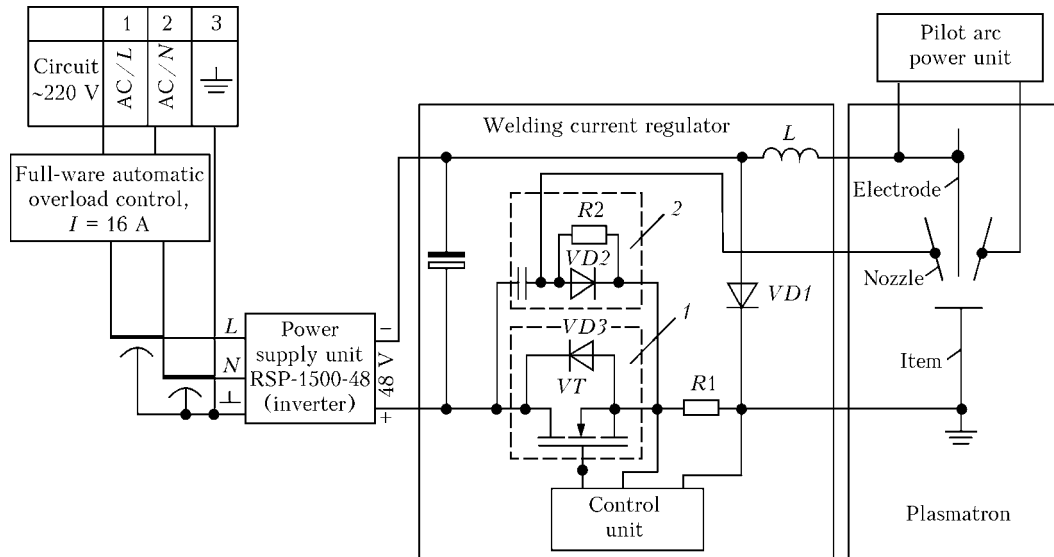
Such a source consists of RSP-1500-48 inverter and chopper. Its diagram is shown in the Figure and is similar to schematics described in works [1, 2], with the difference that the energy accumulated in the snubber capacitor, at transistor unblanking is released not to R_2 , but to the arc through the electrode or plasmatron nozzle.

Study [3] gives analysis of downconverter operation for ohmically capacitive load in linear approximation in the steady-state mode (not at first switching-on) for electronic equipment. A feature of the considered material is the fact that the converter operates for arc load (non-linear element of electric circuit) in a broad range of adjustment of arc current, for instance 5–50 A at different arc voltage drops, dependent on plasmatron nozzle channel, arc length, kind and flow rate of shielding gases, in the range of frequencies safe for hearing.

A detailed and integral description of operation of power source circuit will also be beneficial for welding technologists using microplasma in technological processes of treatment of various materials.

Plasmatron is the microplasma welding tool. Its preparation for operation requires feeding plasma gas (argon), igniting the pilot arc and positioning it so that the plasma plume flowing out of the plasmatron channel, touched the anode – item. Mode of short-circuiting and ignition of the short-circuiting arc is not considered in this work.

At switched on power supply unit and applying control voltage to the gate, transistor is unblanked, power source voltage U_p comes to electrode–item discharge gap, leading to ignition of straight polarity arc. Arc current grows gradually due to self-induction. When it has reached value I_m assigned by control unit, transistor is switched off. Voltage drop on inductance changes polarity, $VD1$ diode is opened, and inductance starts powering the arc. Energy stored in it during unblanked state of transistor, is released into



Block-diagram of a microplasma power source: 1 – transistor module; 2 – snubber

the arc during time τ_0 of transistor blanked state. If τ_0 is long, energy is completely released from inductance. In this case, converter generates individual current pulses with exponential shape of their descending part. As τ_0 decreases, pulses become closer, and a moment comes when there is no pause between them. Further decrease of τ_0 leads to the subsequent pulse being superposed on the descending part of the previous pulse, thus forming lower current level I_0 . Inductance releases only part of its energy. Upper current level I_m is assigned by control unit. The lower τ_0 , the higher I_0 level, i.e. $I_0 = f(\tau_0)$. Difference between I_m and I_0 determines the amplitude of arc current ripple. On the one hand, ripple amplitude should be small, as in this case the strength of sound radiation of the arc decreases, and, on the other hand, decrease of ripple amplitude narrows the range of current adjustment and essentially increases converter switching frequency.

At high values of current I_m the probability of double arc formation in the plasmatron becomes higher, and at high arc current ripple the quality of weld metal protection becomes worse. Fluctuations in the arc column develop in synchronism with current ripple. Arc column now expands at current rise, now contracts at its decrease. These fluctuations are transmitted to the shielding gas zone, leading to air inflow. The same phenomenon is also found in pulsed welding with zero current component between the pulses. At limited power of the power supply unit current amplitude $I_m > I_p$ (nominal value of power source current) can be provided by buffer electrolytic capacitor connected at converter input. Its high capacity allows generating current pulses of a high amplitude, greatly exceeding the load current of power supply unit I_p . During time τ_1 of transistor unblanked state, the arc is practically powered by the capacitor. After transistor blanking, power supply unit further charges the capacitor up to voltage U_p and restores capacitor energy losses. Therefore, maximum current amplitude

$I_m \gg I_p$ is limited not by power supply unit current, but by transistor type. For instance, transistor GA200SA60U passes current of 100 A, while transistor SKM180A allows raising current up to 180 A.

Let us consider the operation of downconverter at direct current with certain assumptions. Arc voltage drop (at $I_a \geq 5$ A) [4] and inductance value are independent on arc current. We will neglect all the electric losses on chopper active and passive elements. These losses require additional consumption of power of the power supply unit. They are described in detail in [2]. Assumptions made do not have any influence on analysis of welding current regulator operation, they just simplify mathematical analysis. During investigations all these losses are allowed for in the form of converter efficiency.

It is known that to generate current I_m power supply unit should spend energy not only for powering the arc, but also for energy accumulation in the inductance. When transistor is blanked, this energy comes back into the circuit and powers the arc with the switched off power supply unit. It gives to the arc as much energy as has accumulated in it.

At transistor switching on the current does not immediately reach its nominal value, as with ballast rheostat, but rises gradually. Self-induction phenomenon consists in inducing additional electromotive force, proportional to the rate of current variation, but with the opposite sign. Therefore, Ohm's law for arc welding can be written as follows:

$$U_p - U_a - LdI/dt = IR$$

$$\text{or } dI/dt + (R/L)I = (U_p - U_a)/L, \tag{1}$$

where U_a is the arc voltage drop; L is the choke inductance; R is the ohmic resistance of the power circuit; I is the current; t is the current time.

Let us consider the regularity of current increase at switched on transistor. Under the impact of power supply unit voltage U_p applied to electrode-item dis-



charge gap, main arc is excited and current starts rising.

Separating variables in equations (1) and performing integration, we have

$$\begin{aligned} -RdI/(U_p - U_a - IR) &= (R/L)dt; \\ U_p - U_a - IR &= A \exp(-Rt/L). \end{aligned} \quad (2)$$

Integration constant A is determined from initial conditions: at $t = 0, I = I_0 > 0$. It is obvious that $A = U_p - U_a - I_0R$. Omitting intermediate computations, we obtain

$$I = (U_p - U_a)(1 - \exp(-Rt/L))/R + I_0 \exp(-Rt/L). \quad (3)$$

To simplify analysis we will use Taylor expansion and will limit ourselves to linear term of the series. In this case, expression (3) becomes

$$I = I_0 + (U_p - U_a - I_0R)t/L. \quad (4)$$

It is seen that current I rises linearly (similar to [3]). When value I_m has been reached, control unit switches off the transistor. Duration of the time of transistor unblanked state during which current I rises from I_0 up to I_m is calculated by the following formula:

$$\tau_1 = (I_m - I_0)L/(U_p - U_a - I_0R). \quad (5)$$

Note that current I is not only arc current, power supply unit current, but also current of energy accumulation in inductance L . At switched off transistor power supply unit is disconnected ($U_p = 0$) and the arc is powered from inductance L through releasing diode $VD1$, bypassing shunt $R1$. Current I starts decreasing from value I_m to I_0 . From equation (2), omitting mathematical computations, we obtain

$$I = I_m - (U_a + I_mR_0)\tau/L. \quad (6)$$

Here $R_0 = R - R_1$.

It is seen that current decreases linearly in time. At $\tau = \tau_0$ equation (6) becomes

$$I_0 = I_m - (U_a + I_mR_0)\tau_0/L. \quad (7)$$

Duration of transistor blanked state is equal to

$$\tau_0 = (I_m - I_0)L/(U_a + I_mR_0) \approx (I_m - I_0)L/U_a. \quad (8)$$

Let us denote ratio τ_1 to τ_0 through β . Taking into account expressions (5) and (7), neglecting terms I_0R and I_mR_0 in view of their smallness compared to U_p and U_a , β becomes

$$\beta \approx U_a/(U_p - U_a). \quad (9)$$

The shape of arc current pulse is close to isosceles triangle, if $2U_a$ is negligibly smaller than U_p . Parameter β is equal to about 0.85 at $U_a = 22$ V and $U_p = 48$ V. If $U_p \gg 2U_a$, then τ_1 becomes shorter, β becomes smaller, and switching frequency increases 1.47 times at $U_p = 60$ V compared to $U_p = 48$ V.

Period of one cycle also decreases $T = (\tau_1 + \tau_0)$. Replacing τ_1 through β , we have

$$T = \tau_0(1 + \beta). \quad (10)$$

Using equations (4)–(8) it is easy to determine average values of arc current I_a , and power supply unit current I_p within one cycle (period T). Omitting mathematical computations, they become

$$I_a = (I_m + I_0)/2, \quad I_p = (I_m + I_0)U_a/(2U_p). \quad (11)$$

Analyzing expression (11), we come to the conclusion that $I_a > I_p$ and it is the greater, the smaller the arc voltage drop and the higher voltage U_p of power supply unit.

In the actual converter power supply unit spends the energy not only for accumulation and powering the arc, but also for electric losses in the chopper. They are the smaller, the higher the quality and the more rational the wiring.

Ratio of power released in the arc, to power consumed from the power supply unit, is the converter efficiency, i.e.

$$(U_a I_a)/(U_p I_p) = \eta, \quad \text{or } I_a/I_p = \eta U_p/U_a. \quad (12)$$

If we connect the ammeters at converter input and output, they will show different values. Ammeter in the arc circuit will show greater current than ammeter in the power supply unit circuit. Ratio of these currents is the current gain factor. Measured current gain factor was equal to 1.64, and calculated converter efficiency $\eta = 0.75$ (at $U_a = 22$ V and $U_p = 48$ V). In [2] it is equal to 0.75–0.81. This discrepancy is possibly accounted for by the fact that the current ratio was measured on a mock-up, and not on the actual converter.

Let us consider one more important characteristic of the converter — ratio of current I_0 to I_m . They are set and regulated by control unit.

Let us denote this ratio as α . From (8) we have

$$1 - \alpha = (U_a/L)(\tau_0/I_m). \quad (13)$$

It is easy to see that α parameter does not depend on current I_m , if τ_0 parameter is linearly related with current I_m by ratio $\tau_0 = \gamma I_m$ (γ is the coefficient of proportionality, $s \cdot A^{-1}$). Then (13) becomes

$$\alpha = 1 - (\gamma U_a/L) \quad (14)$$

and ratio of I_0 to I_m no longer depends on I_m in the entire range of its adjustment. This means that at adjustment of current I_m it is also necessary to adjust parameter τ_0 , connected to it by a linear relationship. Development of such a control unit is the objective of further research.

In analog control circuits not only current I_m is adjusted, but also parameter τ_0 has a fixed value. If the circuit of control by parameter τ_0 is constructed so that at arc current, for instance $I_a = 20$ A, parameter



$\alpha = \alpha_0$, then at adjustment of current $I_a > 20$ A parameter α increases, i.e. $\alpha > \alpha_0$. Difference between currents $I_m - I_0$ decreases $(1 - \alpha) < (1 - \alpha_0)$. This only improves the microplasma welding process and weld quality. At arc currents $I_a < 20$ A, parameter α starts decreasing ($\alpha < \alpha_0$) and difference $I_m - I_0$ increases. With decrease of current I_a current I_0 quickly tends to zero. This is due to the fact that energy accumulated in the inductance, decreases quadratically with decrease of current I_m . This energy, long before repeated unblanking of the transistor, is completely released into the arc and current $I_0 = 0$. Arc runs in the form of individual current pulses, even with pauses between them. Welding process with interruption of arc current continuity makes weld formation difficult, and sometimes impossible. This exactly is the main disadvantage of the control circuit with fixed τ_0 value. Thus, the need for upgrading the current control circuit of the converter as part of the power source for microplasma welding has been substantiated.

It is interesting that even with such a control circuit there exists α_1 value which is independent on current I_m , i.e. has a constant value in the entire range of arc current adjustment. This is the case when difference of currents $I_m - I_0$ multiplied by certain number δ , is equal to arc current, i.e. when $I_a = \delta(1 - \alpha_1)I_t$. Equating the righthand part of this equation to the righthand part of equation (11) and cancelling I_m , we have

$$(1 + \alpha_1)/2 = \delta(1 - \alpha_1) \tag{15}$$

or $\delta = (1 + \alpha_1)/(2(1 - \alpha_1))$.

Using equations (7)–(9) and (15), arc current becomes

$$I_a = \delta U_a(U_p - U_a)/(U_p LF), \tag{16}$$

where F is the switching frequency.

Differentiating I_a for U_a and equating the derivative to zero, we find that current I_a reaches its maximum value I_{max} :

$$I_{max} = \delta U_p/(4LF) \text{ at } U_a = 0.5U_p. \tag{17}$$

At the same time I_{max} is determined, proceeding from maximum power transmitted by arc power supply unit, i.e.

$$I_{max} = \eta W_p/U_a = 2\eta W_p/U_p \text{ at } U_a = 0.5U_p, \tag{18}$$

where W_p is the power of power supply unit.

Equating righthand parts of (17) and (18), we find

$$\delta = 8\eta W_p LF/U_p^2. \tag{19}$$

Substituting values of parameters η , U_p , W_p into (19) and making the calculations, we find $\delta = 1.171875$ (at $LF = 2 \cdot 10^{-5} \text{ H} \cdot 1.5 \cdot 10^4 \text{ Hz} = 0.3$). Substituting this value of δ into (15), we calculate $\alpha_1 = 0.4$.

From (11) we calculate $I_a = 0.7I_m$. We get the same value of arc current I_a from difference $\delta(I_m - I_0)$, i.e. we have an identity, and expression (16) becomes

$$I_a = 1.167U_a(U_p - U_a)/(U_p LF) \text{ at } \alpha_1 = 0.4. \tag{20}$$

Stable operation of current regulator with release of choke energy to the arc through diode $VD1$ is possible only at $U_a < 0.5U_p$. At U_a approaching $0.5U_p$ emf of self-induction decreases, and when it becomes smaller than U_a , choke stops releasing the energy to the arc. At transistor unblanking emf is summed up with U_p and the rate of current rise increases approximately 2 times. Emf of self-induction increases by as many times. Under certain circumstances, the process becomes uncontrollable, which is dangerous for the transistor. Thus, the arc length can be changed only in the zone of $U_a < 0.5U_p$.

Equation (20) is interesting, as it allows calculation not only of the range of adjustment of current I_a , but also of frequency range safe for hearing. If we assign constant product $I_a L$, frequency F will no longer depend on current I_a , i.e. converter choke should be made to have a ferrite core, the inductance of which decreases with rise current of I_a .

It is not easy to calculate such a choke not only because magnetic susceptibility of ferrite changes with heating temperature, but also because it has a complex dependence on magnetic field intensity. In such a case it is possible to use an experimental graphic dependence $L = f(I_a)$. This dependence is easily derived, if the choke is loaded by current from a storage battery (for instance, car battery) and current is adjusted by a rheostat, and inductance is measured, for instance, by emittance measuring device E7-15 or UT603 instruments.

Although in mathematical analysis the functions are not graphically assigned, their graphic presentations are often used, as easy visibility and illustrativeness of the graph make it an indispensable auxiliary means of studying the functions. Note that with increase of current I_a inductance of a choke with a ferrite core tends to a constant value in the limit, when ferrite magnetization reaches saturation. If at current $I_a = 50$ A inductance has reached a constant value, for instance $L = 20 \mu\text{H}$, and at current $I_a = 5$ A it is equal to $200 \mu\text{H}$ ($I_a L = 10^{-3}$), current converter will operate at constant frequency of 13.9 kHz in the entire range of current adjustment $I_a = 5-50$ A (at $U_p = 48$ V, $U_a = 22$ V and $\alpha_1 = 0.4$). Proceeding from the fact that F is a constant value, equation (20) can be presented as

$$I_a LF = 1.167U_a(U_p - U_a)/U_p < 13.9. \tag{21}$$

Righthand part of this equation for microplasma welding is a constant value at unchanged arc length $U_a = \text{const}$. At microplasma welding $U_a < 22$ V, depending on selection of shielding gas, arc length [4], as well as plasmatron nozzle channel diameter. Therefore, for this welding process RSP-1500-48 power supply unit with 48 V voltage is quite acceptable, the more so since the upper limit of U_a adjustment reaches 56 V.



It is not difficult to make choke on ferrite experimentally. The smaller the inductance, the smaller its weight and overall dimensions, material and labour costs for its manufacture. Even if the inductance differs only slightly from $I_a L = 10^{-3}$, frequency at arc current adjustment is «floating» a little. The main thing is for it not to leave the zone safe for hearing.

Let us consider the operation of buffer capacitor. Let us assume that the capacitor charged up to voltage U_p , is disconnected from the power supply unit, and the arc is loaded through the converter. The arc runs until the capacitor has discharged to voltage $U_c = 2U_a$.

Amount of energy ΔW_c spent by the capacitor for powering the arc, is written as

$$\Delta W_c = \eta C(U_p^2 - 4U_a^2)/2, \quad (22)$$

where C is the capacitor capacity; η is the converter efficiency.

During period T the arc consumes energy $I_a U_a T$. Dividing ΔW_c by energy consumed by the arc, we will find number of cycles N :

$$N = \eta C(U_p^2 - 4U_a^2)F / (2U_a I_a). \quad (23)$$

Substituting the above values of parameters (U_p , U_a , F , η) and performing calculations for $C = 5.6 \cdot 10^{-3}$ F, we have $N = (8.4, 5.6, 4.2, 2.8)$ at currents $I_a = (50, 75, 100, 150)$ A, respectively. These calculations show that the electrolytic capacitor as part of downconverter is absolutely necessary in case of low-power inverter power supply units. Arc current can 1.5–2 times exceed the load current of the power supply unit.

One power supply unit RSP-1500-48, even at a lower converter efficiency $\eta = 0.75$, transmits 1125 W of power to the arc. For microplasma welding at $U_a = 22$ V arc current is equal to 51 A, and at $U_a = 18$ V current $I_a = 62.5$ A. Current gain factor is equal to 1.62 and 2, respectively. Here current consumed from power supply unit is equal to 31 A, which is equal to 97 % of maximum load current. At inverter connection by the circuit shown in the Figure, with feed-through capacitors it operated in a stable manner for arc equivalent with ballast rheostat for 45 min even with overload by power by 13 %.

Thus, the power supply unit power is the first limiter of arc current. Arc current can be increased 2 times, if two such units are connected in parallel.

Developer envisages parallel operation of the units for a common load. However, not every transistor can switch high arc currents. Second limiter for arc current, namely maximum collector current I_{coll} comes into force here, i.e.

$$I_{coll} \geq I_m = 1.4286I_a \text{ or } I_a \leq 0.7I_{coll}. \quad (24)$$

When GA200SA60 transistor is used in the converter the power source is limited from above by current $I_p = 70$ A, and for transistor SKM180A — by arc current $I_a = 126$ A. Therefore, GA200SA60 transistor is recommended for power source with one power supply unit RSP-1500-48, and SKM180A transistor — for operation of two power supply units in parallel.

CONCLUSIONS

1. A region of stable operation of the converter was established, which is determined by arc voltage drop $U_a < 0.5U_p$.

2. It is shown analytically that a converter with inductive accumulator is current amplifier. Gain factor is directly proportional to product of ηU_p and inversely proportional to arc voltage drop.

3. Inductance of a choke with a ferrite core decreases with current rise and tends to a constant value, when core magnetization reaches saturation. Such a choke ensures a smooth adjustment of arc current and maintains the frequency in the selected range, if $LI_a \approx \text{const}$.

4. Dependence of arc current on voltage drop across it, power supply unit voltage, choke inductance and frequency, was determined allowing calculation of the range of arc current adjustment with acceptable ripple amplitude in the frequency range safe for hearing.

5. It is shown that it is possible to develop a modern small-sized power-intensive highly-dynamic power source for microplasma welding for arc voltage drop $U_a < 0.5U_p$ on the basis of batch-produced inverter power supply units and downconverter.

1. Korotynsky, A.E., Makhlin, N.M., Bogdanovsky, V.A. (2002) About design of electronic controllers of welding current for multistation welding systems. *The Paton Welding J.*, **12**, 16–24.
2. Kunkin, D.D. (2008) System for TIG welding process control of low-thickness steels. *Ibid.*, **12**, 12–14.
3. Pilinsky, V.V. (1985) *Source of secondary power supply with transformerless output for electronics*. Kiev: KPI.
4. (1979) *Microplasma welding*. Ed. by B.E. Paton. Kiev: Naukova Dumka.



TECHNOLOGICAL STRENGTH AND ANALYSIS OF CAUSES OF WELDABILITY DETERIORATION AND CRACKING

V.V. DERLOMENKO, K.A. YUSHCHENKO, V.S. SAVCHENKO and N.O. CHERVYAKOV

E.O. Paton Electric Welding Institute, NASU, Kiev, Ukraine

Criteria for evaluation of sensitivity to hot and cold cracking by different methods applied to determine technological strength were considered. Dependence of the sensitivity of material to cracking on its degradation was evaluated by the Varestreint-Test method. It is shown that cracking in all cases is caused by degradation of the material in certain temperature conditions and stress-strain state.

Keywords: *weldability, degradation, thermal stress, hot cracks, cold cracks, technological strength, test methods, brittle temperature range*

The heterogeneous «heating ↔ cooling» cyclic temperature effect leads to formation of thermal stresses in a welded joint. The presence of this state, along with probable structural changes of material, local deformation processes and residual stresses, causes substantial deterioration of properties of the material of a joint, i.e. its degradation. Different welding technologies may cause different degradation levels [1], which, according to the data of studies [2, 3], can serve as a criterion for evaluation of weldability. Obviously, if the material of the joint reaches the level of degradation that is higher than the tolerable one, this will lead to irreversible changes in its properties, such as cracking and fracture of the joint, or to its inadmissible performance.

In the last years, researchers have developed various technological strength test methods, which allow evaluating the sensitivity to hot and cold cracking in individual regions of a welded joint, or crack resistance of the entire joint [4–12]. These methods induce a limiting stress-strain state in the weld and joining zone, in which the degradation effects show up in metal. Technological strength takes into account only the material and technology, i.e. it considers only the possibility of formation of a joint, and ignores the factors of fitness of the resulting properties for the specified service conditions. Allowance for the latter factor is a necessary condition for evaluation of weldability [1]. However, it is beyond the scope of this article.

Consider some methods used to evaluate the technological strength during the solidification process (hot cracks) and their criteria.

The technological tests were developed to simulate conditions taking place in fabrication of real welded structures, e.g. multilayer welds in welding and cladding, and circumferential welds in welding or welding-in of pipes. The absence of the crack-type defects

in test samples was indicative of a good weldability of metal, which made it possible to come to welding of real parts and motivate adequacy of the chosen welding technologies and consumables.

The qualitative tests for evaluation of the sensitivity to hot cracking include the following: «circular patch weld» [4], criterion of the presence or absence of macro- or microcracks; test specimen BWRA (British Welding Research Association) with a circumferential multilayer weld for austenitic steels [5], criterion of the presence or absence of cracks in the multilayer weld and HAZ metal; Kihlgren–Lacy specimen [5] – presence or absence of cracks in the multilayer weld; H-specimen [5] – presence or absence of macro- or microcrack in the third test weld; and T-specimen [6] – presence or absence of crack in the test weld.

The «semi-quantitative» tests [4] for evaluation of the sensitivity to hot cracking include the following: Kautz specimen [5] – the sensitivity to hot cracking is considered moderate if the total length of the cracks in the fourth test weld is not in excess of 25 mm; Huxley specimen [5] – depending on a particular case, a criterion can be the average length of a crack in the weld, or the average crack length to section length ratio; cruciform thin-sheet specimen [5] – ratio of the length of the welds with cracks to the total length of the welds, Braun–Boveri specimen [5] – quantity and length of cracks in the welds; segmented-groove circular restraint specimen [7] – total crack length to weld length ratio; Tekken specimen with slots [5], Houldcroft cracking test, circular patch specimen, and U.S. Navy circular-patch specimen [7] – crack length to total weld length percentage ratio.

Alloys and welding consumables are investigated, and welding parameters and conditions are optimised by using the qualitative and semi-quantitative tests. The evaluation criteria are presence or absence of hot cracks and their quantity, and absolute or relative length of cracks. This type of the tests characterises



properties of alloys in terms of their technological strength, but does not allow discriminating its components, such as strength and ductility in the crack zone, shape and temperature limits of the ductility-dip range (BTR, DTR). That is, these tests fix only the fact of the presence of cracks at specified technological parameters in metal investigated, but they do not consider temperature and deformation conditions leading to initiation of cracks.

The quantitative tests for evaluation of the sensitivity to hot cracking include the Bollenrath test [5], where the crack inducing deformation of the weld is adjusted by adjusting the distance between the clamps; Bauman MSTU composite sheet test [5], where the criterion is a minimum width of a sheet at which a crack is not formed; Bauman MSTU test for tubular specimens [5], i.e. length of a region from the tube edge to an insert, at which there are no cracks; IMET (Baikov Institute of Metallurgy and Materials Science) test for a thin-sheet material [5], i.e. maximum length of the weld to notch, at which there are no cracks; MSTU-LTP test [4], i.e. width of a plate at which there are no cracks; Lehigh test [7], maximum depth of slots at which there are no cracks; and U.S. Naval Research Laboratory test [7] with a keyhole slot, i.e. distance from the hole to the weld pool at the moment of crack initiation, or length of a crack. In turn, as a criterion for evaluation of the sensitivity to hot cracking the quantitative tests use design parameters of a joint, which provide its rigidity and serve as a comparative criterion that is proportional to the weld deformation rate [4].

The methods for quantitative evaluation of hot crack resistance of metal with forced deformation of a welded joint include the LTP-1-6 test [8], Ates and Frederiks, IMET-2, Blanshet and Murex tests [5], i.e. critical strain rate V_{cr} leading to crack formation; MSTU test [5], i.e. critical angular strain rate ω leading to crack formation; PVR test [9], Vareststraint-Test and TransVareststraint-Test [10], and strain-to-fracture test [11], i.e. critical strain ε_{cr} leading to crack formation.

It can be assumed on the basis of the above criteria that the main cracking condition of both technological tests and quantitative test methods for determination of hot crack resistance of metal with forced deforma-

tion is achievement of a critical value of ε_{cr} within a certain temperature range in the crack formation region, which, in opinion of the authors of [2, 3], is related to degradation of metal.

Consider the methods for evaluation of cold crack resistance of steels in welding by using the same scheme: cruciform test specimen [4] – presence or absence of cracks; Tekken test specimen [4] – critical cooling rate leading to initiation of crack; circular-deposit test specimens, Cranfield and TsNIIMash [4] – critical quantity of shrinkage beads causing crack; Lehigh test specimen [4] – maximal depth of slots at which there are no cracks; VMEI (Higher Electrical Engineering Institute in Varna), TsNIITS and «circular-patch» test specimens [4] – critical geometric size of a specimen causing its rigidity; LTP MSTU and IMET 4 test specimens [12] – critical stress value to time-to-fracture ratio in hydrogen-containing environment; TRC [12] – critical stress value, below which there is no crack under a load that is normal to or directed along the weld; and incubation period for crack initiation.

As seen from some of the above methods used to evaluate resistance of steels to cold cracking, in welding these evaluation criteria can be similar to those used to evaluate hot cracking:

- qualitative (presence/absence of cracks (yes/no));
- semi-quantitative (relative length of cracks, critical cooling rate, critical initial temperature, and critical quantity of shrinkage weld beads);
- quantitative (critical geometric size of a specimen causing its rigidity, minimal stress at which the cracks are formed, set of welding conditions under which a crack is not formed, and critical strain rate and value at which a crack is formed).

As a rule, the cold crack resistance tests are the delayed fracture evaluation methods. This means that time to crack formation may amount from several minutes to several days or more, depending on the effect of ambient stress and long-time process of diffusion of hydrogen into the zones with an increased stress. Presumably, the main cause of hydrogen-induced cracks is reaching the limiting local concentration of hydrogen due to the presence of strains and stresses of a critical level in regions of a welded joint at a

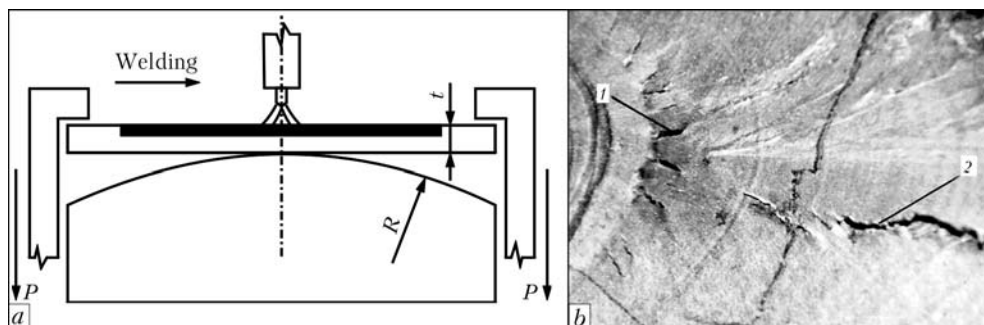


Figure 1. Scheme of dynamic deformation applied by using the Vareststraint-Test method (a), and characteristic cracks formed in welding of alloys with high nickel content (b): 1 – BTR; 2 – DTR

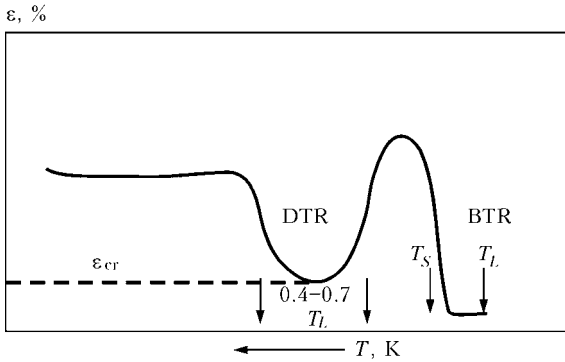


Figure 2. High-temperature ductility of metal with regions containing characteristic types of hot cracks

given temperature, i.e. under conditions of local degradation of metal leading to its embrittlement.

Consider the degradation processes in more detail by an example of high-alloy steels and heat-resistant nickel alloys from the standpoint of their technological strength in fusion arc welding, proceeding from the criterion of formation of hot cracks in the welded joint.

Figure 1 shows the scheme of the Vareststraint-Test method and regions of formation of cracks in regulated bending of the welded joint during welding.

The experimental procedure provides for tungsten-electrode through-penetration welding of a plate using no backing. The initial part of the weld is made without deformation. The pneumatic drive that moves the clamps down is switched on at the time moment when the weld pool is located over the upper point of the mandrel. This process is not stopped at this moment, but is continued for some more time. As a result, metal of the weld pool and all zones both in the weld and HAZ is subjected to a preset deformation, which initiates hot cracking. Strain ϵ of the external layers of a specimen in bending is calculated from formula $\epsilon = \frac{t}{2R} \cdot 100\%$, where t is the thickness of the plate welded, and R is the radius of the mandrel on which the specimen is bent [13].

The cracks initiated at high temperatures (Figure 2), which are close to the solidification tempera-

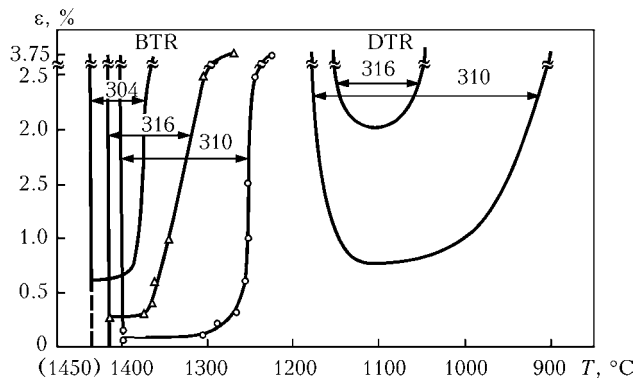


Figure 3. Brittle temperature ranges for welds on austenitic stainless steels of the 304, 310 and 316 types determined by the Vareststraint-Test method

ture, form the so-called high-temperature brittle range (BTR [13]). It extends from liquidus temperature T_L to a region a bit lower than the solidus temperature (approximately by 100–150 °C). The low-temperature brittle range (DTR [13]) is in a temperature range of $(0.4-0.7)T_L$. Critical strain ϵ_{cr} , above which the cracks are formed, is approximately 0.1–1.5 % for different chrome-nickel steels.

Experimental data on evaluation of crack-inducing temperature-deformation conditions are shown in Figures 3 and 4 for a number of welded joints on stainless steels, and for heat-resistant nickel alloys with polycrystalline and single-crystal structure. For instance, steel AISI 304 (analogue of domestic steel 12Kh18N9) is insensitive to cracking (Figure 3), steel AISI 316 (analogue of steel 10Kh17N13M2) has moderate sensitivity, and steel AISI 319 (analogue of steel 20Kh23N18) exhibits an increased sensitivity to cracking [13, 14]. In turn, polycrystalline and single-crystal nickel alloys with the γ -phase content of 50 and 60 %, respectively, are characterised by low crack resistance.

The sensitivity to cracking has two fundamental points, which are worthy of notice.

The first point is a critical level of strain, ϵ_{cr} , above which macrocracks are formed in the weld and HAZ metal at certain temperatures. In our case, this characteristic is one of the weldability criteria, i.e. it is based on evaluation of the sensitivity to

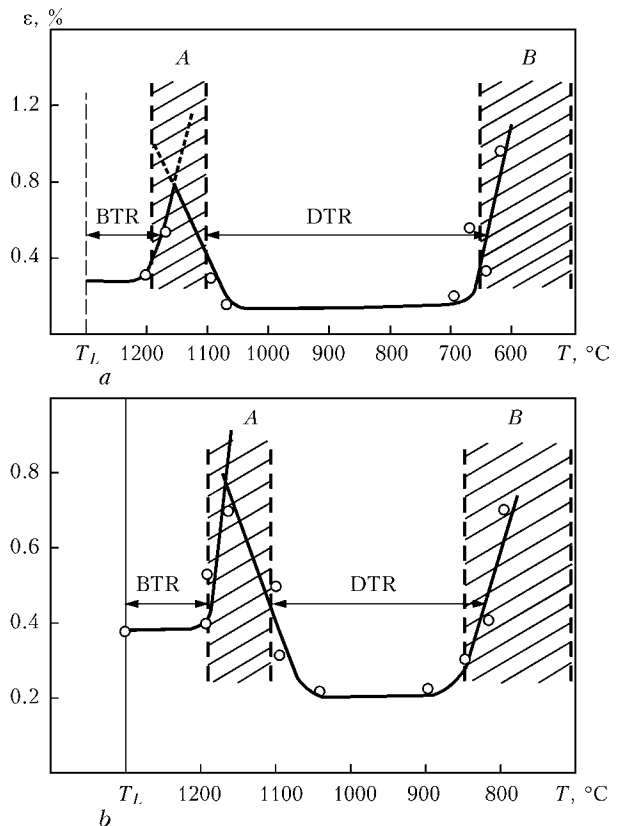


Figure 4. Brittle temperature ranges of welds on polycrystalline alloy with $\gamma' = 50\%$ (a) and single-crystal alloy with $\gamma' = 60\%$ (b)



Characteristics of brittle temperature ranges and critical stresses for cracking determined by TransVarestraint-Test method

Steel or alloy grade	BTR, °C	DTR, °C	ϵ_{cr} , %	
			BTR	DTR
304	1450–1420	–	0.75	–
316	1415–1375	1150–1050	0.25	2.00
310	1400–1300	1175–1000	0.10	0.75
Ni-based, $\gamma' = 50$ %, polycrystal	T_L –1190	1110–670	0.28	0.15
Ni-based, $\gamma' = 60$ %, single crystal	T_L –1190	1105–790	0.38	0.20

cracking. The values of ϵ_{cr} in BTR and DTR are given in the Table.

The lower the value of ϵ_{cr} , the higher is the sensitivity of material to hot cracking, or the lower is the safety factor for crack resistance.

The second point is the character of variations in the $\epsilon_{cr} = f(T)$ curve. As a rule, the temperature curve of ductility has nominal values in the zones between BTR and DTR, as well as from the end of DTR to room temperature (Figure 4, a, b). The zones of nominal ductility are dashed and designated as A and B. Note that in both temperature ranges, i.e. BTR and DTR, where the crack resistance of the weld is much lower, a set of mechanical properties changes towards deterioration. That is, the degradation of metal takes place. This is evidenced by the course of the $\epsilon = f(T)$ curve, angles of its inclination and width of the ductility-dip zone. The welding technology under such conditions can accelerate the degradation of metal by absolute values of the criterial properties, which characterise weldability of steel or alloy of a given chemical composition and production method. Therefore, the numerical indicator of weldability and its absolute value depend on the effect of the welding technology on a corresponding degradation of physical properties of metal, i.e. its sensitivity to cracking. In this case, this is a change of deformability with respect to the initial or stabilised state of a given material.

The causes of formation of cracks can possibly be explained proceeding from comparative analysis of the stress-strain state in the welded joints on high-nickel alloy JS-26, which is sensitive to cracking, and austenitic stainless steel 03Kh20N16AG6, which is resistant to cracking. The explanation was based on evaluation of weldability by the degree of degradation. Current values of longitudinal stresses and plastic strains were determined depending on the temperature at the point located at a distance of 0.5 mm from the fusion line both on the branch of heating to T_{max} and on the branch of cooling to 20° by using experimental data and calculation methods. It follows from the calculation data shown in Figure 5 that the level of tensile longitudinal stresses in nickel alloy reaches about 920 MPa, this corresponding to the yield stress in the ductility-dip temperature range, while the value of plastic strain is approximately 1.75 %, which is

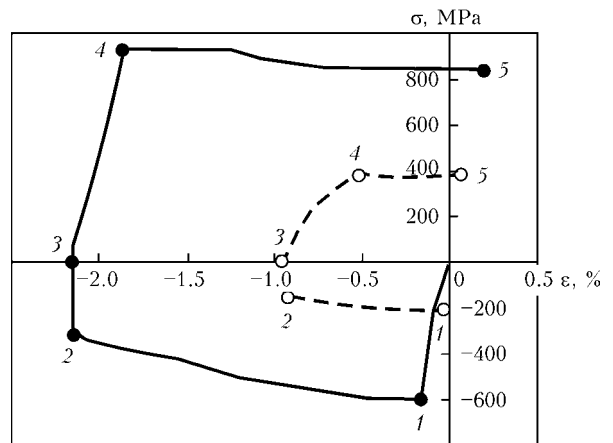


Figure 5. Calculated evolution of stresses and strains in welding of nickel alloy and austenitic steel: points 0–2 – heating, 2–5 – cooling; solid curve – nickel alloy JS-26, dashed curve – steel Kh20N16AG6

almost an order of magnitude higher than $\epsilon'_{cr} \approx 0.15$ %. Therefore, conditions for intensive degradation of metal were thus created, which showed up in formation of cracks in DTR. The level of stresses in austenitic steel was also close to the yield stress and amounted to 390 MPa, and that of plastic strain was about 0.5 % at $\epsilon'_{cr} \approx 4$ %. As the degradation of metal does not reach the level that causes cracking, the steel belongs to those that are easy to weld [15].

Therefore, this proves correlation between the technological strength and weldability, and that they can be evaluated by the degree of degradation of metal. In this case they can be evaluated from strain ϵ , which, when it reaches a critical value, causes cracking of a welded joint at certain temperatures that are characteristic of a welding cycle.

CONCLUSIONS

1. The above methods for determination of technological strength have different criteria. They can be used to investigate a wide range of materials joined and welding technologies. Deterioration of crack resistance and sensitivity to delayed fracture and embrittlement of material up to formation of discontinuities (micro- and macrocracks), which is indicative of occurrence of the processes causing a negative change in properties of the material, are the criteria



that are generally used to evaluate the technological strength (weldability).

2. Any deterioration of properties occurring with time under certain conditions of thermal-load and additional effects on metal, which are characteristic of welding, leads to a limiting state of metal, which causes formation of discontinuities of an inter- or transcrystalline character and degradation.

3. The degradation of properties of metal of the joint should be regarded as a universal criterion for evaluation of the technological strength and, hence, weldability.

1. Yushchenko, K.A., Derlomenko, V.V. (2005) Analysis of modern views on weldability. *The Paton Welding J.*, **1**, 5–9.
2. Yushchenko, K.A., Derlomenko, V.V. (2005) Materials weldability criteria. *Ibid.*, **8**, 68–70.
3. Yushchenko, K.A., Derlomenko, V.V. (2006) Weldability and changes in physical-mechanical properties of welded joints. *Fiziko-Khimich. Mekhanika Materialiv*, **2**, 89–93.
4. (1979) *Welding in machine-building*: Refer. Book. Vol. 3. Moscow: Mashinostroenie.

5. Shorshorov, M.Kh., Erokhin, A.A., Chernyshova, T.A. et al. (1973) *Hot cracks in welding of heat-resistant alloys*. Moscow: Mashinostroenie.
6. (1991) *Welding and materials to be welded*. Vol. 1: Weldability of materials: Refer. Book. Ed. by E.L. Makarov. Moscow: Metallurgiya.
7. Stout, R.D., Dorville, W.D. (1978) *Weldability of steels*. New York: Welding Res. Council.
8. Hrivnak, I. (1984) *Weldability of steels*. Ed. by E.L. Makarov. Moscow: Mashinostroenie.
9. Wilken, K. (1998) Investigation to compare hot cracking tests of externally loaded specimen. *IIW Doc. IX-1923–98*.
10. Savage, W.F., Zuntic, C.D. (1965) The Vareststraint Test. *Welding J.*, **44**(10), 433–442.
11. Nissley, N.E., Lippold, J.C. (2003) Development of the strain-to-fracture test for evaluating ductility-dip cracking in austenitic alloys. *Ibid.*, **82**(12), 355–364.
12. Shorshorov, M.Kh., Chernyshova, T.A., Krasovsky, A.I. (1972) *Weldability tests of metals*. Moscow: Metallurgiya.
13. Kamoi, K., Machora, Y., Ohmosy, Y. (1986) Effect of stacking fault precipitation on hot deformation of austenitic stainless steel. *Transact. of ISIJ*, **26**(2), 159–166.
14. Yushchenko, K.A., Savchenko, V.S., Chervyakov, N.O. et al. (2010) Probable mechanism of cracking of stable-austenitic welds caused by oxygen segregation. *The Paton Welding J.*, **5**, 5–9.
15. Savchenko, V.S., Yushchenko, K.A., Zvjagintseva, A.V. et al. (2007) Investigation of structure and crack formation in welded joints of single crystal Ni-base alloys. *Welding in the World*, **51**(11/12), 76–81.

TREATMENT OF THE SURFACE OF ALUMINIUM-MATRIX COMPOSITE MATERIALS BY CONCENTRATED ENERGY SOURCES

N.V. KOBERNIK¹, G.G. CHERNYSHOV¹, R.S. MIKHEEV² and T.A. CHERNYSHOVA²

¹N.E. Bauman Moscow State Technical University, Moscow, RF

²A.A. Baikov Institute of Metallurgy, RAS, Moscow, RF

Studied was the possibility of modifying surface layers of antifriction aluminium alloy AK9 and aluminium-matrix composite materials reinforced with particles of silicon carbide SiC and aluminium oxide Al₂O₃ in melting of surfaces with arc discharge in magnetic field, as well as with pulsed laser beam. It is shown that surface melting is accompanied by substantial dispersion of the initial surface layer structure. Samples after treatment are characterized by mechanical and tribological properties that are superior to those of the initial material.

Keywords: arc surface melting, pulsed laser radiation, reinforced composite materials, magnetic field, modified surfaces

At present designers are showing interest in aluminium-matrix composite materials (CM) reinforced by refractory ceramic particles. Above-mentioned CM are characterized by high wear resistance and tribological properties, making them promising for application in tribounits [1, 2]. A highly important direction of further work is producing wear-resistant antifriction coatings from these CM on parts operating under extreme conditions. Studies [3–8] show the possibility of producing wear-resistant coatings from such materials by argon-arc surfacing with application of filler rods, the deposited coatings being characterized by service properties close to those of cast CM of the same composition. There is a further possibility of improvement of service properties of surface layer of initial CM and deposited coatings by modifying their

structure, as a change of dimensions of structural elements markedly influences the part wear resistance [9].

In [10, 11] it is proposed to apply microplasma discharges, as well as electron beam and laser radiation for modifying the surface. However, such methods of CM surface treatment are not always cost-effective, because of the low treatment speed, as well as the need for application of complex and expensive equipment. In addition, microplasma treatment in vacuum chambers is related to limitations in product dimensions, and in laser treatment it is also necessary to take into account the reflecting properties of the treated material. A more cost-effective and flexible process of CM surface treatment is arc surface melting with magnetic field impact on the arc and molten pool, allowing high-quality dense surface layers of homogeneous composition to be produced [12].

This work presents the results of investigation of the possibilities of arc surface melting in a magnetic



field, as well as surface melting by pulsed laser radiation for modifying the surface layers of cast samples from aluminium alloy AK9 and aluminium-matrix CM strengthened by particles of silicon carbide SiC and aluminium oxide Al_2O_3 .

At modifying of surface layers of aluminium-matrix CM, reinforced by particles of silicon carbide by surface melting, reinforcing phase degradation due to CM melt overheating is possible [13]. This is manifested in formation of a considerable amount of inter-phase reaction products Al_4C_3 and Al_4SiC_4 , this leading to shape loss as a result of corrosion failure in the presence of water vapours, and lowering of CM strength and rigidity. In [3, 14] it is shown that the processes of reinforcing phase degradation can be suppressed at rational selection of treatment modes, surfacing technique and using alloys of Al-Si system with 11–13 wt.% Si as matrix. Therefore, investigations were performed using CM with AK12M2MgN and AK12 matrix alloys and modes recommended in [3–6, 14].

Experiments on modification of surface layer structure by surface melting were conducted on cast plates of aluminium alloy AK9 (GOST 1583–93) of the following composition, wt. %: 9–11 Si; ≤ 1 Cu; 0.2–0.4 Mg; 0.2–0.5 Mn; ≤ 0.3 Ni; ≤ 0.5 Zn; ≤ 1.3 Fe; Al being the base, and dispersion-strengthened aluminium-matrix CM.

Dispersion-strengthened CM were produced by mechanical mixing of reinforcing filler into the matrix melt. CM matrix were aluminium alloys (GOST 1583–93) AK12M2MgN of the following composition, wt. %: 11–3 Si; 1.5–3.0 Cu; 0.3–0.6 Mn; 0.85–1.35 Mg; < 0.5 Zn; 0.05–1.2 Ti; 0.3–1.3 Ni; < 0.8 Fe; < 0.2 Cr; < 0.1 Sn; and AK12: 10–13 Si; < 0.6 Cu; < 0.5 Mn; < 0.1 Mg; < 0.3 Zn; < 0.7 Fe; < 0.1 Ni; < 0.1 Ti; Al being the balance. Fillers were particles of silicon carbide SiC and aluminium oxide Al_2O_3 . Mean diameter of SiC particles was equal to 14 and 28 μm , and for Al_2O_3 it was 40 μm . Before mixing the powders were soaked in an oven for drying, burning out accidental organic contamination and oxidation of free silicon. Powder mixing into the melt was performed

by pan-type mixer. CM plates were produced by pouring the composite melt into the mould.

Surface melting by arc discharge in magnetic field of surface layer of cast samples was performed by an arc running in argon between tungsten electrode and item at straight polarity direct current in the center of a four-pole magnetic system [12]. Arc current was $I_a = 100$ A, surface melting rate — $v_{s,m} = 14$ m/h, magnetic induction $b = 0.048$ – 0.120 T.

Surface melting by pulsed laser radiation was performed in QUANT-15 unit with pulse power $W_p = 815, 1500$ and 2250 W and degree of defocusing (or distance from beam focus to sample surface) $\Delta f = 1, 3$ and 5 mm, providing heated spot diameter $d_s = 0.3, 0.9$ and 1.5 mm at lens focal distance of 0.5 mm. Pulse time t_p was set at 4 ms, and pulse frequency $F_p = 1$ Hz. Surface melting rate was selected so as to ensure point overlap factor $K_{ov} = S/d_s = 0.5$, where S is the step at superposition of individual spots, argon being used as shielding gas.

Modified surface structure was studied in Leica DMILM optical microscope using image analysis program Qwin, as well as in scanning electron microscopes Leo 430i and FEI Quanta 3D FEG fitted with attachments for X-ray microprobe analysis (XRMPA).

Mechanical properties were determined by measurement of microhardness by depth of deposited metal in Wilson Wolpert 432SVD instrument at the load of 0.5 N, as well as measurement of Brinell hardness in an all-purpose Wilson Wolpert 930 N instrument by indentation of 2.5 mm sphere at 620 N load.

To assess modification effectiveness dry sliding friction tests of as-cast initial samples and those after surface melting by an arc in magnetic field were conducted. Friction was performed in MTU-01 unit (TU 4271-001-29034600–2004) by the following schematic: rotating bushing (counterbody from steel 40Kh with more than *HRC* 45 hardness) over washer (samples from CM with modified surface) at 18 – 60 N load and sliding velocity of 0.39 m/s. Testing included registering the moment of friction and mass change

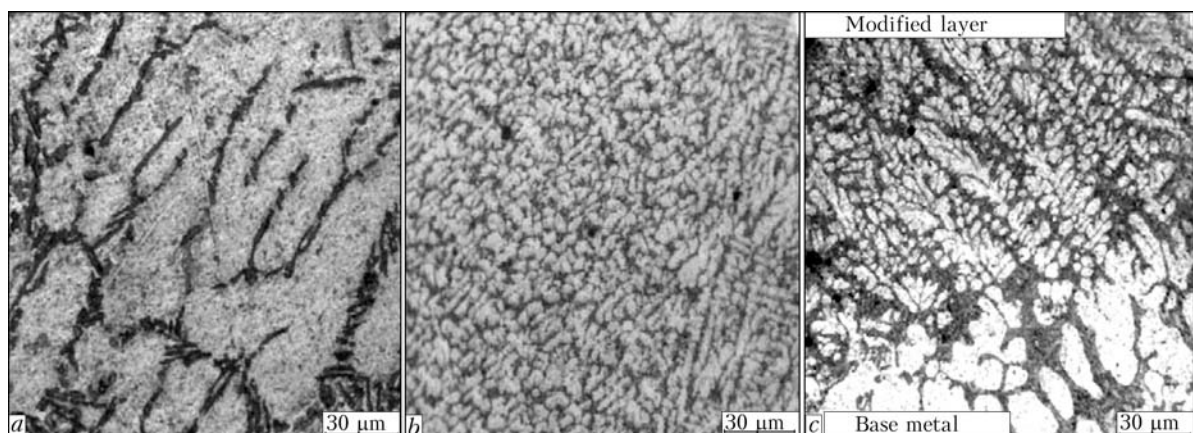


Figure 1. Microstructures of AK9 alloy in the initial (cast) condition (a), of upper part of modified layer (b) and fusion line (c) after treatment by an arc in the magnetic field ($b = 0.048$ T)



by weighing each sample before and after testing with the accuracy of $\pm(0.5 \cdot 10^{-3})$ g. First stage of triboloading of 15 min duration at the load of 18 N and sliding velocity of 0.39 m/s was regarded to be running-in one.

Sample behaviour during dry sliding friction was assessed by bulk intensity of wear I_V , friction coefficient f_{fr} , wear coefficient K and stability coefficient α_{st} . Values of these parameters were determined by the following formulas [15, 16]:

$$I_V = \frac{\Delta m}{\rho L}; \tag{1}$$

$$f_{fr} = \frac{M}{R_m F_1}; \tag{2}$$

$$K = \frac{I_V H}{F_1}; \tag{3}$$

$$\alpha_{st} = \frac{f_m}{f_{max}}, \tag{4}$$

where ρ is the sample metal density, g/mm^3 ; L is the friction path, m ; M is the moment of friction, $N \cdot m$; R_m is the mean radius of the counterbody, mm ; F_1 is the applied load, N ; H is the sample metal hardness, MPa ; f_m , f_{max} are the mean and maximum friction coefficients.

Stability coefficient α_{st} is a dimensionless value and characterizes stability of the process of dry sliding

friction. Wear coefficient K , which is also a dimensionless value, expresses the probability of worn particle separation at friction.

Structure and mechanical properties of surface layers melted by arc discharge in the magnetic field.

Microstructures of samples from AK9 alloy and dispersion-filled CM AK12 + 10 % $Al_2O_{3(40)}$ and AK12M2MgN + 12 % $SiC_{(14)}$ in the initial condition are shown in Figure 1, *a* and Figure 2, *a, d*, respectively. It is seen from the Figures that the cast structure of AK9 alloy consists of coarse cellular-dendritic crystals of $\alpha-Al$ of thickness $\lambda = 30-50 \mu m$ and interdendritic eutectic interlayers. According to XRMPA these interlayers, in addition to $\alpha-Al$ and eutectic silicon also contain nickel, iron and copper aluminides. Thickness λ of $\alpha-Al$ crystals of CM initial (cast) structure is equal to 13-15 μm (AK12 + 10 % $Al_2O_{3(40)}$) and 20-25 μm (AK12M2MgN + 12 % $SiC_{(14)}$), which is somewhat smaller than in AK9 aluminium alloy. This is the consequence of the influence of reinforcing Al_2O_3 and SiC particles, limiting the volumes of melts, in which liquation occurs.

Samples obtained after arc surface melting in a magnetic field are characterized by a sufficiently smooth surface. Influence of magnetic induction on the shape of surface layers, obtained by arc melting under the impact of magnetic field on the arc, was

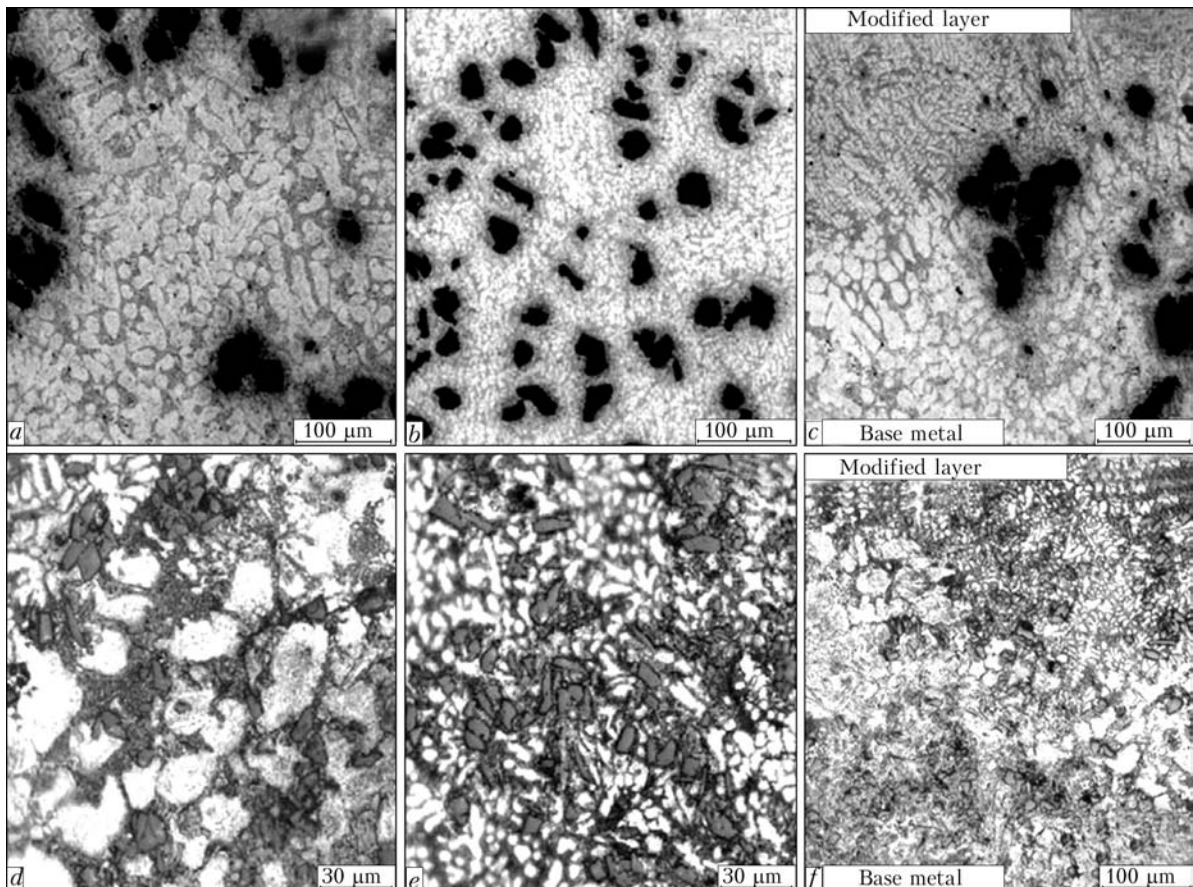


Figure 2. Microstructures of CM AK12 + 10 % $Al_2O_{3(40)}$ (*a-c*) and AK12M2MgN + 12 % $SiC_{(14)}$ (*d-f*) in the initial (cast) condition (*a, d*), of upper part of modified layer (*b, e*) and fusion line (*c, f*) after treatment by an arc in a magnetic field ($I_w = 110$ A; $U_a = = 16$ V; $b = 0.048$ T)



Table 1. Geometrical dimensions of welds made on samples from different materials and at different values of magnetic induction

Sample material	<i>B</i> , mm	<i>h</i> , mm	<i>B</i> , mm	<i>h</i> , mm
	<i>b</i> = 0.048 T		<i>b</i> = 0.120 T	
AK9	7.00	1.20	8.50	0.50
AK12 + 10 % Al ₂ O ₃₍₄₀₎	6.73	1.27	9.27	1.67
AK12M2MgN + 12 % SiC ₍₁₄₎	6.60	2.00	8.07	2.40

studied on transverse macrosections of surface-melted samples. Measurements of geometrical dimensions of welds showed that all the materials are characterized by increase of width *B* and surface melting zone at increase of magnetic induction (Table 1), as a higher degree of arc defocusing is achieved. Change of penetration depth *h* depending on magnetic induction is not so evident, but the tendency to its decrease is preserved.

Microstructures of samples from AK9 alloy after modifying treatment by an arc discharge in the magnetic field are shown in Figure 1, *b*, *c*. The Figures show a considerable dispersion of the initial structure caused by high rates of cooling of the thin layer of molten metal. Parameter λ decreases to 5–7 μm (Figure 1, *b*). Near the fusion line the dispersity of the surface melted layer structure is somewhat lower as a result of partial inheritance of substrate structure at epitaxial solidification, as well as lower initial rate of melt solidification (Figure 1, *c*).

Figure 2, *b*, *c*, *e*, *f* shows microstructures of samples from dispersion-filled CM of AK12 + 10 % Al₂O₃₍₄₀₎ and AK12M2gN + 12 % SiC₍₁₄₎ compositions, respectively. Surface treatment of samples by arc melting with the impact of magnetic field on the arc results in refinement of the initial matrix structure (thickness is equal to 3–4 and 4–5 μm , respectively). Volume fraction and size of reinforcing Al₂O₃ and SiC particles do not change.

SiC particles in treated surface layers of a sample of AK12M2MgN + 12 % SiC₍₁₄₎ CM preserve their initial cleavage faceting, which is indicative of an absence of intensive interphase interaction between filler and matrix melt during arc surface melting (Figure 2, *b*, *e*). In addition, redistribution of reinforcing particles occurs during surface treatment. The high cooling rate, inherent to this technological process, leads to a uniform distribution of reinforcing particles in the matrix (Figure 3).

Table 2. Composition across the depth of treated layer of AK12M2MgN + 12 % SiC₍₁₄₎ CM (XRMPA)

Measured section	Al, wt.% (at.%)	Si, wt.% (at.%)
Base metal	91.58 (91.88)	8.42 (8.12)
Near the fusion line (from modified layer side)	96.30 (96.44)	3.70 (3.56)
Near the surface	83.08 (83.63)	16.92 (16.37)

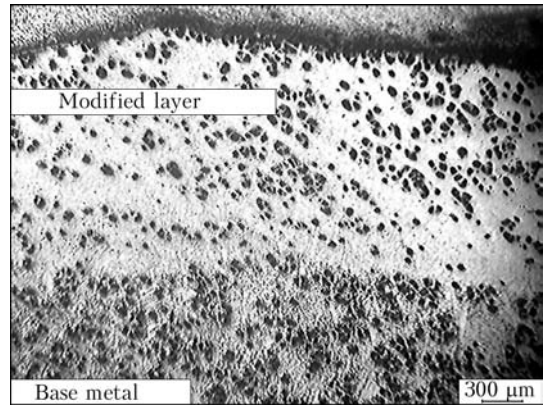


Figure 3. Macrostructure of AK12 + 10 % Al₂O₃₍₄₀₎ CM after treatment by an arc in a magnetic field ($I_w = 110 \text{ A}$; $U_a = 16 \text{ V}$; $b = 0.120 \text{ T}$)

As a result of treatment the composition across the surface layer thickness changes. Near the fusion line silicon content in the layer decreases, and the zone adjacent to the sample surface is noticeably enriched in silicon compared to the initial structure (Table 2). This is caused by liquation characteristic for directional solidification of the surface-melted layer from the fusion line towards the layer surface.

Refinement of matrix structure and increase of uniformity of filler distribution in the surface layers of dispersion-filled CM after modifying treatment leads to increased hardness of surface layers compared to the initial state of AK9 alloy and dispersion-filled CM (Figure 4). Change of magnetic induction values from 0.048 up to 0.120 T practically does not affect the hardness of surface-melted layer.

Modification of the structure of aluminium alloys and CM by surface treatment by arc melting in a magnetic field improves their wear resistance and tribological characteristics. Values of bulk intensity of wear I_v and wear coefficient K , both for AK9 model sample and for dispersion-filled CM decrease significantly, particularly at increase of the load (Figure 5). This may be due to refinement of dimensions of silicon crystals and relative dimensions of sections of aluminium-based solid solution, increasing the resistance to abrasive and adhesion wear of samples [9]. Absence of degradation of reinforce-

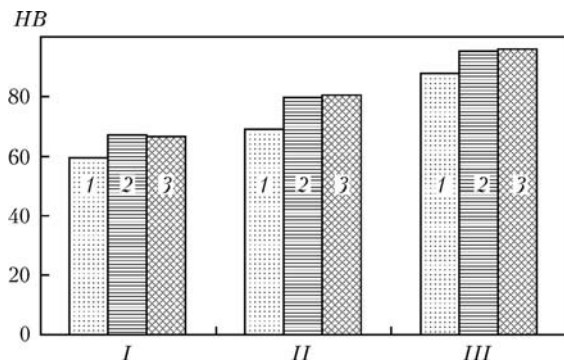


Figure 4. Hardness of samples from AK9 alloy (*I*), AK12 + 10 % Al₂O₃₍₄₀₎ (*II*) and AK12M2MgN + 12 % SiC₍₁₄₎ (*III*) in the initial condition (1) and after treatment by the arc in a magnetic field at *b* = 0.048 (2) and 0.120 (3) T



$I_e \cdot 10^{-3}, \text{mm}^3/\text{m}$

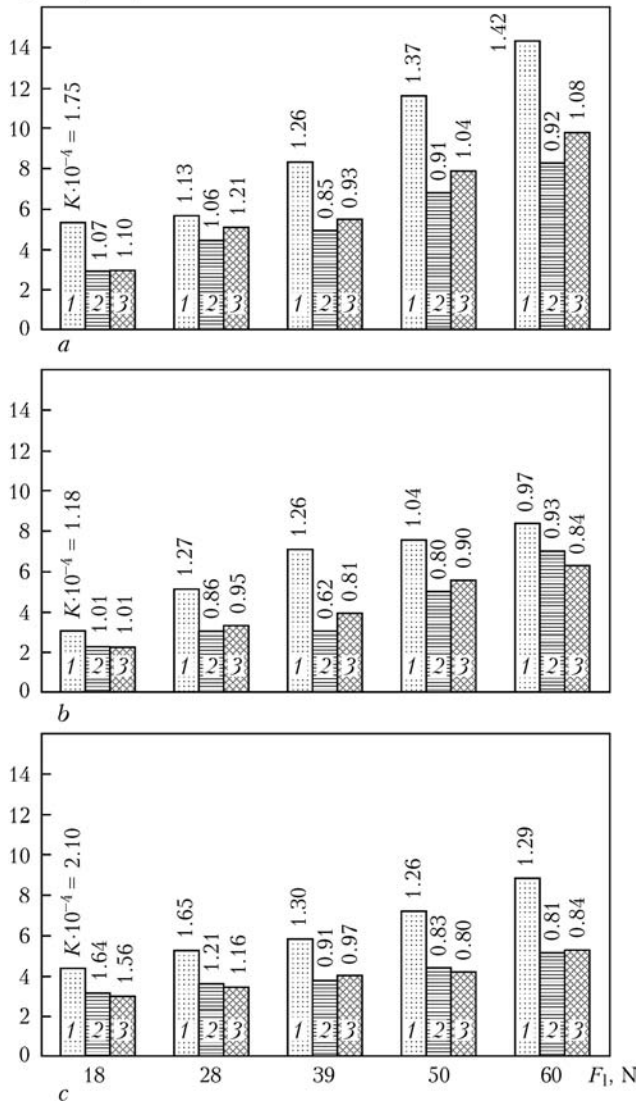


Figure 5. Change of bulk wearing intensity I_e and wear coefficient $K \cdot 10^{-4}$ of samples from AK9 alloy (a), CM AK12 + 10% $\text{Al}_2\text{O}_{3(40)}$ (b) and AK12M2MgN + 12% $\text{SiC}_{(14)}$ (c) depending on load F_1 under the conditions of dry sliding friction: 1 – initial state; 2, 3 – after modification of the surface layer at $b = 0.048$ and 0.120 T

ing particles in the deposited layers of dispersion-filled CM also has an important role.

Normalized friction coefficients of samples ($f_{\text{mod}}/f_{\text{in}}$ is the ratio of friction coefficient of modified sample to friction coefficient of initial sample) depending on the applied load are given in Figure 6. It is seen from the Figure that in the entire range of triboloading modified samples from AK9 model alloy have equal or smaller values of friction coefficient compared to cast samples (Figure 6, a). Modified dispersion-filled CM feature a somewhat higher friction coefficient at the initial stages of testing at up to 39 N load compared to the initial condition. However, at high loads the values of friction coefficients become similar (Figure 6, b, c) that may be related to formation of a transition layer close in composition and dispersity during dry sliding friction process.

During dry sliding friction the subsurface layers are exposed to strong plastic deformation, traces of

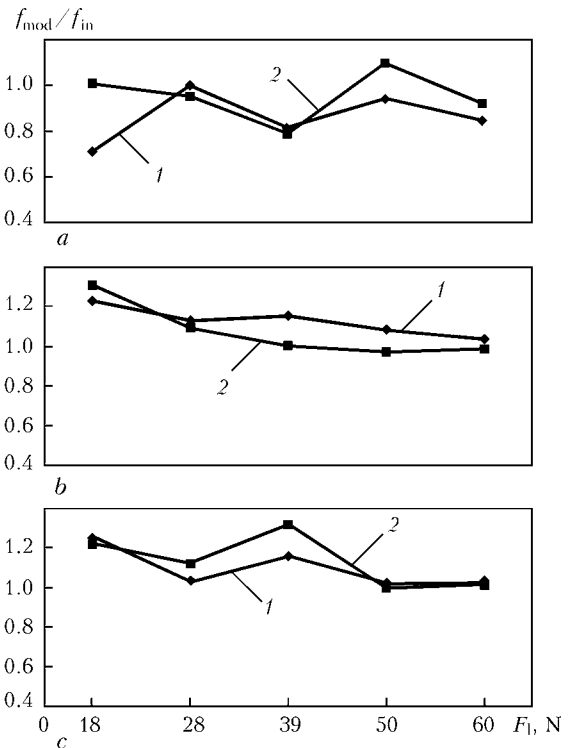


Figure 6. Change of normalised friction coefficient $f_{\text{mod}}/f_{\text{in}}$ of samples of AK9 (a), CM AK12 + 10% $\text{Al}_2\text{O}_{3(40)}$ (b) and AK12M2MgN + 12% $\text{SiC}_{(14)}$ (c) after modifying treatment depending on applied axial load at $b = 0.048$ (1) and 0.120 (2) T

which in the form of rotation of dendrite axes in the sliding direction can be observed on transverse microsections of the samples after friction tests (Figure 7, a). Width of plastic deformation zone of CM cast samples is equal to about $250 \mu\text{m}$, and that of modified samples decreases to $150 \mu\text{m}$. At testing at axial load of 60 N a transition layer formed during friction is clearly visible on contact surfaces of the modified sample. According to XRMPIA it is a mechanical nanostructured mixture of the material of counterbody and tested sample, as well as their oxides (Figure 7, b). Appearance of iron or its oxides can be due to abrasive impact on the counterbody of reinforcing dispersed particles of Al_2O_3 , SiC, as well as silicon crystals in the composition of AK9 and AK12M2MgN alloys. The more finely-dispersed is the microstructure of the sample tested by friction, the more intensive are the processes of nanostructuring in the transition layer, which promotes lowering of friction coefficient and protects the sample from wear.

Initial samples, as well as samples after modifying treatment, are characterized by the coefficient of stability of the process of sliding friction without lubrication close to a unity (Table 3), which is inherent to antifriction materials and is indicative of friction process stability. It is seen that surface melting by an arc in the magnetic field leads to an increase of the coefficient of stability of samples from dispersion-filled CM, its high values (not lower than 0.9) being preserved even at maximum axial loads.

Structure and mechanical properties of surface layers melted by pulsed laser radiation. Surfaces

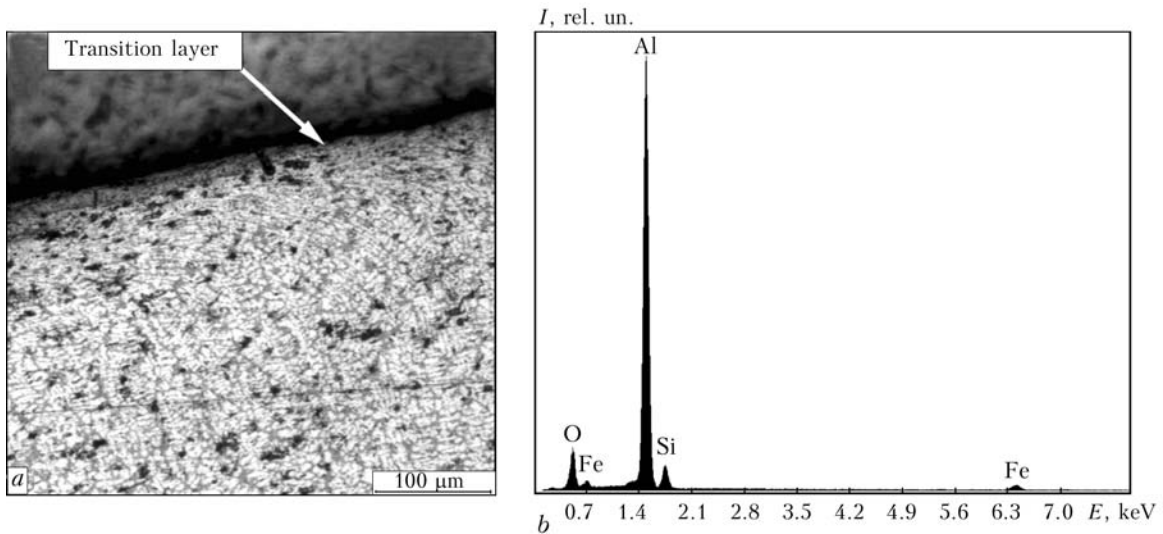


Figure 7. Microstructure of modified sample from AK9 alloy after friction tests (a) and elemental composition of the transition layer according to XRMPE (b)

melted at the smallest value of beam defocusing ($\Delta f = 1$ mm or $d_s = 0.3$ mm) have pronounced roughness and a multitude of dents in the entire range of studied values of pulse energy. Such a state of melted surface is indicative of exceeding the optimum density of laser radiation E_{opt} . Such exceeding results in formation of a considerable fraction of vapour-gas phase, leading to considerable spattering and evaporation of base metal. Melted surfaces, obtained at defocusing $\Delta f = 3$ and 5 mm, have a smooth surface. Width of the strip molten in one pass is not more than 1.5 mm.

Figure 8 shows microstructures of samples from AK12M2MgN + 5 % SiC₍₂₈₎ CM surface-melted by pulsed laser radiation. In CM melted surface layer the reinforcing phase is present and the particles preserve their dimensions and cleavage faceting in the entire range of the studied modes. λ values in different modes of laser surface melting for $\Delta f = 1/3$ mm are given below:

W_p, W	812.5	1500	2250
$\lambda, \mu\text{m}$	1.90/1.90	1.80/1.70	1.54/1.60

Treatment by laser beam results in refining of the initial structure of the matrix by an order and more (in as-cast condition CM has $\lambda = 30 \mu\text{m}$).

In addition to metallographic investigations of the metal of beads produced by surface melting, their hardness measurement was also performed at the degree of defocusing $\Delta f = 1$ mm, and also in the base metal at 5 mm distance from the fusion line (it is equal to HV 130 MPa). Results of hardness measurement are given below:

W, W	815	1500	2250
HV, MPa	161	175	180

Obtained results show that microhardness increases with increase of pulse power, which is the consequence not only of refinement of matrix alloy structure after laser surface melting, but also additional alloying of the matrix by the reinforcing phase.

Degree of refinement of the structure of aluminium-matrix CM at surface melting by pulsed laser radiation is higher than in surface melting by an arc

Table 3. Values of stability coefficients α_{st} of dry sliding friction of samples in the initial condition and after treatment by welding arc in a magnetic field

Sample material	Treatment state and mode	α_{st} at applied axial load F_1, N				
		18	28	39	50	60
AK9	Initial	0.87	0.91	0.92	0.93	0.90
	Treatment at $b = 0.048 T$	0.93	0.84	0.85	0.82	0.85
	Treatment at $b = 0.120 T$	0.87	0.81	0.82	0.85	0.84
AK12 + 10 % Al ₂ O ₃₍₄₀₎	Initial	0.94	0.93	0.86	0.88	0.81
	Treatment at $b = 0.048 T$	0.81	0.85	0.95	0.95	0.97
	Treatment at $b = 0.120 T$	0.95	0.87	0.98	0.94	0.98
AK12M2MgN + 12 % SiC ₍₁₄₎	Initial	0.98	0.91	0.91	0.88	0.85
	Treatment at $b = 0.048 T$	0.98	0.91	0.95	0.94	0.89
	Treatment at $b = 0.120 T$	0.96	0.94	0.93	0.95	0.93

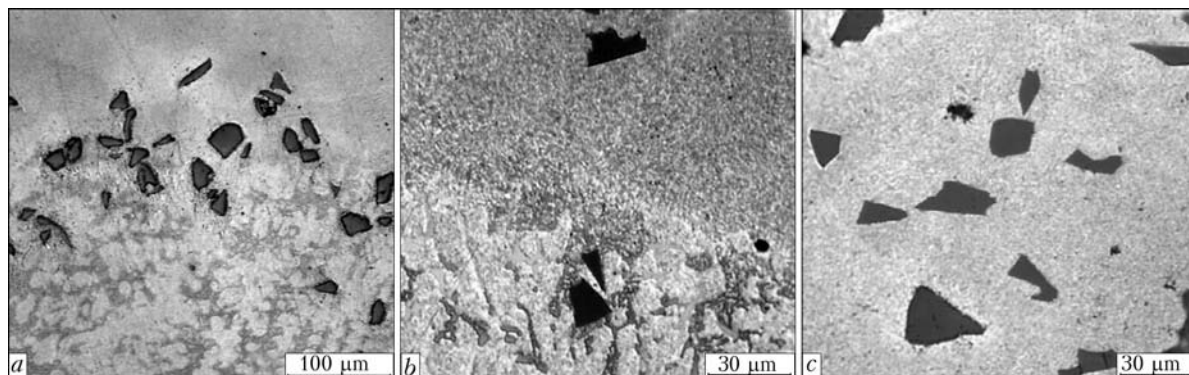


Figure 8. Microstructures of AK12M2MgN + 5 % SiC₍₂₈₎ CM after treatment by pulsed laser radiation ($\Delta f = 1$ mm; $W_p = 2250$ W): *a*, *b* – fusion line; *c* – central part

discharge in a magnetic field. However, the efficiency of arc surface melting is much higher (minimum width of surface melted strip at arc melting is equal to 6.6 mm with the above treatment method at the speed of 14 m/h, and at laser treatment at the speed of 2.7 m/h it is 1.5 mm).

CONCLUSIONS

1. Possibility of modification of surface layers of aluminium alloy AK9 and aluminium-matrix CM at arc melting of the surface in magnetic field and surface melting by pulsed laser radiation is shown.

2. At treatment of AK9 alloy by arc surface melting in a magnetic field, parameter λ decreases more than 7 times, for AK12 + 10 % Al₂O₃₍₄₀₎ CM – 4 times, at treatment of AK12M2MgN + 12 % SiC₍₁₄₎ CM – more than 5 times. Application of four-pole magnetic system allows adjustment of geometrical dimensions of surface melting zone (width and depth) and dispersity of the produced structure.

3. At surface melting by pulsed radiation a greater refinement of CM structure is observed. λ parameter for AK12M2MgN + 5 % SiC₍₂₈₎ after laser treatment decreases 16 times, however, surface melting process efficiency is much lower than at arc treatment.

4. Treated surfaces acquire mechanical and tribotechnical characteristics superior to those of the initial material.

5. Process of arc surface melting with impact of a magnetic field on the arc and the melt can be applied to produce high-quality wear-resistant surface layers from aluminium-matrix CM of a uniform composition.

- Chernyshova, T.A., Kobeleva, L.I., Bolotova, L.K. (2001) Discretely reinforced composites with aluminium alloy matrices and their tribological properties. *Metally*, **6**, 85–98.
- Chernyshova, T.A., Kobeleva, L.I., Bolotova, L.K. et al. (2005) Behavior in dry sliding friction of dispersion filled composites on the base of aluminium alloys with different level of strength. *Perspect. Materialy*, **5**, 38–44.
- Kobernik, N.V., Brodyagina, I.V., Chernyshov, G.G. et al. (2005) Argon arc cladding of dispersion-strengthened aluminium matrix composites. *Fizika i Khimiya Obrab. Materialov*, **4**, 67–71.
- Kobernik, N.V. (2008) Production of wear-resistant coatings by argon arc cladding of matrix of aluminium alloy AK12M2MgN particles SiC. *Zagot. Pr-va v Mashinostroenii*, **3**, 13–17.
- Kobernik, N.V. (2008) Argon arc cladding of composites of Al–SiC system. *Izvestiya Vuzov. Mashinostroenie*, **2**, 74–80.
- Kobernik, N.V., Chernyshov, G.G., Mikheev, R.S. et al. (2009) Argon arc cladding of wear-resistant composite coatings. *Fizika i Khimiya Obrab. Materialov*, **1**, 51–55.
- Kobernik, N.V. (2009) Producing of wear-resistant coatings of Al–SiC system composites by argon arc cladding. *Scarka i Diagnostika*, **1**, 25.
- Kobernik, N.V., Chernyshov, G.G., Mikheev, R.S. et al. (2009) Influence of method of filler material producing on formation of composite deposited coatings. *Ibid.*, **4**, 18–22.
- Stroganov, S.B., Rotenberg, V.A., Gershman, G.B. (1977) *Alloys of aluminium with silicon*. Moscow: Metallurgiya.
- Lapteva, V.G., Kuksenova, L.I., Ivanov, V.A. et al. (2008) Effect of microplasma treatment on properties of near-surface layer of specimens of different structural materials. In: *Proc. of Sci.-Techn. Conf. on Tribology for Machine Building* (Moscow, 2008). CD-ROM, Sect. 3, **19**.
- Biryukov, V.P. (2008) Laser hardening of friction surfaces by high-power gas, solid-state and fiber lasers. *Ibid.*, **7**.
- Akulov, A.I., Bul, B.K., Chernyshov, G.G. et al. *Magnetic system*. USSR author's cert. 654964. Publ. 1979.
- Chernyshova, T.A., Kobeleva, L.I., Shebo, P. et al. (1993) *Interaction of metal melts with reinforcing filler materials*. Moscow: Nauka.
- Mikheev, R.S., Kobernik, N.V., Chernyshov, G.G. et al. (2006) Effect of pulse laser radiation on structure and properties of aluminium-matrix composites. *Fizika i Khimiya Obrab. Materialov*, **6**, 17–22.
- Chichinadze, A.V., Berliner, E.M., Braun, E.D. et al. (2003) *Friction, wear and lubrication (tribology and triboengineering)*. Moscow: Mashinostroenie.
- Fuks, I.G., Buyanovsky, I.A. (1995) *Introduction to tribology*: Manual. Moscow: Neft i Gaz.

REPAIR OF SHIP HULL STRUCTURES OF ALUMINIUM ALLOY AMg6 USING ELECTRODYNAMIC TREATMENT

L.M. LOBANOV¹, N.A. PASHCHIN¹, V.P. LOGINOV¹, A.G. POKLYATSKY¹ and A.I. BABUTSKY²

¹E.O. Paton Electric Welding Institute, NASU, Kiev, Ukraine

²G.S. Pisarenko Institute for Problems of Strength, NASU, Kiev, Ukraine

The electrodynamic treatment (EDT) of welded joints from aluminium alloys AMg6 in ship hulls was carried out. The effect of 50–60 % reduction of initial stressed state was obtained at EDT of full-size samples of welded joints. Technological recommendations for EDT of ship welded hulls were worked out. A high process efficiency was shown by monitoring welded joints of hulls after EDT.

Keywords: aluminium alloys, ship hull structures, butt joints, residual stresses, electric current pulse, electrodynamic treatment, technological recommendations, service life, impact loads, vibration loads

Currently the welded hull structures of aluminium alloys are widely used in small-tonnage shipbuilding. It is connected with the fact that aluminium hulls as compared to steel ones and those of glass plastic have smaller weight at equal displacement, thus reducing the operational costs, in particular, for fuel.

Specific operational conditions of rapid ships, such as high level of vibration and impact loads, lead to damages of welded joints of hulls which are eliminated by repair welding. In number of cases the values of residual stresses (RS) in structural elements of a hull after repair exceed an admissible level which leads to fracture of welded joints and makes further operation of a ship impossible. Therefore it is necessary to conduct investigations of progressive and technological methods of controlling RS in the hulls of aluminium ships, which include treatment of structure using pulses of electric current of different duration and configuration. One of the methods of current influence is electrodynamic treatment (EDT) based on initiation of current charges in the workpiece causing formation of local fields of plastic deformations in it, facilitating relaxation processes in treated metal which in their turn results in decrease of general level of RS in the structure [1–4].

The purpose of this work is to study technological capabilities of EDT to control RS in repair welding of trailer cutters (TC) of aluminium alloy AMg6.

At the modern stage of development of small-size shipbuilding in Ukraine, TC became ever more popular due to mobility of movement on the land using special trailer trolley.

The welded TC (Figure 1), the hulls of which were the object of current investigation, had $7.70 \times 2.63 \times 1.20$ m dimensions in length, width and height, respectively. The necessity in minimizing the mass characteristics of hulls, connected with their transportation on the land, resulted in decrease of the thickness

of applied sheet blanks from 5.0–6.0 to 2.5–3.0 mm which allowed decrease of mass of a hull by 30 %. The decrease in thickness of lining strakes is compensated by strengthening of rigidity of longitudinal-transverse load-carrying section, and the preset geometry of a hull in the area of a deck 1, bottom 4 and forward tip of a keel 2 is provided by a rigid profile of a tubular section. The transverse rigidity in forward and stern tips is preset by vertical 3 and inclined 6 welded supports, and conjugating of stringer set of a bottom and boards with a stern is performed using plain links, i.e. knees 5. The fitting out of a hull with longitudinal and transverse links provided its minimal deviation from its preset geometry. Therefore longitudinal bending did not exceed 5 mm, and transverse one – 3 mm, that contributed to achievement of the satisfied hydrodynamic characteristics of a ship. Meantime, the high rigidity of a hull in combination with small thicknesses of a load-carrying section and lining make it less resistant to impact and vibration loads in comparison with ships of a conventional design.

During service of a batch of TC, damages in welded joints appeared in some of them that did not allow the further service of ships. The location of characteristic damages of hulls is shown in Figure 2. In tip part the cracks were observed in welds of strengthening the tip winch 1, joints of tip support 2, 3 and in

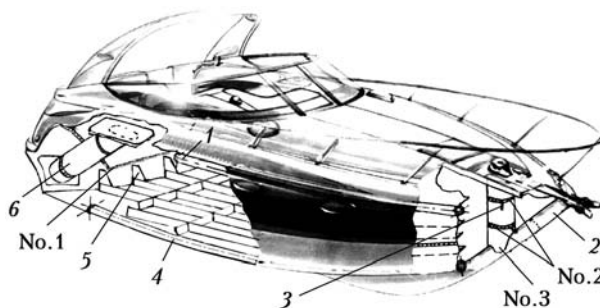


Figure 1. Scheme of welded structure of TC hull of alloy AMg6: 1 – strengthening of deck; 2 – tip tail of keel; 3 – tip support; 4 – bottom strengthening; 5 – knee; 6 – stern support; No.1 – stern strengthening weld; No.2 – support weld; No.3 – weld of support fastening at the stem

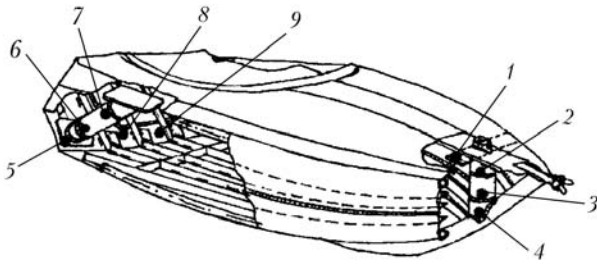


Figure 2. Location of characteristic damages of TC: 1 – tip winch strengthening; 2–4 – damages of tip support; 5–7 – places of damages of stern support; 8, 9 – stern strengthening under the engine

the places of its fastening at the keel 4. In stern tip the damages occurred in fasteners of supports to the stern 5 and in welds of supports 6, 7 and also strengthening under the engine 8, 9.

The operability of structures was renovated using repair technologies developed for manufacturing large-size hull of oceanic race yacht of aluminium alloy AMg5M [5]. After the defect was determined its marking was conducted by a marking tool with further mechanical preparation using disc milling cutter for all thickness of a joint. The V-shape crack trepanning with an angle, not exceeding 30°, was used. The length of repair weld exceeded the length of prepared area by 30 mm on each side for guaranteed remelting of microcracks. The butt joints 2–4, 6, 7 (see Figure 2) during repair of circumferential welds of tip and stern supports with thickness of wall of up to 3 mm were performed for one pass by manual non-consumable electrode welding in argon using filler rod of 2 mm diameter of the SvAMg6 grade. Welding current was 120 A, and argon consumption – 7 l/min. Rectilinear areas of overlapped welds of thickness (3 + 6) mm during repair of strengthening of winch 1 and stern supports 5 were performed by welding at current 200 A with filler wire of 3 mm diameter. The similar condition was applied for repair of T-joints of stringers of stern strengthening 9 of the thickness (3 + 6) mm (Figure 3). The damages in the corners of stern strengthening 8, welded of sheets of different thickness (3 + 6) mm, were eliminated using mechanical

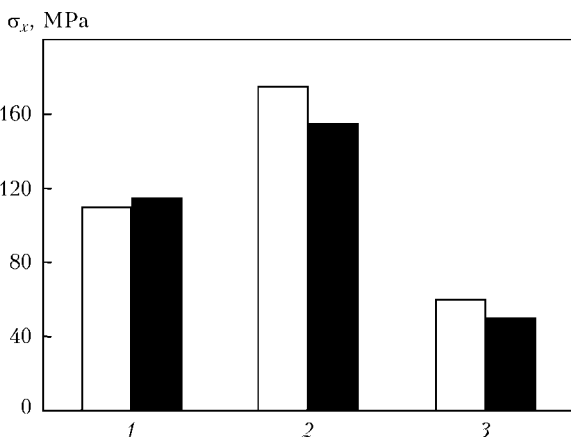


Figure 3. Longitudinal RS in the specimens of longitudinal (white columns) and circumferential (black) welds: 1 – initial RS; 2 – after repair welding; 3 – after EDT

V-groove preparation for the depth of 3 mm from a face surface of welds with further pre-welding at the current not exceeding 150 A.

After completion of repair procedures the damage of repaired welds at minimal run of ships was observed in some cases. The repeated repair welding led to overheating of metal which deteriorated its mechanical properties. Basing on the analysis of service damages it was suggested that their possible reason was high level of RS in renovated joints. This was connected with the fact that ships were manufactured using method of unit-by-unit assembly, providing free shrinkage of welds in welding and, as a consequence, minimal level of RS in the joints. Repair procedures were carried out in ready bodies under the conditions of «rigid fastening» of damaged elements, which excluded free realization of shrinkage shortenings and, as a result, increased the level of RS. The combination of impact and vibration loads with high level of RS in renovated elements of a body leads to damageability of a ship at minimal run.

As far as there are no conditions for realization of free shrinkage during repair of welded joints of TC to control the level of RS, the EDT was applied. To evaluate the influence of repair welds and their further treatment on the level of RS in damaged units of TC the full-scale specimens of structural hull elements were manufactured. The specimens of longitudinal butt joint of strengthening of stern of variable thickness (3 + 6) mm of the size 400 × 400 (see Figure 1, weld No.1), and a pipe of 300 mm length, 100 mm diameter with wall thickness of 3 mm with central circumferential weld as a support specimen (Figure 1, weld No.2) were used. Conditions of manual welding of specimens were in compliance with accepted ones in manufacturing of hulls. The measurements of initial values of longitudinal RS along the central axis of a weld were carried out using mechanical strain gauge with 30 mm base. The technological operations of preparation and rewelding of damages at regular condition accepted during repair of ship stern were carried out on specimens. Then EDT of specimens were carried out using a series of current pulses. The treatment was performed using manual tool representing cylindrical electrode of copper of the grade M1, which is arranged in the isolated casing [2]. The energy of current pulse at EDT is transferred during touch of manual tool in a specified area of the surface being treated.

After repair welding and treatment the current measurements of RS in welds were carried out, the results of which are presented in Figure 3. Basing on the data of the Figure it is possible to conclude: if the beginning level of RS in welds did not exceed 120 MPa, then after the repair of circumferential and longitudinal welds it increased, respectively, by 35 and 60 % and reached 155–175 MPa, which can negatively influence the service characteristics of material. After performance of EDT the values of RS decreased

more than by 65 % and did not exceed 50–60 MPa which is proved by efficiency of this kind of treatment.

On the basis of results of the carried out experiments on EDT of specimens of longitudinal and circumferential butts the following technological recommendations on pulsed treatment of problematic welded elements of hulls of small ships of alloy AMg6 were worked out: before EDT of welds in the compartment of a ship it is necessary to clean the area being treated from foreign objects, tool, cable and hose lines; to provide access of manual tool to the area of treatment at the distance of not less than 20 mm from the fusion line of a weld; not to admit positioning of manual tool in a specified point of treated surface for more than one current discharge; to perform EDT in lower and horizontal position of manual tool in the direction from middle to edges of a weld; to perform EDT of circular and circumferential welds in broken order.

On the basis of developed recommendations the treatment of structural elements of welded hulls of TC of alloy AMg6 in the amount of seven units was performed. The EDT of welded joints of tip and stern compartments and also some areas of load-carrying section after repair welding was performed (Figure 4).

In the period of navigation of 2009 the monitoring was made on welded joints of ship hulls, where EDT after repair welding was performed. The results of inspection showed that for the current period TC ran without damages from 300 up to 1320 km, no traces of damages in a form of microcracks in treatment area were detected.



Figure 4. EDT of welded joints of stern strengthening of TC hull

Therefore it can be concluded that EDT is the efficient method of prolonging the service life of thin-wall hull structures of aluminium alloys after repair welding.

1. Lobanov, L.M., Pashchin, N.A., Loginov, V.P. et al. (2005) Application of electric pulse treatment of structural elements to extend their service life (Review). *The Paton Welding J.*, **11**, 19–23.
2. Lobanov, L.M., Pashchin, N.A., Loginov, V.P. et al. (2007) Change of the stress-strain state of welded joints of aluminium alloy AMg6 after electrodynamic treatment. *Ibid.*, **6**, 7–14.
3. Lobanov, L.M., Pashchin, N.A., Loginov, V.P. et al. (2007) Effect of electrodynamic treatment on stressed state of welded joints on steel St3. *Ibid.*, **7**, 6–8.
4. Lobanov, L.M., Makhnenko, V.I., Pashchin, N.A. et al. (2007) Features of formation of plastic deformations at electrodynamic treatment of welded joints of St3 steel. *Ibid.*, **10**, 7–11.
5. Lobanov, L.M., Pavlovsky, V.I., Grishchenko, A.N. et al. (1993) Ensuring of accuracy in fabrication of welded hull of ocean racing yacht. *Avtomatich. Svarka*, **3**, 40–43.

HIGH-QUALITY HOSE PACKS FOR UNDERWATER WELDING AND CUTTING

V.N. MARTINOVICH¹, N.P. MARTINOVICH¹, V.A. LEBEDEV², S.Yu. MAKSIMOV², V.G. PICHAK² and I.V. LENDEL³

¹SPA «Vitok» Ltd., Donetsk, Ukraine

²E.O. Paton Electric Welding Institute, NASU, Kiev, Ukraine

³Pilot Plant for Mechanical Welding Equipment, Ilnitsa, Ukraine

Considered are examples of design of special cable products to be used with mechanized equipment for semi-automatic welding, surfacing and cutting. Possibilities of new cable developments for manufacture of hose holders are shown, their advantages and technical characteristics are analyzed, and fields of their efficient application were outlined. Special attention is given to cables employed to power semi-automatic systems operating under extreme conditions.

Keywords: arc welding, semi-automatic devices, service lines, cable, hose holder, structure, manufacture, service conditions

The mechanized equipment for welding, surfacing and cutting is traditionally upgraded through improving characteristics of welding current sources, feed mechanisms, control and regulation systems [1, 2] etc. Consideration is also given to other components of this type of the equipment. These are the elements of service lines (welding cables, hose holders), which are

based on special cable [3]. The problems addressed with the help of semi-automatic devices are so diverse (various electrode wires, environment and service conditions etc.) that they require a special approach to elements of the service lines and, naturally, determine differences in their designs. And whereas the problem of selection of welding cables for conventional conditions is solved through a choice of what is already commercially manufactured in sufficient quantities and proved good (for example, flexible trailing weld-

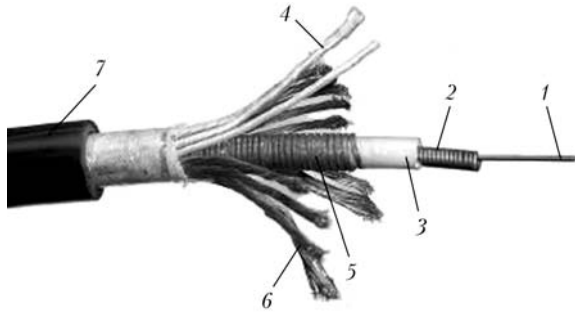


Figure 1. Appearance of cable KPESGU for mechanized welding equipment (1-7 – see the text)

ing cable KOG), special service conditions (mechanized underwater welding) require cables with new characteristics. To a greater extent, this concerns the cable products underlying development and manufacture of domestic different-application hose holders. The main function of a guide channel in the hose holder is to provide feed of an electrode wire without jerks and jams at a preset algorithm of movement in modulated working modes, and movements with regulated pulse components.

The aim of the present study is to consider the possibility of using them in semi-automatic systems for solid and flux-cored electrode wire welding by an example of new developments of special cables.

Up to now the semi-automatic devices for gas-shielded welding have been completed with hollow electric welding cables of the KPES grade. A hollow internal channel in them is made in the form of an externally insulated steel spiral with a power conductor and control conductors wound on it, and a rubber skin applied on top. In addition, the use was made of cables of the KPESG grade and foreign cables of similar design. The hollow internal channel in them is made in the form of a polymeric, sufficiently rigid tube with a power conductor and control cables wound on it, and a rubber skin applied on top. In their technical level, these electric welding cables do not meet the up-to-date requirements. Main disadvantages of

these cables are their significant rigidity and short life time. Besides, design of the KPES cable does not provide for a shielding gas to be fed via it to the welding zone, and design of the KPESG cable does not guarantee that the channel will retain its shape after kinks of the cable and application of transverse loads to it, which cause deformation of the plastic channel, thus hampering installation of a removable guide channel for wire into it.

To avoid the said disadvantages of the welding cables, the Design Bureau of the E.O. Paton Electric Welding Institute in collaboration with SPA «Vitok» Ltd. developed and manufactured the new designs of hollow reinforced flexible electric welding cables of the KPESGU grade with a rubber skin and of the KPESGUV grade with a polyvinylchloride (PVC) skin. These cables are intended to supply the direct current at an operating voltage of up to 100 V, or the 50 Hz frequency alternating current at a voltage of up to 42 V, to feed the electrode wire and shielding gas to the welding zone, and feed the control signals.

Appearance of a hollow flexible reinforced electric welding cable with copper conductors is shown in Figure 1. It comprises hollow elastic plastic or rubber channel 3 wound around with metallic single-wire cylindrical spiral 5, with the strands 6 of the main conductor and control conductor 4 wound on it, and protective rubber or PVC skin 7 applied on top of them. Channel 3 provides feeding of a shielding gas to the welding zone. Also, it houses replaceable steel spiral 2 for feeding of welding wire 1. A replaceable tube from fluoroplastic or carbon-reinforced plastic is installed instead of the steel replaceable spiral when using this design for development of a hose holder to feed wires of aluminium alloys.

The presence of the hollow channel in the form of elastic polymeric tube wound around with a cylindrical metallic spiral provides a substantial increase in flexibility of the cable at any ambient temperature and in its life time, as well as retention of the cylindrical form of the elastic polymeric tube (channel) at any kinks of the cable. This ensures an easy change of the replaceable guide channel (replaceable steel spiral or plastic channel), which fails rather quickly because of its wearing by the welding wire.

Quantity and nominal cross-section of the conductors (main and control), nominal inside diameter of the channel and outside diameter of the cable are given in the Table.

Tests of different designs of the hose holders made by using the above cable proved their high reliability. Comparison with the hose holders of the well-known German Company BINZEL was carried out in worst-case situations at sharp kinks of the cable (at an angle of 90° or more) with a kink radius formed under a load of 200–300 kN. This is a case that often takes place in manipulation with the hose holder, in particular, in transportation or turning of the feed mecha-

Technical characteristics of cables for mechanized welding equipment

Nominal section of conductor, mm ²		Nominal diameter of channel tube, mm		Diameter of spiral of channel, mm, not more than
Main	Control	Internal	External	
10	From 0.35 to 1.00	5.0	6.5	8.3
12		5.0	6.5	8.3
16		5.0	6.5	8.3
25		6.5	8.1	10.0
35		6.5	8.1	10.0
35		7.5	9.5	11.3
50		7.5	9.5	11.5
70		7.5	9.5	11.9
50		9.0	11.0	12.9
70		9.0	11.0	13.4

nism because of pulling of the hose holder. Feeding of the wire through the channel of the BINZEL hose holder is hampered after a few such cycles, whereas the hose holder based on the KPESGU cable retains its performance. Tests of said cable in a set with the hose holder, conducted by feeding different-diameter electrode wires of Sv-08G2S type through its channel showed that the 1.2 mm diameter wire can move with allowable outlet speed fluctuations at a channel length of 3.5–4.5 m, and the 1.6–2.0 mm diameter wire – at a channel length of 6 m. Thus, it is obvious that the new design of the cable provides significant widening of the maintenance zone for semi-automatic welding and surfacing devices.

The KPESGU cables are gradually introduced into designs of modern types of the hose holders manufactured in Ukraine (PPMWE, Ilnitsa) and Russia («Linkor» Company, Stavropol).

It should be noted that manufacture of cables with sections of the main conductors, sections of the control conductors, their quantity, diameters of elements of the channel and cable other than those indicated in the Table is permitted after agreement with a consumer.

Development of a cable to power electric drives of the feed mechanisms and systems for control and regulation of the semi-automatic devices for welding and cutting at significant depths (more than 200 m) is a very difficult problem [4].

We conducted integrated investigations of mechanical strength and electric characteristics (heating, attenuation of control signal and voltage drops on power wires) of the cable. The flexible, armored and reinforced cable of the KGBU grade, the cross-section of which is shown in Figure 2, was developed and manufactured by SPA «Vitok» Ltd.

The cable is designed for control of the equipment for underwater welding at direct current voltage of up to 220 V. It is made from flexible copper conductors insulated by PVC elaston: two conductors 1 with the 2.5 mm² section, three twisted pairs of conductors 2, 3 and 5 with the 0.75 mm² section, screened with foiled film (forlsan, alumoflex) and copper wire 4 with the not less than 0.15 mm diameter, laid longitudinally under the foiled film.

All twisted pairs and conductor are twisted around central conductor. Polyethyleneterephthalate film PET-E 6 with overlap of not less than three layers, flexible armor in the form of turns of single-wire spiral 7 made from the (0.85 ± 0.10) mm thick and (2.5 ± 0.3) mm wide flat steel wire with an axial gap between its turns, which is not more than two widths of the wire, reinforcing polyester threads 8 and PVC skin 9 are laid in series over the twisted conductors.

Conductors of the twisted pairs are stranded with each other at a strand pitch of not more than 10 external diameters of the strand. The foiled film is wound on a twisted pair with overlap of not less than 10 %.

The external diameter of the cable is not more than 20.5 mm, the minimum internal radius of a kink loop of the cable is not less than its 7 external diameters, and tensile strength of the cable is not less than

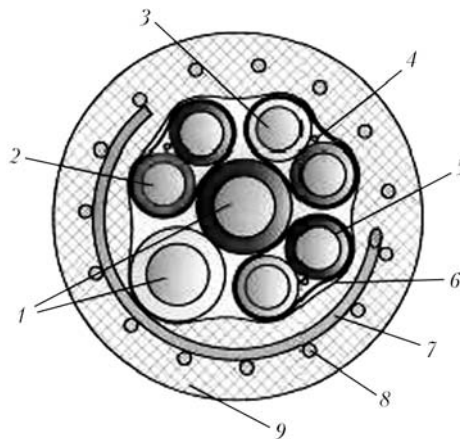


Figure 2. Cross-section of cable for semi-automatic underwater welding and cutting device (1–9 – see the text)

1900 N. An estimated weight of the cable is 0.61 kg/m.

The presence of the flexible steel flat wire armor provides the required strength characteristics of the cable in axial and radial directions (in the case of operation in deep-water environment) by maintaining the necessary flexibility.

Tests of the cable, including in water environment with 3.5 % salinity, showed its high quality. It has almost no analogues to the combination of its parameters.

Unique equipment for continuous winding of non-rotating metal single-wire cylindrical spirals on any billets, for example, in the form of flexible tubes, cable conductors, including twisted ones, was developed and manufactured on the basis of inventions [5, 6] by «Vitok» Ltd. for production of the above cables. Many new designs of load-carrying cables featuring an increased flexibility, enhanced explosion, electrical and fire safety properties are developed and manufactured by using such spirals as a flexible armor. Their service life increased not less than three times, compared to cables with similar conductors but without flexible armor. These developments can be used for welding, surfacing and cutting equipment operating under extreme conditions.

It should be noted that Ukraine has a high-efficiency enterprise «Vitok», which manufactures the high-quality wide-application cables. This enterprise is fitted with the in-house equipment providing a complete manufacture cycle by using advanced materials. The enterprise can develop and produce special designs of cables by request of a customer and in correspondence with his requirements.

1. Belfor, M.G., Paton, V.E. (1974) *Equipment for arc and slag welding and surfacing*. Moscow: Vysshaya Shkola.
2. Lebedev, V.A., Pichak, V.G., Smolyarko, V.B. (2001) Pulsed wire feed mechanisms with pulse parameter control. *The Paton Welding J.*, 5, 27–33.
3. Chvertko, A.I., Pichak, V.G. (1983) *Equipment for arc and slag welding and surfacing*. Kiev: Naukova Dumka.
4. Yushchenko, K.A., Lebedev, V.A., Pichak, V.G. et al. (2009) New generation of semi-automatic machines for underwater mechanized welding and cutting. *Svarka i Diagnostika*, 4, 31–37.
5. Martinovich, N.P., Putilov, E.P. *Device for spiral winding*. USSR author's cert. 1440590. Publ. 07.01.87.
6. Martinovich, N.P. *Device for spiral winding*. USSR author's cert. 1688961. Publ. 24.08.89.

*Non-destructive testing*

ULTRASONIC DIAGNOSTICS OF SERVICE DEFECTS IN STRUCTURES OF OIL AND GAS INDUSTRY

V.A. TROITSKY, V.P. DYADIN and E.A. DAVYDOV
E.O. Paton Electric Welding Institute, NASU, Kiev, Ukraine

Results of diagnostics of petrochemical equipment conducted by specialists of the E.O. Paton Electric Welding Institute during the last 10 years were analyzed. The most characteristic regions of the apparatuses susceptible to service damage were determined, and methods for testing them by ultrasonic inspection were suggested. It is noted that the most frequent error in repair of welded joints on heat-resistant steels is their incomplete tempering in the zones of contact of elements made from different structural materials. Recommendations are proposed to select materials at replacement of equipment that exhausted its specified service life.

Keywords: *welded structures, service defect, diagnostics, low-temperature hydrogen delamination, crack, high-temperature cracking, heat treatment, medium impact, ultrasonic testing*

In connection with an abrupt increase of energy carrier prices and wear of the main equipment, a considerable part of enterprises of oil and gas industry are in need of technical re-equipment. Performance of reconstruction is associated primarily both with the need to reduce power inputs in manufacture of a particular type of product, and with increase of the depth of processing the used raw materials.

In view of the fact that a significant part of expensive equipment has been in operation for 20–30 years, only its stage-by-stage upgrading can be considered.

Hence the need for further use of part of processing equipment which has exhausted its specified service life, which, in its turn, requires development of more accurate means of non-destructive testing (NDT) and assessment of the possibility of its further operation.

Sufficiently advanced methods of ultrasonic (US) testing have been introduced over the recent years, which are based on analysis of the time of arrival of diffracted US waves reflected from sharp edges of internal defects. These methods, conditionally designated as TOFD, SAFT, tandem, etc. allow finding cracks, corrosion, hydrogen and other cracking which develop in service.

The main service conditions of welded structures usually include the contacting medium, loads, temperature, radiation and time of their aggregate effect.

Load influence is differentiated by duration of impact and rate of application (static, cyclic, dynamic, etc.). Loads may arise both from external impact and inherent deformations at structural transformations and non-uniform heating. In combination with the shape of welded joints and structural elements, com-

plex local stresses are induced, which affect the strength and further performance of welded structures.

Distinction is made between the cyclic and dynamic nature of loading, which is also regarded as one of the most heavy-duty modes of welded structure operation. Many steels are sensitive to the rate of load application, particularly in the presence of stress raisers, which, in its turn, requires performance of heat treatment after welding and making more stringent requirements to norms of NDT of critical elements.

To ensure welded structure stability under the impact of high compressive forces, thickness of used metal and shape of structural elements have the main role. Temperature requirements are also significantly dependent on the material. For instance, ferrous metals are characterized by lower strength in the presence of stress raisers, which predetermines certain requirements to selection of metal, its heat treatment and to admissible defect dimensions.

A special situation arises in the region of high operating temperatures of equipment, where correct selection of the respective high-temperature steel is important. Otherwise it may lead to a change in the material strength and ductility, its structure, thermal embrittlement and fracture at long-term impact.

Medium influence on the structure is even more diverse. For instance, metal corrosion in combination with loads leads to corrosion cracking and fatigue. Temperature and load influence make the situation even more difficult.

Given below are the results of technical diagnostics of petrochemical industry equipment, conducted by PWI staff members over the last ten years.

In addition to acquisition of data on the characteristic defects and improvement of NDT procedures, also various aspects of possible degradation of service properties in structural materials and welded joints

in corrosive media at normal and higher temperatures were studied.

Corrosion damage of petrochemical equipment (PCE) in petroleum processing is caused by its inevitable impurities [1]: sulphur-, chlorine-, oxygen-organic compounds, local water and products of their thermal decomposition. Corrosiveness of the formed components is determined both by raw material composition, and mode parameters of the technological processes in its processing (pressure, temperature, etc.). The following factors causing PCE failure, can be named:

- decomposition of sulphide compounds of oil and chlorides, leading to formation of corrosive components, such as hydrogen chloride and hydrogen sulphide;
- presence of water electrolytic media, promoting corrosion cracking, low-temperature hydrogen cracking, low-temperature hydrogen delamination and hydrogen embrittlement of steels;
- application of alkali agents promoting development of caustic brittleness of welded joints of ferrous metals;
- formation of hydrogen sulphide at high temperatures leading to acceleration of the corrosion processes;
- increase of cooling water aggressiveness;
- formation of acid compounds (naphthenic acid);
- presence of two-phase media, etc.

Considering the mobility of the corrosion media during petroleum processing, conditions are also in place for development of combined forms of corrosion failure (combination of pitting corrosion with corrosion cracking, intercrystalline stress corrosion cracking, etc.).

Many years of inspection of PCE, which operated in a broad range of temperatures, pressure, medium corrosiveness, content of H_2 , H_2S , etc., allowed revealing a large number of cases of low-temperature lamellar-hydrogen damage of apparatus bodies, made from low-carbon and low-alloyed steels. Figure 1 shows a histogram of damage distribution by steel grades against the total number of studied cases. Figure 1 gives a good idea of the actual condition of the equipment on a qualitative level. Metal structures made from steels of 16GS and 09G2S grades show the highest susceptibility to low-temperature lamellar hydrogen delamination, unlike apparatuses made from steel 20 and St3sp (killed) grades.

Analysis of PCE technical condition shows that the difference in the degree of damageability is mainly related to peculiarities of structural texture of metal rolled stock [2] and diffusion processes running along the boundaries of non-metallic inclusion location [3, 4]. This is another confirmation of the need of both reconsidering the class of steels suitable for manufacture of PCE operating in hydrogen sulphide media, and applying US testing procedures based on recording the diffracted US vibrations.

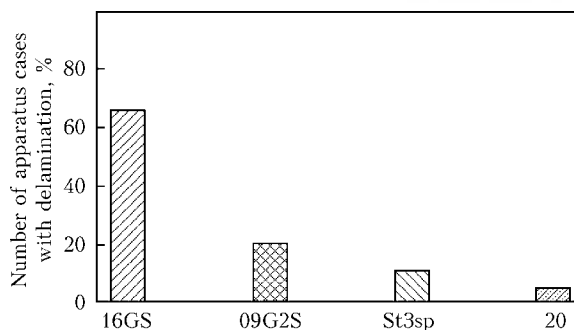


Figure 1. Fraction of apparatus cases in which corrosion damage was detected

A considerable number of cases was found in practice, when equipment manufactured from steels of 09G2S and 16GS grades without knowing more precisely the requirements to their categories, was rejected already after 2–4 years of service. For metal rolled stock with a pronounced zonal segregation occurring at depths equal to half or one third of sheet thickness, lamellar cracking develops in the zone characterized by considerable anisotropy of strength properties in the thickness direction. This type of damage may differ by the rate of its propagation in the sheet plane, and can be of a stepped or plane nature. As damage accumulates, deformation of the thinner wall under the impact of internal pressure can be observed later on.

US inspection of metal rolled stock by P-Scan system showed that at increased sulphur content and more uniform distribution of sulphide inclusions by sheet thickness lamellar cracking mostly is of a stepped nature (Figure 2).

Lamellar hydrogen cracking in PCE made from low-alloyed steels 16GS, 09G2S and low-carbon steel St3sp5, affected gas absorbers, which had been in operation for more than 20 years at 30–50 °C temperatures in media containing 15 % water solution of monoethanolamine (MEA), hydrocarbon gas, as well as H_2 and H_2S in different weight percent.

Figure 3 gives diffractograms of sections of scanning an absorber body from 09G2S steel 48 mm thick. The examined section was removed from the point of corrosive medium input. It is seen that the process of lamellar hydrogen cracking can be both of a plane and step-like nature, with predominant rate of propagation in the direction of rolled stock plane. Step-like nature of cracking in this case is determined by a considerable thickness of the segregation zone. Figure 4 shows the section of scanning the absorber body, located opposite the hydrogen-containing gas input (steel 16GS 28 mm thick). The Figure quite clearly shows two layers sub-

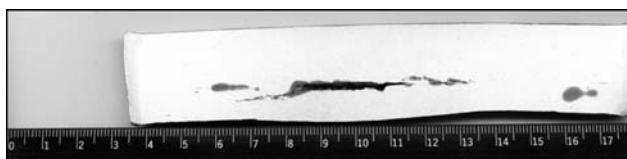


Figure 2. Lamellar cracking across sheet thickness

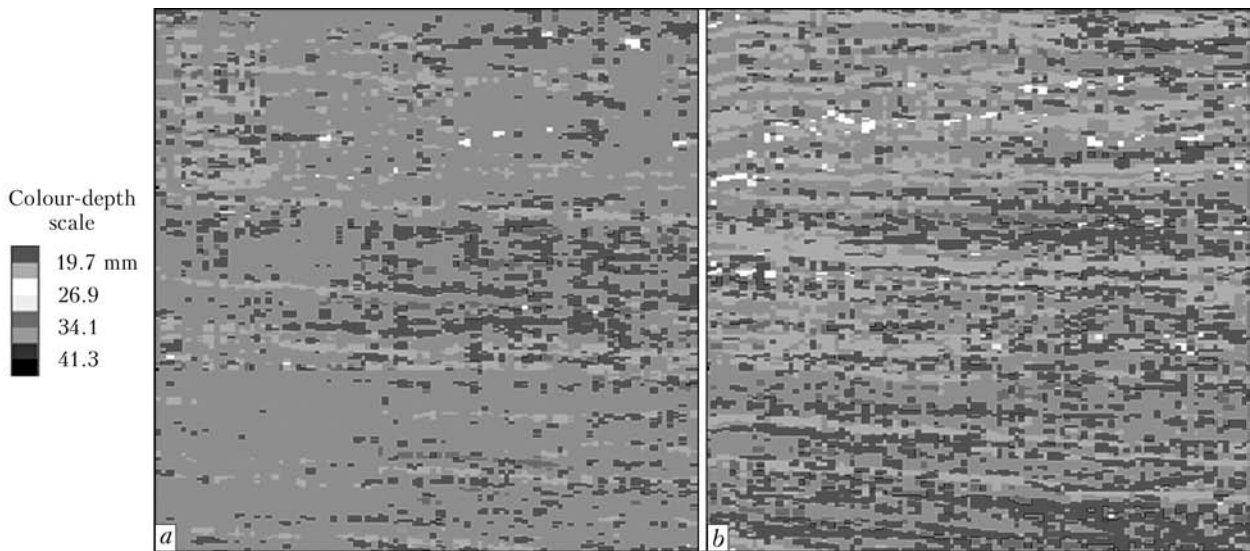


Figure 3. Monitoring of growth of discontinuities in the metal of absorber body from 09G2S steel of 48 mm thickness during one year of operation (reference section of 750 × 750 mm size): *a* – initial scanning; *b* – repeated scanning of the same section after one year

jected to lamellar hydrogen cracking, which are located at depth of 12–16 mm and 18.5–24.0 mm from the outer surface. Layer at the depth of 18.5–24.0 mm is at the final stage, which is indicated by step-like development of the process of cracking along the boundaries of developed discontinuities and visible plastic deformation of the thin wall under the impact of pressure of molised gas in the cavities. Layer at the depth of 12–16 mm is subjected to less intensive cracking. The latter is attributed to its shielding by the layer at the depth of 18.5–24.0 mm.

Section of scanning the body of an absorber made from steel St3sp5 12 mm thick has certain differences in the nature of lamellar cracking from those considered above. As is seen from Figure 5, the dimensions of discontinuities in the sheet plane are somewhat smaller than in Figures 3, 4, and step-like development of lamellar cracking comes to the inner surface.

In this case the predominant development of hydrogen cracking process occurs in the direction of sheet thickness. A similar cracking process is observed for steel 20, which is also associated with the features of structural texture of metal rolled stock and diffusion processes running along the boundaries of non-metallic inclusions.

During diagnostic inspection of PCE special attention was paid to zones subjected to the most intensive lamellar hydrogen cracking. These, first of all, are the region of input of hydrogen-containing products; sections along media interfaces; stagnation

zones; regions of plastic deformations and residual stress zones.

In the region of hydrogen-containing product input, in addition to relatively high content of hydrogen, the impact of the flow (jet) is always present to varying degrees, which promotes diffusion saturation of metal in the contact region, and, as a consequence, leads to higher rates of development of lamellar cracking compared to other parts of the apparatus. As an example, Figure 6 gives ultrasonic evaluation of discontinuities in the section of the column body. The above section was located opposite the inlet for MEA water solution into the apparatus. Unlike other sections of the column, which also had lamellar damage in the metal, the region given in the Figure features a considerable intensity of hydrogen cracking development. As a rule, such regions are of a local nature, allowing their repair to be performed without column dismantling. In recent years cases of complete replacement of shells in product input zones have become more frequent in local petroleum processing enterprises, which except for a considerable increase of the cost of repair operations, does not in any way influence further performance of the equipment.

A quite frequent case is a combination of pitting corrosion with low-temperature hydrogen delamination of metal along the interface of media phase states. As a rule, such locations are in the lower parts of the

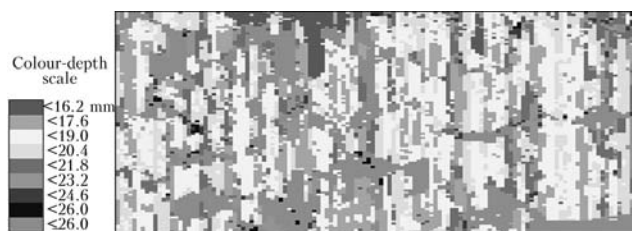


Figure 4. Data on scanning in section of absorber case from 16GS steel 28 mm thick (section size of 250 × 500 mm)

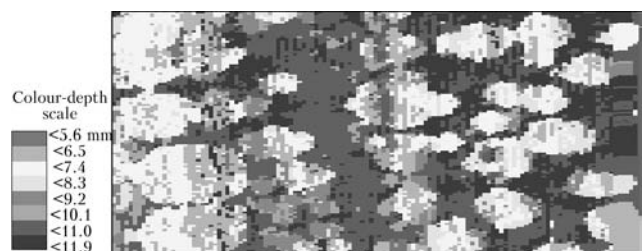


Figure 5. Fragment of scanned section with hydrogen cracking of an element of absorber body from St3sp5 steel 12 mm thick (section size of 250 × 250 mm)

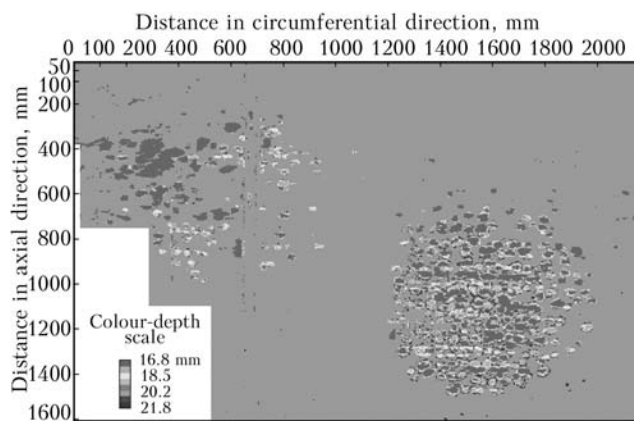


Figure 6. Data of scanning in the section of column body opposite to product input (MEA water solution) (section size of 1600×2000 mm, metal thickness of 22 mm)

apparatus. In this case for separators and heat exchangers the main corrosion zone is located along the apparatus body generatrix on the level of fluctuation of media interfaces or in the wetting zones.

So, Figure 7 gives a combined form of corrosion damage of separator body in the stagnation region which forms because of the protruding nozzle.

Characteristic regions prone to possible intensive low-temperature lamellar cracking in hydrogen-containing media also include regions with residual stresses (for instance, zones of maximum plastic deformations in stamping of elliptical bottoms, locations of welding auxiliary elements to the body, etc.).

Influence of residual stresses in welded joints is rather clearly manifested in diagnostics of alkali tanks, made from steels of 16GS and 09G2S grades. In these apparatuses which are past their specified service life at temperatures above 50°C and alkali concentration of not less than 10 %, central longitudinal cracks are periodically found in T-shaped welded joints of up to 10 mm and greater depth (in a number of cases cracks were observed in near-weld zones of field welds). When ordering this type of equipment, it is recommended to specify its high tempering.

As regards high-temperature hydrogen-sulphide corrosion, this type of damage is observed at service temperatures above 260°C in transfer pipelines, furnace coils and heat exchangers connected to them, in the form of fine shallow wide pits connected to each other. In the pure form such a kind of corrosion fracture is rather easily detectable, however, the high propagation rate requires development of special ap-

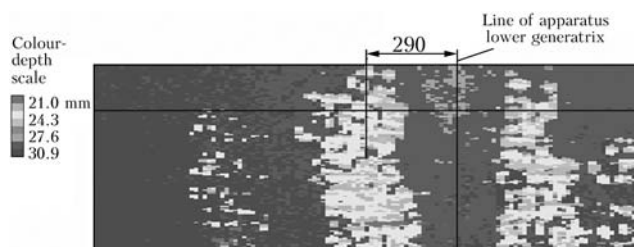


Figure 7. Data on scanning metal with corrosion damage in stagnation zone of separator 32 mm thick from steel 16GS (section size of 500×1750 mm)

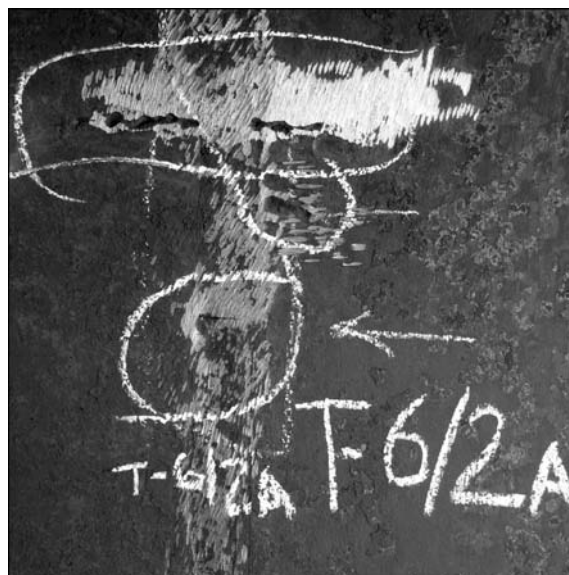


Figure 8. High-temperature cracking of weld of heat-exchanger from 12KhM steel in repair welding zone

proaches to its NDT. In the combined variant, this kind of corrosion damage is the most critical in connection with development of welded joint cracking in the points of fine linear porosity clusters and development of through-thickness cracks. Influence of residual stresses in these cases is particularly high. Despite the fact that practically all the power equipment is made from chromium-molybdenum steels requiring compulsory heat treatment after welding, it is not always possible to eliminate residual stresses completely. During this examination period, PWI experts found a considerable number of cases of welded joint cracking leading to emergency shutdown of critical power equipment and installations as a whole, because of development of through-thickness cracks and product leakage practically in all the petroleum-processing plants of Ukraine. So, Figure 8 gives a section of the weld with a developed crack one year after performance of repair work in power heat exchanger.

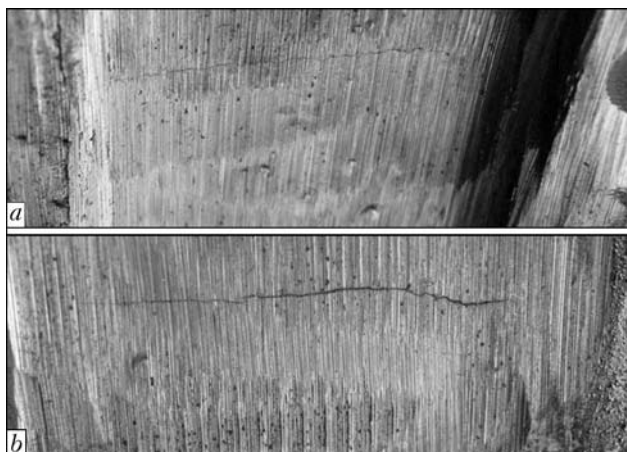


Figure 9. High-temperature cracking of circumferential welds in zone of joint of flange (steel 15Kh5MU) to heat exchanger shell (12KhM) of various thickness: *a* – weld joining heat exchanger shell to bottom of 35 mm thickness; *b* – weld in the zone of joint of 45 mm thickness shell to flange

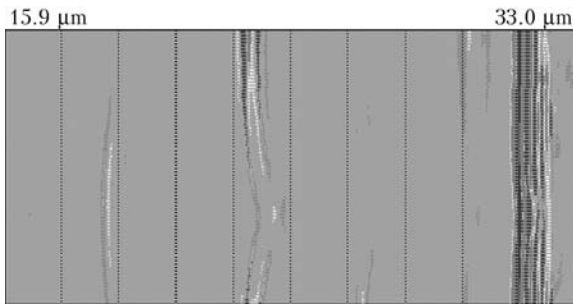


Figure 10. Example of TOFD measurement of a crack in a welded joint which initiated through cracking of facing cladding layer

The most characteristic elements, subjected to such damage, are sections of welded joints in the locations of welding branchpipes, elements of transfer pipelines and heat exchanger shells to flanges. In most of the cases appearance of defects in these joints is related to incomplete tempering of the welded joint because of the difference of joined element materials (Figure 9).

In heat-exchanger equipment the length of such defects is usually not greater than weld width because of the presence of residual compressive stresses in the HAZ metal, restraining their development in this direction. Such limitations are absent in the thickness direction, which is what leads to appearance of through-thickness «short» cracks.

For transfer pipelines such cracking usually occurs along the line of fusion of flange to pipe weld. In this case, bending stresses due to thermal expansion of the pipeline have a quite significant role, which is what leads to partial or complete rupture.

Intercrystalline cracking of protective facing welds and the main cladding layer of the equipment, made from a bimetal, also is a quite frequent phenomenon in petrochemical production. On the other hand, while the depth of intercrystalline cracking of the cladding layer of bimetal is usually limited by cladding thickness due to the presence of a thin martensite interlayer on the boundary of transition to alloyed metal, in facing welds it largely depends on correct selection of welding consumables and welding technology. Several cases were recorded when such violations resulted in extended cracks of a length greater than half of the section [5]. As an example Figure 10 gives the result of measurement of the depth of such a crack using TOFD method. It should be noted that US technology allows a sufficiently accurate (with 1–2 mm error) measurement of crack dimensions, the information

about which is required for assessment of tested facility performance. In regular practice of diagnostic examinations crack dimensions are evaluated by cutting out, which involves a number of technological difficulties. It should be noted that application of TOFD method in structures with a clad surface has a number of special features, so that specialists conducting the measurements are required to have certain qualifications and experience. A higher susceptibility of 10Kh18N10T steel to this type of damage unlike 08Kh13 steel should be noted.

Fatigue fracture, except for tanks, is a quite rare phenomenon in petrochemistry. On the other hand, in a number of enterprises a growth of process cracks was registered in welded joints of supporting parts and coverplates with their propagation into the main body of coke chambers under the impact of thermal cyclic stresses and vibrations.

As regards brittle fractures, practically all the cases occurred after performance of repair-reconditioning operations at incomplete removal of the defect with its subsequent remelting. In most of the cases brittle fracture was caused by strain ageing and hydrogenation of metal ahead of the front of incompletely removed defect. Over the recent years such fractures occurred in repair of vacuum columns in several enterprises of Ukraine and Russia.

CONCLUSIONS

1. Characteristic PCE zones the most prone to damage in service were analyzed. Recommendations are proposed on requirements to selection of structural materials for PCE manufacture and repair, allowing lowering the risk of equipment service damage.

2. An advantage of ultrasonic computerized systems of monitoring the growth of service defects in PCE diagnostics is shown.

1. Shrejder, A.V., Degtyaryova, G.L., Diakov, V.G. (1964) *Corrosion protection of oil refining equipment*. Moscow: Nedra.
2. Girenko, V.S., Bernatsky, A.V., Rabkina, M.D. et al. (1987) Lamellar, lamellar-brittle and lamellar-ductile fracture of welded joints. *Problemy Prochnosti*, **3**, 70–76.
3. Karpenko, G.V. (1960) New ideas about hydrogen effect on properties of steel. *Prykladn. Mekhanika*, **6(4)**, 361–367.
4. Karpenko, G.V., Kripyakevich, R.I. (1962) *Hydrogen effect on properties of steel*. Moscow: Chyorn. i Tsvet. Metallurgiya.
5. Girenko, V.S., Rabkina, M.D., Dyadin, V.P. et al. (1998) Some results of technical diagnostics of vessels and pipelines in petrochemical industry. *Tekhn. Diagnostika i Nerazrushayush. Kontrol*, **3**, 17–24.



10th JUBILEE EUROPEAN CONFERENCE-EXHIBITION ON NON-DESTRUCTIVE TESTING

On June 7–10, 2010 10th Jubilee European Conference-Exhibition on Non-Destructive Testing (10th ECNDT) was held in Moscow. It had a record number of countries-participants over the entire period of conducting such forums — representatives of 65 countries came to Moscow. Total number of registered participants was 1021 persons, participants of conference and exhibition — 1230 persons. Moscow was granted the right to host this event as a result of competition in EFNDT session in Vienna in 2005. 10th ECNDT President was appointed to be V.V. Klyuev, Academician of RAS, President of the Russian Society on Non-Destructive Testing and Technical Diagnostics. Scientific Committee was formed from representatives of 43 countries, and it included 153 known scientists and leaders of national NDT societies.

In keeping with the program of 10th ECNDT a plenary session was held, in which six presentations were made: V.V. Klyuev (Russia) «Nanotechnologies and nanodiagnostics»; Prof. V. Krsteji (Croatia) «EFNDT positioning in European quality infrastructure»; N.A. Makhutov, Corresp.-Memb. of RAS (Russia) «Diagnostics of the state of objects and risk monitoring in large-sized projects»; Dr. M. Farley, ICNDT President (Great Britain) «ICNDT activity in the sphere of international certification of NDT personnel»; Prof. U. Ewert (Germany) «Prospects for mobile computer tomography»; Prof. V.P. Vavilov (Russia) «Thermographic non-destructive testing: brief history, state-of-the-art and tendencies».

Then meetings were conducted in 25 sessions, in which 703 presentations were made on various methods, directions and problems in the field of non-destructive testing and technical diagnostics (NDT and TD).

The following events took place during the Conference:

- EFNDT General Assembly, in which new members of the Board of Directors were elected, report of EFNDT Board of Directors was presented, and updated EFNDT Bylaws were approved;

- ICNDT General Assembly chaired by Dr. M. Farley, ICNDT President, which addressed the following issues: ICNDT 2009 report, coordination of ICNDT operation procedures, discussion of membership fees, 2010–2011 budget, presentation of certificates to new members, interim report on preparation for 18th World Conference on NDT (18th WCNDT), reports of regional divisions;

- EFNDT BoD meeting devoted to 10th ECNDT, discussion of the strategic plan, financial report, 2010–2011 budgets, refinement of EFNDT operation proce-

dures, incorporation of new members, as well as planning the next meeting, which it was proposed to hold in Kiev;

- two meetings of Academia NDT International chaired by Dr. J. Nardoni, President of the Academia, in which 25 full members of Academia from 17 countries of the world took part. 7 new full members and 2 honorary members were elected into Academia. Total number of Academia NDT members is 44 academicians from 21 country. A decision was taken to raise the number of Academia members to 100 in the next 2–3 years, widening of representation geography being important here;

- ICNDT Executive committee meeting in which documents for discussion in ICNDT General Assembly, and key issues of WG1 and WG3 activities were considered, as well as incorporation of new members from Central Asia region;

- Forum on qualification, certification and accreditation. Forum participants representing more than 20 countries discussed the latest changes in ISO 9712 and EN 473 standards and submitted a proposal on uniting the requirements of these standards and creating a common standard on NDT personnel certification;

- EFNDT–ASNT meeting devoted to the features of functioning of American NDT Committee. In addition, issues of NDT personnel training and certification in the USA were considered, in particular a new innovation program aimed at attracting and supporting young specialists;

- meeting of ISO TC 1135 «Non-Destructive Testing», in which more than 60 participants from 20 countries of the world took part.

One of the Conference events was an exhibition of NDT means, in which more than 190 companies from 16 countries and 32 national NDT societies in 151 booths took part.

More than one thousand NDT instruments and systems with application of acoustic, ultrasonic, radiation, vibration, electromagnetic, magnetic, thermal and other testing methods, information booths of ICNDT, EFNDT, national NDT societies of European, Asian, American and African countries were presented in the exhibition.

An innovation competition chaired by Dr. M. Douglas (Canada) was held during the exhibition.

10th ECNDT Diplomas were awarded to six innovative developments:

- small-sized betatron for 2.5 MeV energy for field operation (GOU VPO Tomsk Polytechnic University, RI of Introscopy);

- ACOUSTIC EYE system for NDT of internal condition of tubes of heat exchangers, steam generators and other industrial facilities, having tubes in their structures («Spektr» Ltd.);

- automated facility for eddy current control of bearing rings VISTKON (UNITEST GROUP);

- magnetostriction generators of higher power waveguide waves (Souhtwest Research Institute);

- automated unit «Shilo» for testing girth welds in tube-tubesheet system (TSNK Laboratory);

- AVGUR-T system for external and internal AUST of welded joints and base metal of pipelines and welded T-joints with coverplates (SPC «Ekho+» Ltd.).

In a specially equipped hall leading world manufacturers made 16 presentations of the most advanced equipment. Presentation by Harry Passi (Sonotron NDT Company) on «Ultrasonic testing with phased array application. Result visualization in keeping with

the actual geometrical dimensions and shape of the object of control», as well as US flaw detector on phased arrays ISONIC 2009 generated participants' interest.

As part of Exhibition activities, a competition of exponent companies for the «Best Booth of ECNDT 2010» was held. By the results of an anonymous poll of more than 300 specialists a commission headed by D. Gilbert, Editor-in-Chief of Insight Journal, determined the winners. These were booths of the following companies: OLYMPUS, Spektr, General Electric, South African Institute for NDT (in the nomination «Best Booth of the National NDT Society»).

In the official meeting devoted to closing of the 10th Jubilee Conference its results were summed up and countries-organizers of the next international conferences were presented, namely of 18th International Conference in SAR, and 11th European Conference in Czechia in 2014.

Dr. S.V. Klyuev, RF

INTERNATIONAL CONFERENCE ON WELDING CONSUMABLES

The 5th International Conference «Welding consumables. Technologies. Production. Quality. Competitiveness», devoted to the 20th anniversary of Association «Elektrod», took place in Artyomovsk, Donetsk region, in the period of June 7–11, 2010. The organizers of the Conference were Association «Elektrod» of enterprises of CIS countries and CJSC «Artemmashzavod «VISTEK». 44 specialists from 29 enterprises and organizations of Ukraine, Russia and Kazakhstan participated in the work of the Conference. I.M. Livshits, the president of the Association, general director of CJSC «SVAMA», opened the work of the Conference. N.I. Yatchenko, general director of VISTEK, delivered a welcome speech to the participants of the Conference. Prof. V.N. Shlepakov, leading staff scientist of the E.O. Paton Electric Welding Institute, presented the greeting speech of Prof. B.E. Paton to the participants of the Conference.

The program of the Conference included 25 papers and presentations, many of which were included into the Collection prepared by the International Association «Svarka». One part of the papers was devoted to covered electrodes and technology of their manufacture, and another part described the problems of development, production and application of solid wires, flux-cored wire and fluxes for mechanized arc welding. During two plenary sessions the lecturers presented their papers, commented upon their content before the participants of the Conference and answered the questions of the audience.

In the paper «Methods of modernization and development of electrodes for manual arc welding and surfacing» Dr. I.N. Vornovitsky (OJSC SPA «TSNIIT-MASH») explained new criteria of quality and algorithm of processes of development of electrodes to solve the problems of providing high quality of their manufacturing and stability of welding-technological characteristics. On the example of operation of preparation of coating mass the advantages of intensive mixers over roller ones in improvement of key characteristics of electrodes, such as productivity (increases), losses of metal for waste and spattering (decrease), manoeuvrability of electrode (improves) are shown. O.V. Dzyuba (SPC «Svarochnye materialy», Krasnodar) reported about new technology of increase of modulus of liquid glasses designed for manufacturing welding consumables. For this purpose the methods of electrolysis were suggested to be used, applied for desalination of sea water. In the paper some properties of obtained soluble-glass materials are analyzed.

I.M. Livshits («Izhorskie svarochnye materialy», Ltd., RF) reported in his speech that the results of optimization of the technology of manufacturing of flux of the grade 48 KRF-16, intended for welding of structures of nuclear power plants, allowed considerable decrease of sulphur and phosphorus content in deposited metal.

I.N. Zvereva, engineer (OJSC «MKM-METIZ», Magnitogorsk, RF) told about advantages of lubrica-



tion of the grade PANLUBE S622T of the company PAN CHEMICALS (Italy), revealed at manufacturing electrode cores of the wire produced in large-lot line of wire rod drawing after mechanical removal of scale from its surface. High adaptability of the process including stability of drawing, high efficiency of lubrication holdup, absence of dusting and «burning» of lubrication material is observed. Lubrication is easily removed from the surface of the wire in the process of washing out, which is confirmed by results of evaluation of amount of lubrication on the surface of rods after operation of cutting. Two papers of I.M. Livshits are dedicated to actual problems of production and application of electrodes of general purpose. In the first one the attempts to change electrodes UONI-13/55 are analyzed, which were 70 in the last year with the new developments to improve their manufacturability in the process of production, to increase the welding-technological characteristics, and also physical-mechanical characteristics of welds performed by them. The paper concerns the results of the previous works (TsU-6, TsU-7 of TsNIITMASH, ANOD of the E.O. Paton Electric Welding Institute, UONI-13/45AA and UONI-13/55AA of TsNII KM «Prometey»), and also the challenged developments carried out in the frames of state program «Magistral». The second paper concerns speculations, made by some manufacturers of electrodes, on far-fetched problem of influence of the coating colour on welding-technological and operational properties of electrodes.

Dr. V.G. Lozovoj (SPC «Svarochnye materialy») comprehensively reported in his work about experience of large group of authors, accumulated during tests and application of Russian electrodes LB-52 TRU instead of foreign ones in welding of blast furnace of Novolipetsk Metallurgical Works. The paper is saturated with practical data and is recommended to those involved in development and application of low-hydrogen electrodes designed for welding and repair of objects of metallurgical complex.

Dr. A.E. Marchenko (the E.O. Paton Electric Welding Institute) devoted his paper to the analysis of physical-chemical nature and results of investigation of strength of electrode coatings. It was shown that strength of electrode coatings, manufactured using binder in the form of a liquid glass, is provided by hydrant shapes of alkali silicates occurred during dehydration of liquid glass at heating of electrodes not more than to 200 °C. The structure of silicate binder is considerably deteriorated in the course of high-temperature heat treatment (400 °C), to which low-hydrogen electrodes are subjected. As a result, the hydrate forms of silicates possessing binding (adhesion) properties completely disappear in it. Moreover, high-temperature heating and cooling of electrodes provoke the inner stresses in the coating, caused by inadmissible shrinkage of silicate matrix and also difference of coefficients of thermal expansion of ma-

trix and filler in the coating on one hand and coating and rod on the other hand.

The paper of Dr. Marchenko, prepared together with engineer N.A. Protsenko (the E.O. Paton Electric Welding Institute), describes the new edition of international standards ISO 9000 and ISO 9001 and their national versions in Ukraine and also prospect of issuing of a new standard ISO 9004.

In the review, prepared by Drs A.E. Marchenko and N.V. Skorina (the E.O. Paton Electric Welding Institute) and also engineer V.P. Kostyuchenko (OJSC «Mezhgosmetiz-Mtsensk») the detailed technical characteristics and advantages of low-hydrogen electrodes with two-layer coating, which are available at international market of welding consumables, are given and prospects of their development and production in CIS countries are shown.

Dr. Marchenko presented the paper «Grounding and experimental investigation of the system of deoxidization and microalloying of metal, deposited by low-hydrogen special-purpose electrodes», prepared by a group of authors headed by Prof. I.K. Pokhodnya. As far as in welding using coated electrodes the welding zone is not very reliably protected from surrounded air, as during use of other welding consumables, titanium in deoxidation system Mn-Si-Ti acts not only as a deoxidizer, but also as a nitride-forming element. Such «doubling» does not allow its use as microalloying element for effective control of impact toughness of weld metal. To increase protective capacity of coating, it is necessary to increase relation $\text{CaCO}_3:\text{CaF}_2$ in coating and its thickness. Under the given conditions combining titanium as microalloying element with boron it is possible to increase impact toughness of weld metal not only at room but also at negative temperature down to -60 °C.

Engineers P.A. Kosenko and N.A. Solovej devoted their paper to the problems of production of welding consumables at SE «Pilot Plant of Welding Consumables of the E.O. Paton Electric Welding Institute of the NAS of Ukraine» (OZSM). It is outlined in this paper that under the present economic conditions at the market of welding consumables the quality of output products and rendered services have the primary significance for successful functioning of enterprise. The acting system of quality management by the standard ISO 9001:2000 was certified in 2007. Now the preparation for its recertification in accordance with statements of new version of standard set into force in 2009 is carried out. Nowadays OZSM fully prepared his test laboratories for accreditation according to ISO/IEC 17025:2006. In its market activity it was reoriented to the work with small organizations and outlet sale of electrodes. In a tiny package the most challenging grades of electrodes began to be packed. The packing line of productivity of about 470 boxes of 1 kg mass per hour was designed and manufactured. A new package, manufactured of strong mi-

crocorrugated cardboard and made in brand style and white-blue colors, traditional for OZSM, will provide proper storage of electrodes and satisfy the demands of consumers.

The paper of the specialists of the E.O. Paton Electric Welding Institute, presented by Prof. V.N. Shlepakov, was devoted to the question of application of flux-cored wires for welding structures of units of metallurgical and mining production. In the paper the analysis of structural defects revealed in the units of mentioned productions after their continuous operation was given. The characteristics of developed flux-cored wires and technologies of their application for mechanized and automatic welding of these structures were described. The results of tests of offered technology showed increase in productivity of welding operations by 1.5–2 times. The welding consumables are saved, the level of residual stresses in welded joints is decreased and their operation reliability increased. The basic principles of use of offered technology on the different objects of metallurgic complex were defined.

V.N. Shlepakov also presented the paper «Bases of formation of compositions of flux-cored wires at high welding efficiency». He outlined that the solution of problems of mechanized welding of steels of increased and high strength is defined by technological and metallurgical requirements which are specified to welded joints, and high productivity of process of wire electrode melting must be combined with low specific heat input into a near-weld zone. This is achieved using tubular gas-shielded flux-cored wires with a metallic type of core, in content of which the volume of filler does not exceed 1.5 %. The correlation of fractions of metallic and gas slag-forming parts of a core is determined in accordance with the required level of alloying of deposited metal. To protect molten metal

from air the gas mixtures based on argon should be applied. This provides stable arc burning, decrease of number of short circuits, and character of transfer of electrode metal transforms from drop into spray one.

In conclusion part of his paper the author made review of aspects of production and application of seamless flux-cored wire, where he generalized the multi-year foreign and domestic experience in this question. It was included into Collection as a separate paper. The principle of modernization of three grades of electrodes — ANO-21, ANO-4 (rutile coating, design of PWI) and UONI-13/55 (low-hydrogen coating, design of TsNIIM, Russia), carried out by the E.O. Paton Electric Welding Institute, was reported by engineer O.I. Folbort (the E.O. Paton Electric Welding Institute). The modernization of electrodes AHO-21 was made to widen their assortment and expecting a maximum possible use of raw materials of the Ukrainian manufacturers. The modernization of the electrodes ANO-4 and UONI-13/55 was caused by necessity of fulfillment of requirements, which are specified by Russian National Agency for Control and Welding (NAKS) to the products delivered both to Russia and also to Federation by foreign producers. S.Yu. Ryabov, chief engineer of «Silikat Ltd.» (St. Petersburg), reported about production of silicate lumps, designed for manufacturing welding electrodes, their characteristics and terms of delivery. A number of planned speeches failed in connection with the fact that reporters did not arrive to the Conference by different reasons and did not participate in its work. Their papers are available for review, as far as they are included into published Collection.

*Dr. A.E. Marchenko,
Eng. P.V. Ignatchenko, PWI*



10th INTERNATIONAL CONFERENCE-EXHIBITION «PROBLEMS OF CORROSION AND ANTICORROSION PROTECTION OF STRUCTURAL MATERIALS. CORROSION-2010»

10th International Conference-Exhibition «Problems of corrosion and anticorrosion protection of structural materials. Corrosion-2010» took place in Lvov in June 8–11, 2010. It was dedicated to 100th birth anniversary of academician H.V. Karpenko, one of the founders of physicochemical mechanics of the materials that is a research direction appeared in the first half of XX century at the turn of mechanics of materials, solid-state physics and chemistry of surface effects.

The problem of corrosion and anticorrosion protection of metal structures and their welded joints is relevant for many branches of industry of Ukraine, including building, transport, machine building, gas-and-oil producing industry, mining, power, metallurgical, chemical and food manufacturing areas.

The annual loss of industry of the developed countries due to corrosion is estimated in 4–5 % of the gross domestic product. At that, more than 15 % of this sum could be saved using known progressive anticorrosion methods of protection. Therefore, protection and reduction of metal loss due to corrosion acquire particularly large importance, especially, in connection with an increase of consumption of different types of metal products in industry and agriculture.

The International Conference-Exhibitions on problems of corrosion and anticorrosion protection in Lvov, became traditional, are brought to familiarize a wide range of specialists with the new theoretical and practical developments in this field of science, current methods for increase of corrosion resistance of different application metal structures as well as establish closer research-production and commercial connections between Ukrainian and foreign specialists. The conference-exhibitions are organized by Ukrainian Association of Corrosion Specialists at the head of its president Prof. V.I. Pokhmursky, Corresponding Member of the NAS of Ukraine. At present time the Association has been joining around 50 research institutions, organizations and enterprises and more 100 individual members.

The representatives of research institutions, commercial companies and industrial enterprises from Germany, Australia, Russia, Ukraine, Poland, Mexico, Kazakhstan, Lithuania, Belarus and other countries participated in work of the jubilee conference-exhibition that is the evidence of its relevance and increasing authority.

The Conference was opened by Prof. V.I. Pokhmursky which represented plenary paper «Role of academician H.V. Karpenko in development of investigations of stress corrosion fracture of metals».

The main questions, touched on the Conference, are fundamental aspects of corrosion and stress corrosion fracture; problems of hydrogen and gas corrosion; new tendencies in development of corrosion-resistant materials and creation with their help of gas-thermal, galvanic and other coatings; modern directions of development of inhibitor, biocide and electrochemical protection; research methods and corrosion control; corrosion and environmental problems; problems of training of corrosion specialists; ways of implementation of the latest methods of anticorrosion protection of equipment for oil-and-gas industry, power and chemical equipment.

The representatives of commercial enterprises paid particular interest to papers of applied character describing the problems of monitoring of metal structures, including gas, oil and water pipelines and their welded joints, electrochemical protection and protective coatings (lecturers: R. Dzhalá, V. Chervatyuk, M. Khoma — H.V. Karpenko PMI of the NASU; S. Polyakov — E.O. Paton Electric Welding Institute of the NASU; Yu. Gerasimenko, G. Vasiliev — NTUU «Kiev Polytechnic Institute»; I. Reformat-skaya — FSUE «L.Ya. Karpov Research Physicochemical Institute» etc.).



Opening of Jubilee Conference-Exhibition. *From the left:* Prof. V.I. Pokhmursky, Corresponding Member of the NASU; *from the right:* V.V. Panasyuk, director of the H.V. Karpenko Physico-Mechanical Institute of the NASU



The PWI Corrosion laboratory represents the Institute on Conference «CORROSION-2010»

Manufacturing companies directly working in area of metal fund protection from corrosion took part in the exhibition: STC H.V. Karpenko PMI of the NASU, SE Engineering Center «Techno-resurs» of the NASU, SE Engineering Center «Lvovantikor» of PMI of the NASU, DE NORA DEUTCHLAND GmbH (Germany), «ZINGA METAL and K» Ltd., «Tech Engineering» Ltd., OJSC «Zaporozhie Plant of Electrical Equipment» etc. A delegation of young scientists under leadership of Prof. S.G. Polyakov presented the E.O. Paton Electric Welding Institute. Themes of presentations and poster papers of representatives of the PWI were relevant applied developments in area of monitoring of man-caused media (soils, subsoil-waters, cooling liquids) with application of electrochemical methods of investigations such as method of

polarization resistance, method of polarization curves and electrochemical noises, which are already used on enterprises of oil-and-gas complex, OJSC «Ukrhidroenergo» and municipal engineering. A development of Corrosion laboratory of the PWI took an important place in exhibition exposition. It was a system of corrosion monitoring of pipelines (SCMP) TU U 33.2-30019801-001:2006 designed for determination of level of protection of pipeline in length and in time according to DSTU 4219; rate of corrosion of pipeline metal from outside; places of protective coating damage; rate of residual corrosion of pipeline metal in a defect of protective coating; current of hydrogen diffusion through wall of pipeline metal; corrosivity of soil in places of pipeline positioning; corrosivity of product being transported; electrochemical potentials: polarization, corrosion, total with ohmic component, transverse and longitudinal gradient of potentials along the whole pipeline length as well as their change in time; presence of roaming currents.

SCMP is certified by the «Ukrmetrteststandart» of Ukraine as a mean of measuring equipment that is uncommon for such class of devices measuring instantaneous rate of metal corrosion.

The problems of terminology in area of corrosion protection, development of normative documents in this sphere which would be harmonized with international standards were discussed at final meeting of the Conference.

*Prof. S.G. Polyakov,
Ing. S.A. Osadchuk, PWI*

L.M. LOBANOV IS 70



Professor Lobanov Leonid Mikhajlovich, Dr. of Tech. Sci., academician of the NAS of Ukraine, the honoured worker of science and technology of Ukraine, laureate of Prize of the USSR Council of Ministers, State

Ukrainian Prize, Paton Prize of the NAS of Ukraine, famous scientist in the field of materials science and strength of materials and structures, celebrated his 70th anniversary in September.

Lobanov L.M. graduated from the faculty of industrial and civil building of Kiev Civil Engineering Institute and mechanical-mathematical faculty of Kiev State University. Since 1963 he is working at the E.O. Paton Electric Welding Institute of the NAS of Ukraine, since 1985 — Deputy Director on research work and Chief of Department of optimization of welded structures of new engineering at the Institute.

Scientific activity of L.M. Lobanov is connected with investigations of behavior of materials in welding, development of experimental methods of investigations and control of welding stresses and strains, fabrication of high-efficient welded structures and development of methods and means of their diagnostics.

His works, devoted to development of methods of optic modeling, holographic interferometry, electron



speckle-interferometry and shearography for investigation of stressed state and control of quality of welded joints in the structures of metallic, composite and polymer materials, were widely recognized. The developed methodological approaches and designed devices of a high accuracy and informativity are applied in research organizations and enterprises of Ukraine, CIS countries, China, South Korea.

Owing to the works of L.M. Lobanov and his pupils, the new scientific direction was formed: a deformation-free welding of structures, based on the control of thermal processes during welding to decrease heat input and create preliminary stress-strain states optimized relatively to welding stresses and deformations. The developed methods and technical means of eliminating welding deformations and stresses were used during development of complex «Energiya-Buran» and other rocket-space systems. The radically new are the developed technologies of deformation-free welding of stringer panels and shells of high-strength aluminium and titanium alloys.

Under the supervision of L.M. Lobanov the complex of fundamental investigations in the field of static and dynamic strength of welded joints considering their mechanical heterogeneity and presence of crack-like defects, resistance of welded joints to brittle and laminar fractures and also to fatigue fractures, and of scientific approaches to provide reliability and long life of welded structures keeping requirements towards the decrease of their metal capacity, methods of non-destructive control of quality and diagnostics of welded joints and structures, evaluation and extension of life of welded structures of critical purpose has been performed. New types of high-effective welded structures have been manufactured, which include the light stringer metallic structures, bridge spans, heavy-loaded structures of high-strength steels, unique structures of transformable volume. By his

active participation the State standards of Ukraine regulating requirements to the quality of welded structures and technologies of their manufacture were developed, the system of certification of welding technologies, materials, equipment and structures was organized, the conception of State program on providing technological safety for basic branches of economy of Ukraine was worked out.

L.M. Lobanov took active participation in publishing three-volume edition «Welded Engineering Structures», where the experience on study and development in the field of designing and manufacture of structures, determination of their technical condition and reconstruction was generalized.

L.M. Lobanov conducts an important scientific-organizational work as Chairman of Ukrainian technical committee on standardization in the field of welding, Deputy Chief of Interstate Scientific-Technical Council on welding and related technologies, member of Interdepartmental Council on the problems of scientific-technical security and defense of Ukraine, Deputy Chairman of scientific council on purposeful complex program of the NAS of Ukraine «Problems of life and safe service of structures, constructions and machines». He actively cooperates with international scientific organizations of CIS countries and foreign countries, often presents scientific papers at prestigious scientific forums, heads a number of international projects.

L.M. Lobanov is the author of more than 600 scientific works, including 6 monographs, 60 author's certificates and patents. He supervised the theses of 8 Dr. of Techn. Sci. and 15 Candidates of Techn. Sci.

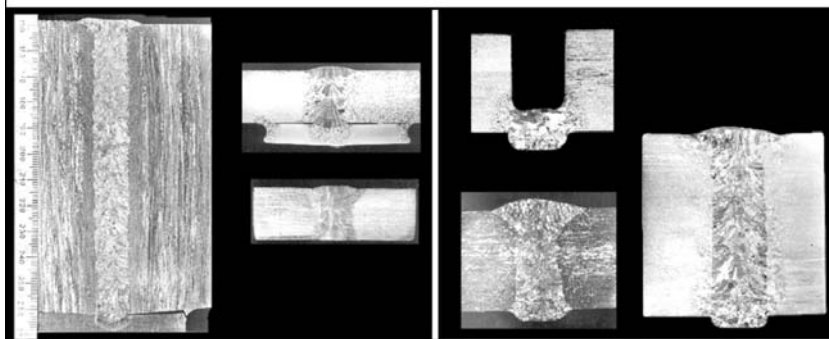
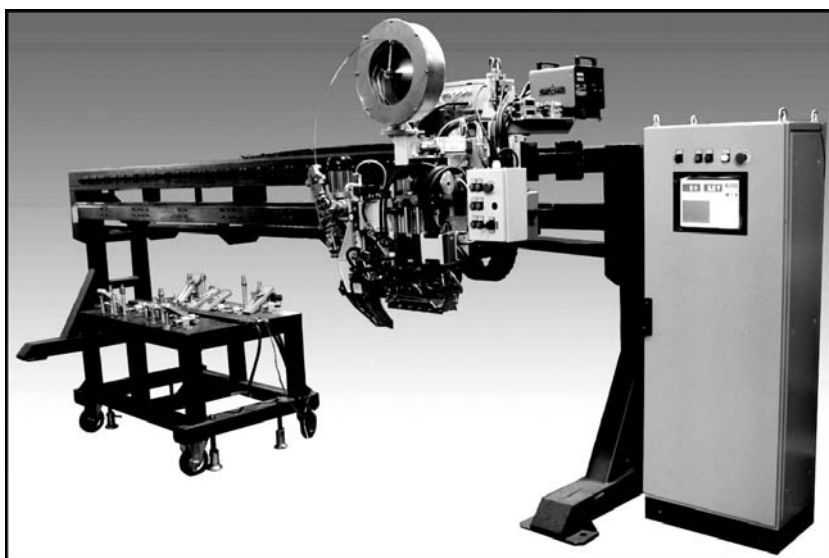
He is awarded with orders «For services» of II and III degree and Badge of Honour, decoration of Presidium of the NAS of Ukraine «For Scientific Achievements», medal of Yu.V. Kondratyuk for participation in space activity and many other medals and decorations.

NEWS

NARROW-GAP WELDING OF HIGH-STRENGTH TITANIUM ALLOYS OF UP TO 110 MM THICKNESS

A technology and portal type unit for narrow-gap arc welding of titanium and high-strength titanium alloys of up to 110 mm thickness were developed in the E.O. Paton Electric Welding Institute. The technology provides for application of TIG welding process with magnetically-impelled arc and feed of filler wire in narrow gap of 8–12 mm width. An alternating devia-

tion of arc to side walls of narrow-gap groove is achieved due to its magnetic control and, respectively, uniform fusion of vertical walls with deposited bead as well as beads between themselves is attained. An electric arc burns under constricted conditions in narrow-gap welding, besides, at that, except tungsten electrode a guide for filler wire and magnetic circuit of electromagnet are situated in the gap groove that makes control of the process of welding difficult for operator. A small-size video camera VK-27, equipped with right angle attachment and designed for TV monitoring of process of TIG welding of structures from titanium and titanium alloys with up to 500 A current was developed for visual control of welding process and control of a state of tungsten electrode and position of filler wire in the groove.



tion of arc to side walls of narrow-gap groove is achieved due to its magnetic control and, respectively, uniform fusion of vertical walls with deposited bead as well as beads between themselves is attained.

An electric arc burns under constricted conditions in narrow-gap welding, besides, at that, except tungsten electrode a guide for filler wire and magnetic circuit of electromagnet are situated in the gap groove that makes control of the process of welding difficult

The main advantages of developed technology:

- reduction of weld width and heat-affected zone;
- decrease in volume of deposited metal;
- increase of welding process efficiency;
- reduction of welding process laboriousness;
- providing of high quality of welded joints independent on thickness of elements being joint;
- strength of welded joint — at the level not less than 0.9 of strength of the base metal.



DEVELOPED IN PWI

INSTALLATION NK 362M

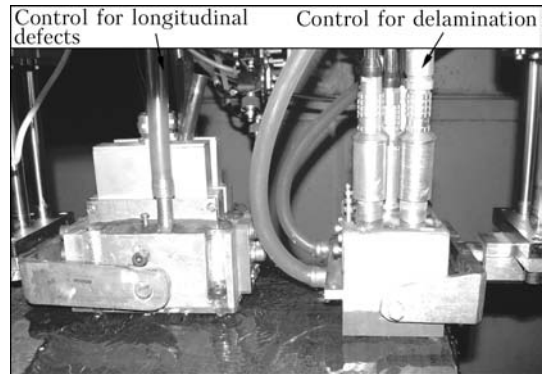
It is designed for automatic ultrasonic control of end areas of pipes of diameter of 508–1420 mm with 7–50 mm thickness of wall.

The installation provides:

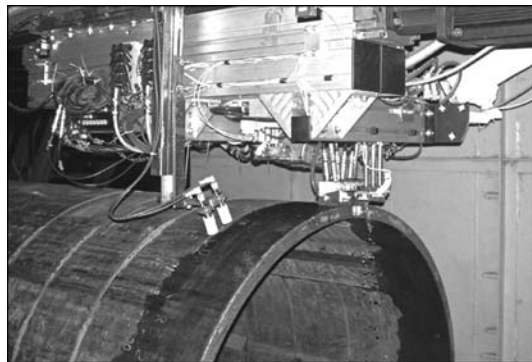
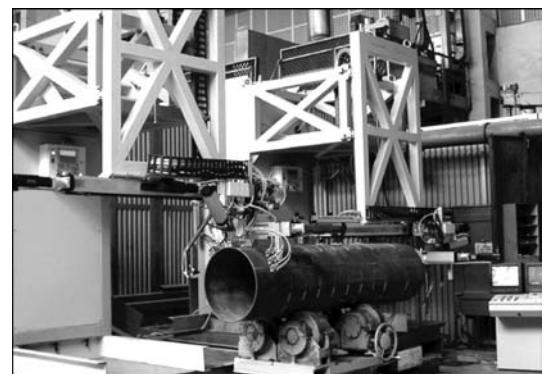
- sounding of both ends of pipes around the whole perimeter across the wall thickness, detection of defects of delamination type on the width of 60 mm from the end and longitudinally oriented defects of crack type on the width of 30 mm from the end;
- automatic control of quality of acoustic contact in all flaw detection channels.

The following operations are automatically performed in the installation:

- record and storage of information about the process and results of control;
- output of light and sound signal about presence of flaw;
- output of light and sound signal about inadmissible deterioration of quality of acoustic contact;
- diagnostics of equipment operation and sending of messages to the device of man-machine interface;



Local-immersion acoustic heads



- preparation and transfer of necessary information about results of control and installation operation to workshop database;
- making marks of different colors on the pipe surface, defining location of defects and areas with unsatisfactory acoustic contact.

Multichannel ultrasonic flaw detector is designed on the base of «Socomate» boards.

Basic technical characteristics of the installation NK 362M

Parameter	Value
Working frequency, MHz	2.5; 4.0
Linear control speed, m/min	max. 20
Range of speed control	not less than 1/100
Number of US channels on the base of «Socomate» boards, pcs	16
Frequency of tracking of sounding pulses along each channel provides pulsing for 1 mm	not less than 2
Reserve of sensitivity along channels in dynamic mode, dB	not worse than 12
Incontrollable area on the ends of pipes, mm	not more than 10
Incontrollable area in the region of a weld, mm	not more than 15
Water consumption, l/min	not more than 50
Power consumption, kV·A	not more than 8



INSTALLATION NK 364

It is designed for automatic ultrasonic testing of solid-rolled railway wheels made on GOST 10791 and specifications as well as wheels of foreign standards UIC, AAR in a processing line of their production of 760–1092 mm diameter.

The following operations are automatically performed in the system:

- record and hold of the results of testing;
- defect light and sound alarm signals;
- light and sound alarm signal of inadmissible loss of quality of acoustic contact;
- equipment operation diagnostics and display of a messages on human-machine interface device;
- preparation and transfer of necessary information about results of testing and operation of system into a shop database.



The system has 6 acoustic locally immersion blocks for testing:

- rim in axial direction;
- rim in radial direction;
- hub;
- disk;
- disk in axial direction by inclined transducers;
- flanges.

Systems of AUST of railway wheels successfully passed metrological certification in Ukraine, Russia and guarantee tests and were introduced in commercial operation.

Capacity of the system makes 70 wheels per hour.

Main performance characteristics of NK 364 system

Operating frequency, MHz	2.5–5.0
Wheel speed, rpm	5–20
Number of US channels, pcs	20 (40)
Time instability of response level for 8 h of work, dB	not more than 2
Instability of response level on width of testing zone at 70 mm depth, dB	not more than 0.5
Frequency of movement of monitoring pulses through each channel provides pulsing per 1 mm	not less than 1
Margin of response level in channels in dynamic conditions, dB	not worse than 8
Uncontrolled zone of side surfaces of controlled areas, mm:	
internal side surface of a rim; wheel disk	not more than 5
external side surface of a rim (for direct PET), internal and external side surfaces of a rim (for inclined PET); thread, side surfaces of a hub	10
Size of acoustic gap, mm:	
in control of rim and disk of a wheel for direct and inclined transducers, operating in immersion variant	10–40
in control of wheel hub for direct transducers, operating in gap variant	0–3
Initial edge of control zones monitoring accuracy, mm	±0.5
Consumed power, kV·A	not more than 12